



UNIVERSIDAD NACIONAL AUTÓNOMA DE MÉXICO
PROGRAMA DE MAESTRÍA Y DOCTORADO EN INGENIERÍA
INGENIERÍA AMBIENTAL – AGUA

**POLYHYDROXYALKANOATES PRODUCTION USING MICROALGAE-BACTERIA
CONSORTIA UNDER ENVIRONMENTAL CONDITIONS**

TESIS

QUE PARA OPTAR POR EL GRADO DE:
DOCTOR EN INGENIERÍA

PRESENTA:

M.I. ENRIQUE ROMERO FRASCA

TUTOR PRINCIPAL

DR. GERMÁN BUITRÓN MÉNDEZ, INSTITUTO DE INGENIERÍA

COMITÉ TUTOR

DRA. CLAUDIA ETCHEBEHERE ARENAS, IIBCE URUGUAY

DR. ARMANDO GONZÁLEZ SÁNCHEZ, INSTITUTO DE INGENIERÍA

Santiago de Querétaro, Querétaro, abril de 2024



Universidad Nacional
Autónoma de México

Dirección General de Bibliotecas de la UNAM

Biblioteca Central



UNAM – Dirección General de Bibliotecas
Tesis Digitales
Restricciones de uso

DERECHOS RESERVADOS ©
PROHIBIDA SU REPRODUCCIÓN TOTAL O PARCIAL

Todo el material contenido en esta tesis esta protegido por la Ley Federal del Derecho de Autor (LFDA) de los Estados Unidos Mexicanos (México).

El uso de imágenes, fragmentos de videos, y demás material que sea objeto de protección de los derechos de autor, será exclusivamente para fines educativos e informativos y deberá citar la fuente donde la obtuvo mencionando el autor o autores. Cualquier uso distinto como el lucro, reproducción, edición o modificación, será perseguido y sancionado por el respectivo titular de los Derechos de Autor.

THESIS JURY:

Chair: Dr. Héctor Arturo Ruiz Leza

Secretary: Dr. Julián Carrillo Reyes

1st examiner: Dr. Armando González Sánchez

2nd examiner: Dra. Claudia Etchebehere Arenas

3rd examiner: Dr. Germán Buitrón Méndez

This research was conducted in the following facility (or facilities):

Laboratory for Research on Advanced Processes for Water Treatment, Academic Unit Juriquilla,
Instituto de Ingeniería, Universidad Nacional Autónoma de México

Laboratory of Environmental Biotechnology, INRAE Occitanie-Montpellier

THESIS DIRECTOR:

Dr. Germán Buitrón Méndez

.....

SIGNATURE

Acknowledgments

There are no proper words to express my sincere gratitude and admiration for my thesis and research adviser, Germán Buitrón Méndez. He has motivated me to become an independent researcher and demonstrated the value of critical thinking. He also showed what a clever and hardworking scientist can do.

My genuine gratitude must also go to the members of my thesis advisory and exam committee: Claudia Etchebehere Arenas, Armando González Sánchez, and Guillermo Quijano Govantes. They generously gave their time to offer me helpful suggestions, insights, and comments toward improving my work.

I am also most grateful to the collaborators at Laboratoire de Biotechnologie de l'Environnement, INRAE Occitanie-Montpellier for lending me their expertise and intuition to my scientific and technical problems: Jérôme Hamelin, Kim Milferstedt, and Julie Jimenez.

The financial support from Consejo Nacional de Humanidades, Ciencias y Tecnologías (CONAHCYT) through the CONAHCYT-OAS-AMEXCID Scholarship Program (grant no. 855766) is acknowledged.

This thesis was framed within the context of SEP-CONAHCYT-ANUIES-ECOS NORD Mexico-France scientific cooperation framework through project number 296514 'Caracterización morfológica y funcional de gránulos fototróficos utilizados en el tratamiento de aguas' and within Programa Iberoamericano de Ciencia y Tecnología para el Desarrollo (CYTED) though project number 320RT0005 'RENUWAL - Red iberoamericana para el tratamiento de efluentes con microalgas'.



GOBIERNO DE
MÉXICO

EDUCACIÓN
SECRETARÍA DE EDUCACIÓN PÚBLICA



CONACYT
Consejo Nacional de Ciencia y Tecnología



Summary

There is an urgent demand for innovative and sustainable solutions to address the growing environmental and wastewater treatment challenges. Conventional methods, like activated sludge processes, have long been the cornerstone of municipal wastewater treatment plants. However, increasingly stringent environmental and water reclamation regulations have evidenced the poor performance of activated sludge processes regarding energy consumption and nutrient removal. In response to these challenges, microalgae-bacteria consortia have emerged as a promising approach. This approach involves recovering organic matter and nutrients from wastewater and converting them into added value bioproducts using carbon dioxide and sunlight. In this context, the production of polyhydroxyalkanoates, such as polyhydroxybutyrate, by microalgae-bacteria cultures has gained attention for valorizing the generated biomass. However, the production yields of microalgae-based polyhydroxyalkanoates have been relatively modest, leading microalgae biomass to more immediate and practical applications like soil fertilization. This research evaluated nitrogen limitation and dissolved oxygen management as stress factors to increase polyhydroxyalkanoate accumulation in microalgae-bacteria biomass when it is produced using municipal wastewater under environmental conditions.

The structure of the present thesis was divided into four experimental parts, delineated following an initial review of the current state of the art. The first part of the experimental work was to screen and identify the microalgal biomass-producing polyhydroxyalkanoates from the incubation of municipal activated sludge. To this end, samples of activated sludge and municipal wastewater primary effluent were collected and subjected to continuous illumination to generate a microalgae-bacteria consortium under lab conditions. Nile red staining and micromanipulation techniques were used to identify and separate polyhydroxyalkanoates-producing microalgae. The production of polyhydroxybutyrates was quantified under nitrogen limitation in selected strains using gas chromatography and compared to *Chlorella sorokiniana* obtained from freshwater sources. The production of polyhydroxybutyrate was lower than 5 mg g dried biomass⁻¹ (0.5% dCW) in mixed microalgae consortium from activated sludge and mixed *Chlorella sorokiniana* dominant consortium. In contrast, polysaccharides production for activated sludge biomass was 460 ± 16 mg glucose g dried biomass⁻¹ (41% dCW) whereas 320 ± 24 mg glucose g dried biomass⁻¹ (30% dCW) were observed for *Chlorella sorokiniana* dominated consortia.

The second experimental part was dedicated to maximizing the production of polyhydroxyalkanoates as polyhydroxybutyrate in selected microalgae-bacteria consortia. A combined strategy of nitrogen limitation and low dissolved oxygen concentration was selected using the cyanobacterium *Synechocystis* sp. Polyhydroxybutyrate production was maximized to 95 mg L⁻¹ (12% dCW) by combining nitrogen limitation with low oxygen concentration conditions (1.2 mg O₂ L⁻¹). Moreover, low oxygen conditions also lowered the growth performance and photosynthetic activity yield in *Synechocystis* sp. compared to higher dissolved oxygen concentrations (≥ 6.5 mgO₂ L⁻¹), suggesting that hypoxia limited futile electron-consuming processes competing with the synthesis of polyhydroxybutyrate.

The third experimental part assessed the best performing conditions from the previous experimental part for simultaneous nutrient removal and polyhydroxybutyrate production in municipal wastewater. *Synechocystis* sp. cultures were adapted and grown in municipal primary effluent under environmental conditions until nitrogen-limited conditions were reached (12 d). Afterward, short photo-dense pulses of light (≥ 2000 $\mu\text{mol m}^{-2} \text{s}^{-1}$) were applied to inhibit oxygen evolution from microalgae while wastewater-borne bacteria consumed dissolved oxygen. This oxygen stripping protocol resulted in a low dissolved oxygen concentration (5.7 mg O₂ L⁻¹). Results from this experimental part confirmed that *Synechocystis* sp. and wastewater-borne bacteria, in combination with the nitrogen limitation and oxygen management strategy, were able to remove 92% of chemical oxygen demand, 99% of ammonia, and 88% of phosphorous. Moreover, the low dissolved oxygen concentration attained higher polyhydroxybutyrate production yields (80 mg L⁻¹ or 10% dCW) compared to earlier studies in waste effluents without oxygen management.

The fourth experimental part evaluated the biomass potential for soil fertilization using the microalgae-bacteria consortia biomass obtained in the first experimental part to possible use as a source of organic matter, nitrogen, and phosphorus. Therefore, a biochemical fractionation method was used based on sequential chemical extraction and fluorescence spectroscopy. Microalgae-bacteria biomass in the form of loose flocs from the first experimental part and other morphological structures from photobioreactors fed with wastewater and mineral medium were harvested and lyophilized. The dried biomass was then subjected to a series of extractions to separate the biochemical compounds into different fractions, all with varying degrees of accessibility for soil microorganisms and complexity. Loose flocs from the first experimental trial were hardly extractable, with more than 50% of its organic matter, nitrogen, and phosphorus content considered

non-extractable. However, their extractability improved when subjected to nitrogen-limited conditions, where less than 10% of the organic matter, nitrogen, and phosphorus content was deemed non-extractable.

The overall results from this work provided the scientific knowledge base for microalgae-bacteria simultaneous wastewater treatment and polyhydroxyalkanoates production in municipal wastewater under environmental conditions. Microalgae strains from waste effluents or contaminated sources can produce polyhydroxyalkanoates under nitrogen limitation. However, incorporating oxygen management protocols is necessary to maximize polyhydroxyalkanoates production in mineral medium and municipal wastewater effluent. Microalgae-bacteria biomass with low polyhydroxyalkanoate production under nitrogen limitation was observed as an inherent source of accessible organic matter, nitrogen, and phosphorous to soil microorganisms, offering an alternative downstream process.

Resumen

Existe una demanda urgente de soluciones innovadoras y sostenibles para abordar los crecientes desafíos ambientales y de tratamiento de aguas residuales. Los métodos de tratamiento convencionales como los sistemas de lodos activados han sido usados para el tratamiento de aguas residuales municipales durante mucho tiempo. Sin embargo, el fortalecimiento de leyes y políticas en materia ambiental y de recuperación de agua han evidenciado el bajo rendimiento de los sistemas de lodos activados en cuanto a consumo de energía y eliminación de nutrientes. En consecuencia, los consorcios de microalgas-bacterias han surgido como un enfoque prometedor para recuperar materia orgánica y nutrientes de las aguas residuales y convertirlos en productos de valor agregado utilizando dióxido de carbono y luz solar. La producción de polihidroxicanoatos, incluido el polihidroxiacetato, mediante cultivos de microalgas-bacterias ha surgido como una alternativa para valorizar la biomasa generada. No obstante, los rendimientos de producción de polihidroxicanoatos en microalgas han sido relativamente modestos, dirigiendo la aplicación de la biomasa de microalgas hacia aplicaciones más inmediatas y prácticas como la fertilización del suelo. En vista de ello, la presente investigación evaluó la limitación de nitrógeno y la gestión del oxígeno disuelto como factores de estrés para incrementar la acumulación de polihidroxicanoatos en la biomasa de microalgas-bacterias cuando se produce en aguas residuales municipales bajo condiciones ambientales.

La presente se dividió en cuatro partes experimentales, delimitadas luego de una revisión del estado actual del arte. La primera parte del trabajo experimental consistió en examinar e identificar biomasa microalgal productora de polihidroxicanoatos a partir de la incubación de lodos activados municipales. Para ello, se recolectaron muestras de lodos activados y efluente primario de aguas residuales municipales y se sometieron a iluminación continua para generar un consorcio de microalgas-bacterias en condiciones de laboratorio. Posteriormente, se utilizaron técnicas de tinción con rojo Nilo y micromanipulación para identificar y separar microalgas productoras de polihidroxicanoatos. La producción de polihidroxiacetato se cuantificó bajo limitación de nitrógeno en cepas seleccionadas mediante cromatografía de gases y se comparó con *Chlorella sorokiniana* obtenidas de agua dulce. La producción de polihidroxiacetato fue menor a $5 \text{ mg g biomasa seca}^{-1}$ (0.5% dCW) en los consorcios mixtos de microalgas procedentes de lodos activados y los consorcios mixtos dominados por *Chlorella sorokiniana*. Por su parte, la producción de polisacáridos para la biomasa de lodos activados fue de $460 \pm 16 \text{ mg de glucosa g}$

biomasa seca⁻¹ (41% dCW), mientras que para consorcios dominados por *Chlorella sorokiniana* fue de un 320 ± 24 mg de glucosa g biomasa seca⁻¹ (30% dCW).

En la segunda parte experimental, se buscó maximizar la producción de polihidroxicanoatos, como polihidroxiacetato, en consorcios seleccionados de microalgas-bacterias. Para ello, se eligió una estrategia combinada de limitación de nitrógeno y baja concentración de oxígeno disuelto en la cianobacteria *Synechocystis* sp. Los resultados en esta parte experimental demostraron que la producción de polihidroxiacetato fue maximizada hasta alcanzar 95 mg L⁻¹ (12% dCW) bajo condiciones de limitación de nitrógeno y baja concentración oxígeno (1.2 mg O₂ L⁻¹). Adicionalmente, las condiciones de bajo oxígeno también disminuyeron el rendimiento de crecimiento y la actividad fotosintética en *Synechocystis* sp. en comparación con concentraciones más altas de oxígeno disuelto, lo que sugiere que estas condiciones limitan los metabolismos fútiles que consumen electrones y compiten con la síntesis de polihidroxiacetato.

La tercera parte experimental evaluó las mejores condiciones obtenidas en la parte experimental anterior para la remoción simultánea de nutrientes y la producción de polihidroxiacetato en aguas residuales municipales. Para ello, cultivos de *Synechocystis* sp. fueron cultivados en efluente primario municipal bajo condiciones ambientales hasta alcanzar condiciones de limitación de nitrógeno (12 días). Luego, se aplicaron pulsos cortos y densos de luz ($\geq 2000 \mu\text{mol m}^{-2} \text{s}^{-1}$) para inhibir la producción de oxígeno de las microalgas mientras que las bacterias del agua residual consumían oxígeno disuelto para obtener una baja concentración de oxígeno disuelto (5.7 mg O₂ L⁻¹). Los resultados de esta parte experimental confirmaron que *Synechocystis* sp. y las bacterias del agua residual, en combinación con la estrategia de limitación de nitrógeno y baja concentración de oxígeno, fueron capaces de eliminar el 92% de la demanda química de oxígeno, el 99% de nitrógeno como amoníaco y el 88% de fósforo como ortofosfatos. Además, la baja concentración de oxígeno disuelto logró mayores rendimientos de producción de polihidroxiacetato (80 mg L⁻¹ o 10% dCW) en comparación con estudios anteriores utilizando efluentes sin control de la concentración de oxígeno disuelto.

En la cuarta parte experimental, evaluó la biomasa de consorcios de microalgas-bacterias de la primera parte experimental como una fuente potencial de materia orgánica, nitrógeno y fósforo para la fertilización del suelo. Para ello, se utilizó un método de fraccionamiento bioquímico basado en extracción química secuencial y espectroscopía de fluorescencia. La biomasa de microalgas-bacterias en forma de flóculos sueltos de la primera parte experimental, así

como otras estructuras morfológicas de fotobiorreactores alimentados con aguas residuales y medio mineral, fueron cosechadas y liofilizadas. Los diferentes tipos de biomasa seca fueron luego sometidas a una serie de extracciones para separar los compuestos bioquímicos en diferentes fracciones, todas con grados variables de accesibilidad, para microorganismos del suelo, y complejidad. Los resultados de esta sección demostraron que los flóculos sueltos procedentes de la primera parte experimental eran poco extraíbles, con más del 50% de su contenido de materia orgánica, nitrógeno y fósforo considerado no extraíble. Sin embargo, su extractabilidad fue mejorada cuando se sometieron a condiciones limitadas de nitrógeno, donde menos del 10% del contenido de materia orgánica, nitrógeno y fósforo se consideró no extraíble.

En conjunto, los resultados de este trabajo proporcionaron una base científica para el tratamiento simultáneo de aguas residuales y la producción de polihidroxicarboxilatos en aguas residuales municipales bajo condiciones ambientales. En general, las cepas de microalgas procedentes de efluentes o aguas dulces pueden producir polihidroxicarboxilatos bajo limitación de nitrógeno. Sin embargo, es necesario incorporar protocolos de control de oxígeno para maximizar la producción de polihidroxicarboxilatos en medio mineral y efluente de aguas residuales municipales. Se observó además que la biomasa de microalgas-bacterias con baja producción de polihidroxicarboxilatos bajo limitación de nitrógeno es una fuente inherente de materia orgánica, nitrógeno y fósforo accesibles para los microorganismos del suelo, ofreciendo un proceso alternativo.

Table of Contents

Acknowledgments	i
Summary	ii
Resumen	v
Table of Contents	viii
List of Figures	xi
List of Tables	xiv
1. General Introduction	1
2. Background	4
2.1. Basic theoretical concepts	5
2.1.1. Wastewater treatment	5
2.1.2. Producing biopolymers from microalgae-bacteria consortia	11
2.1.3. Microalgae-bacteria as a platform for polyhydroxybutyrate production	13
2.1.4. Valorization of microalgae-bacteria biomass as biofertilizers	19
2.2. Postulates.....	21
2.3. Hypothesis	22
2.3.1. General hypothesis	22
2.3.2. Specific hypotheses	22
2.4. Objectives.....	23
2.4.1. General objective.....	23
2.4.2. Specific objectives.....	23
2.5. Work strategy	24
3. Assessment of polyhydroxyalkanoates and polysaccharides production in native phototrophic consortia under nitrogen and phosphorous-starved conditions	27
Abstract.....	28
3.1. Introduction	29
3.2. Materials and methods	31
3.2.1. Source of photoautotrophic biomass	31

3.2.2.	Obtention of polymer-storing photoautotrophic consortia.....	32
3.2.3.	Evaluation of growth and enhancement of polymer production in enriched mixed consortia	33
3.2.4.	Analytical measurements	34
3.3.	Results and discussion.....	35
3.3.1.	Culturing of photosynthetic biomass.....	35
3.3.2.	Enrichment of consortia with polymer-accumulating algae	36
3.3.3.	Evaluation of growth and polymer production enhancement in enriched mixed consortia	38
3.4.	Conclusion.....	42
4.	Municipal wastewater treatment and polyhydroxybutyrate production using <i>Synechocystis</i> sp. under oxygen-controlled conditions	43
	Abstract.....	44
4.1.	Introduction	45
4.2.	Materials and methods	47
4.2.1.	Strain and inoculum preparation	47
4.2.2.	Experimental setup and cultivation conditions	47
4.2.3.	Analytical procedures.....	49
4.2.4.	Statistical analysis	50
4.3.	Results and discussion.....	51
4.3.1.	Growth performance and photosynthetic activity of <i>Synechocystis</i> sp. in mineral medium.....	51
4.3.2.	PHB analysis in the cultures of <i>Synechocystis</i> sp. grown in mineral medium.....	53
4.3.3.	Evaluation of <i>Synechocystis</i> sp. performance grown in municipal wastewater.....	55
4.4.	Conclusion.....	60
5.	Bioaccessibility characterization of organic matter, nitrogen, and phosphorus from microalgae-bacteria aggregates.....	61
	Abstract.....	62
5.1.	Introduction	63
5.2.	Materials and methods	65
5.2.1.	Origin, morphology, and preparation of microalgae-bacteria aggregates samples..	65

5.2.2. Assessment of total organic matter, total nitrogen, and total bioavailable phosphorus content...	66
5.2.3. Sequential chemical extraction for organic matter, nitrogen, and phosphorus fractions characterization	67
5.2.4. Fluorescence spectroscopy analysis for molecular complexity characterization.....	68
5.2.5. Statistical analyses.....	69
5.3. Results and discussion.....	69
5.3.1. Morphology of microalgae-bacteria aggregates samples.....	69
5.3.2. Total organic matter, total nitrogen, and total bioavailable phosphorus content in microalgae-bacteria aggregates	71
5.3.3. Extractable fractions of organic matter, nitrogen, and phosphorus in microalgae-bacteria aggregates	73
5.3.4. Effect of starvation	76
5.3.5. Complexity of microalgae-bacteria aggregates.....	78
5.4. Conclusion.....	80
6. General conclusion and future perspectives	81
References	84
Thesis products	108
Supplementary material	111
Figures	112
Tables.....	114
Methods	119
Polyhydroxyalkanoates content using gas chromatography	119
Polyhydroxyalkanoates using Nile red fluorescent staining	121
Polysaccharides content using phenol-sulfuric method.	121
Storage of photoautotrophic microorganisms	123

List of Figures

Figure 2.1. Process flow diagram for wastewater treatment using conventional activate sludge process.	6
Figure 2.2. Schematic representation of microalgae and bacteria mutualistic interaction.	10
Figure 2.3. Molecular structure and main types of polyhydroxyalkanoates based on the number of carbon atom ($n = 1$ to 2), with R representing possible alkyl functional group and X representing the repeating monomeric units, ranging from 100 to 30,000.	14
Figure 2.4. Fundamental pathways related to starch, glycogen, and polyhydroxybutyrate biosynthesis in eukaryotic microalgae and cyanobacteria under nitrogen limitation. Solid arrows represent one step reactions, while dotted arrows represent stepwise reactions. Metabolites: GP, Glycerate 3-phosphate; 1,3BPG, 1,3-Bisphosphoglycerate; GAP, 3-phosphoglyceraldehyde; FBP, Fructose 1,6-biphosphate; F6P, Fructose 6-phosphate; X5P, Xylulose 5-phosphate; Ru5P, Ribulose 5-phosphate; RuBP, Ribulose 1,5-biphosphate; 3-HB-CoA, (S)-3-Hydroxybutyryl Coenzyme A; ACT, aconitate; ICIT, isocitrate; 2-OG, α -ketoglutarate; Suc-CoA, Succinyl-CoA; Suc, Succinyl; FUM, fumarate; MAL, malic acid; OAA, oxaloacetic acid. Enzymes: Rubisco, ribulose 1,5-bisphosphate carboxylase; PGK, 3-phosphoglycerate kinase; GAPDH, glyceraldehyde 3-phosphate dehydrogenase; FBA, Fructose-bisphosphate aldolase; FB Pase, fructose 1,6-bisphosphatase; TKL, transketolase; RPE, ribulose 5-phosphate 3-epimerase; PRK, phosphoribulokinase. GPI, phosphoglucose isomerase; PGM, phosphoglucomutase; AGPase, ADP-glucose pyrophosphorylase; UDPase, UGP-glucose pyrophosphorylase; SS, starch synthases; GS, glycogen synthases; SP, starch phosphorylase; GP, glycogen phosphorylase; ENO, enolase; PK, pyruvate kinase; PDHC, pyruvate dehydrogenase complex; PHA-A Acetyl-CoA acetyltransferase; PHA-B Acetoacetyl-CoA reductase; PHA-C PHA synthase; CS, citrate synthase; AHD, aconitate hydratase; ICDH, isocitrate dehydrogenase; OGDH, 2-oxoglutarate dehydrogenase; SDH, succinate dehydrogenase; FHD, fumarate hydratase; MDH, malate dehydrogenase.	16
Figure 2.5. Extracted chemical fractions and their common biochemical composition from the stability and bioaccessibility prediction model (ISBAMO).	20
Figure 2.6. Work strategy diagram.	26
Figure 3.1. Microscopic images illustrating the microbial composition of (a) non-axenic <i>Chlorella</i> consortium observed in bright field visible light microscope at 40X; (b) the microbial composition	

of predominantly photoautotrophic consortium observed in bright field visible light microscope at 40X; (c) polymer accumulating *Chlorella* strains in non-axenic *Chlorella* consortium observed under fluorescence microscope at 40X after straining with Nile red dye; (d) polymer accumulating *Chlorella* and unicellular cyanobacteria strains in predominantly photoautotrophic consortium observed under fluorescence microscope at 40X after straining with Nile red dye.....37

Figure 3.2. Biomass concentration during *Chlorella sorokiniana* dominated consortium (a) and mixed photosynthetic consortium (b) cultures in nutrient unbalanced growth medium. Error bars represent standard deviation of the mean value.39

Figure 3.3. Changes in PHA (X) and polysaccharides (Δ) values *Chlorella sorokiniana*-dominated consortia (a) and mixed photosynthetic consortium (b) cultures in nutrient unbalanced growth medium. Error bars represent standard deviation of the mean value.41

Figure 3.4. Phosphorous and dissolved inorganic carbon (DIC) dynamics for (a) *C. sorokiniana*-dominated consortium and (b) mixed photosynthetic consortium cultures under nutrient stressed conditions. Bold lines represent time intervals were phosphorous was added. Error bars represent standard deviation of the mean value.42

Figure 4.1. Boxplot showing the dissolved oxygen concentration measured in *Synechocystis* sp. cultures during mineral medium trials. The lower boundary of the box indicates the 25th percentile, a line within the box marks the median, and the upper boundary of the box indicates the 75th percentile. Whiskers (error bars) above and below the box indicate the 90 and 10th percentiles, respectively. Black circles indicate the mean value. Nitrogen addition (+N) and nitrogen-limited (-N).....48

Figure 4.2. Changes in the (a) biomass concentration and (b) photosynthetic activity of *Synechocystis* sp. cultures during the growth stage and the accumulation stage.53

Figure 4.3. PHB content in *Synechocystis* sp. cultures during growth and accumulation stages in the mineral medium.....54

Figure 4.4. Boxplot showing the dissolved oxygen concentration in wastewater and in cultures of *Synechocystis* sp. in wastewater during growth and accumulation stages. The lower boundary of the box indicates the 25th percentile, a line within the box marks the median, and the upper boundary of the box indicates the 75th percentile. Whiskers (error bars) above and below the box indicate the 90 and 10th percentiles, respectively. Black circles indicate the mean value.56

Figure 4.5. Monitoring of (a) biomass growth and (b) photosynthetic activity in *Synechocystis* sp. cultures performed in municipal primary effluent during growth and accumulation stages.59

Figure 4.6. PHB content in *Synechocystis* sp. cultures during growth and accumulation stages using municipal wastewater.60

Figure 5.1. Representative images of (a) loose flocs, (b) consolidated flocs, (c) smooth granules, and (d) filamentous granules.70

Figure 5.2. Contribution of each extracted biochemical fraction to the total organic matter (TOM), total nitrogen (TN), and total bioavailable phosphorus (TBP) in loose flocs (LF), consolidated flocs (CF), smooth granules (SG), and filamentous granules (FG).74

Figure 5.3. Contribution of each extracted biochemical fraction to the total organic matter (TOM), total nitrogen (TN), and total bioavailable phosphorus (TBP) observed for loose flocs and filamentous granules before and after starvation conditions.77

Figure 5.4. Fluorescence complexity index (FCI) for the different biochemical fractions from loose flocs and filamentous granules before and after starvation conditions.79

Figure S3.1. Microscopic imaging of non-stressed polymer accumulating photoautotrophic strains observed under fluorescence microscope at 40X after straining with Nile red dye. Any observed fluorescence, only a dark field.112

Figure S3.2. Indoor cultivation of *C. sorokiniana* dominated consortium in FP-PBR under nutrient-rich (left) and nutrient-unbalanced (right) conditions. Note yellowish color.113

List of Tables

Table 2.1. Operating parameters for activated sludge processes in municipal wastewater treatment facilities.	7
Table 2.2. Operating parameters for microalgae-bacteria based wastewater treatment.....	9
Table 2.3. Biomass composition of some microalgae species, expressed as percentage of dry cell weight (% dCW).....	11
Table 2.4. Physical and thermal properties of polyhydroxybutyrate and their comparison with petroleum-based plastics.	17
Table 2.5. Dominant species and average polyhydroxybutyrate production in microalgae-bacteria consortia cultivated in waste streams under photoautotrophic conditions.	18
Table 3.1. Characteristics of growth medium used for photoautotrophic biomass generation. All values are the means of independent replicates ($n=2$) \pm standard deviation.	32
Table 3.2. Biomass concentration growth rate and biomass productivity in each culture. All values are mean of independent replicates ($n=2$) \pm standard deviation.....	39
Table 5.1. Physical and morphological characteristics of microalgae-bacteria aggregates. See Figure 1 for representative images of the different sample types.	70
Table 5.2. Total organic matter (TOM), total nitrogen (TN), and total bioavailable phosphorus (TBP) in different microalgae-bacteria aggregates. Lowercase letters indicate significant differences ($p \leq 0.05$) between samples for each parameter.	71
Table S5.1. Organic matter content in each fraction extracted from microalgae-bacteria aggregates. Lowercase letters indicate whether there are significant differences ($p \leq 0.05$) between fractions extracted for each sample. Percentage in terms of Total Organic Matter content.	114
Table S5.2. Nitrogen content in each fraction extracted from microalgae-bacteria aggregates. Lowercase letters indicate whether there are significant differences ($p \leq 0.05$) between fractions extracted for each sample. Percentage in terms of Total Nitrogen content.....	115
Table S5.3. Total bioavailable phosphorous content in each fraction extracted from microalgae-bacteria aggregates. Lowercase letters indicate whether there are significant differences ($p \leq 0.05$) between fractions extracted for each sample. Percentage in terms of Total Bioavailable Phosphorous content.	116

Table S5.4. Initial concentration of the BG-11 growth medium used for the cultivation of loose flocs under nutrient reduced conditions for bioaccessibility of organic matter, nitrogen, and phosphorous and molecular complexity assessment. 117

Table S5.5. Initial concentration of the nitrate mineral salt growth medium used for the cultivation of filamentous granules under nutrient reduced conditions for bioaccessibility of organic matter, nitrogen, and phosphorous and molecular complexity assessment. 118

1. General Introduction

Valuable bioproducts, like bioplastics and biofertilizers, from microalgae have attracted much interest because of their potential to replace petroleum-based products and their well-known drawbacks. Today, the cultivation and use of photoautotrophic microorganisms like eukaryotic microalgae and cyanobacteria (prokaryotic microalgae) have received increasing scientific attention. This is due to their ability to grow in waste effluents and their propensity to create and store intracellular polymers of interest like polyhydroxyalkanoates (PHAs). These intracellular polymers are becoming increasingly popular due to their potential for bioplastic production (Park and Lee, 2023; Chong et al., 2022). The primary interest in photoautotrophic microorganisms that produce PHAs stems from their ability to store carbon through oxygenic photosynthesis, which implies minimal culture needs and the use of carbon dioxide as a carbon source.

Most studies on the production of PHAs from photoautotrophic microorganisms generally employ pure or genetically modified cultures of cyanobacteria under nitrogen limitation (Price et al., 2020). Compared to eukaryotic microalgae, cyanobacterial cells have an incomplete Krebs cycle that allows them to store excess intracellular carbon, *i.e.*, Acetyl-CoA, and reduction equivalents, *i.e.*, NADPH, in the form of PHAs (De Philippis et al., 1992). However, the strictly controlled processes in pure and genetically modified cultures often lead to high production costs and, thus, expensive products. Therefore, wastewater-borne mixed cultures could be a more sustainable alternative to produce PHAs derived from cyanobacteria. The utilization of mixed cultures to produce biomass and polymers implies the lack of sterilization of substrates or reactors and the use of cheaper equipment that could ultimately help reduce the production costs compared to pure or genetically processes. However, growing cyanobacteria in such a variable media implies certain disadvantages, including competition with other microorganisms, *e.g.*, eukaryotic microalgae and heterotrophic bacteria, and nitrogen and phosphorus concentration.

In recent years, several authors have obtained PHAs producing mixed cultures, mostly cyanobacteria, following a two-phase or two-stage approach (Arias et al., 2019; Rueda et al., 2020a). This operation scheme benefits from nitrogen limitation in producing up to 69 mg PHA L⁻¹ (5% as dried cell weight (dCW)) using wastewater (Senatore et al., 2023). Nonetheless, no further studies have focused on improving PHAs production using other abiotic stress factors. Therefore, this manuscript aims to evaluate low dissolved oxygen concentrations and nitrogen limitation to maximize PHAs and biomass production of microalgae-bacteria consortia in municipal wastewater.

Chapter 2 delves into the basic theoretical concepts that govern wastewater treatment and PHAs production utilizing microalgae-bacteria consortia. This chapter also outlines the pertinent postulates that serve as the foundation for the hypotheses of the present research work. In turn, these hypotheses pave the way for formulating a general objective and specific objectives that provide direction and purpose to the investigation. A comprehensive work strategy that details the experimental design employed throughout the investigation is also outlined.

In Chapter 3, PHA producing microalgae species were obtained from mixing activated sludge (AS), as inoculum, and primary effluent, as growth substrate. These waste effluents were sampled from a municipal wastewater treatment plant located in Queretaro, Mexico. Another inoculum from freshwater sources (*Chlorella sorokiniana* dominated) was assessed for PHA production under nitrogen-limited conditions. The former parameter was assessed in the microalgae consortia to confirm the conversion of polysaccharides to PHA. The former parameter was assessed in the microalgae consortia to confirm the conversion of polysaccharides to PHA.

Chapter 4 was dedicated to maximizing the production of PHA in microalgae by manipulating nitrogen and dissolved oxygen concentration in a mineral medium. Due to the low PHA production, and thus high polysaccharides production, obtained in microalgae consortia from Chapter 3, a PHA-producing species (*Synechocystis* sp.) was acquired and tested to confirm these conditions as maximizing conditions in mineral medium (BG-11). Following the confirmation of the best performing conditions for PHA production in microalgae using a mineral medium, the efficacy of these conditions was assessed for simultaneous PHA production and wastewater treatment, *i.e.*, nutrient removal, using municipal primary effluent from a municipal wastewater treatment plant located in Queretaro, Mexico.

In Chapter 5, further experiments were dedicated to valorizing the resulting microalgae biomass from Chapter 3 based on the low PHA production. Given the high polysaccharides production in the biomass, the obtained biomass was subjected to sequential chemical extraction based on ISBAMO (Index of Stability and Bioaccessibility of Organic Matter) and modified P-Olsen. These allowed the quantification of biomass organic matter, nitrogen, and phosphorus content for potential fertilization of soils. Different morphological types of microalgae consortia structures were also evaluated with these methods to determine important variations in organic matter, nitrogen, and phosphorus content. Finally, Chapter 6 culminates with a major conclusion based on the findings obtained in this thesis, along with suggestions and insights for future research.

2. Background

2.1. Basic theoretical concepts

2.1.1. Wastewater treatment

The science and engineering of wastewater treatment has notably evolved over the last century. Initially, the main purpose of wastewater treatment was to remove suspended solids and pathogens, which was typically achieved through unit processes such as settling tanks and trickling filters (Riffat and Husnain, 2022). The onset of industrialization and scientific progress further unveiled the presence of a diverse array of contaminants in wastewater, including organic and inorganic pollutants, toxic chemicals, and other harmful compounds. The nature of these contaminants not only varied based on wastewater origin, *e.g.*, municipal, industrial, or agricultural, but also posed new challenges on wastewater discharge practices. Discharging wastewater without proper treatment in lands or water bodies leads to severe pollution problems, with eutrophication being a prominent concern (Chen et al., 2020). Eutrophication involves the prompt growth of harmful water plants (*e.g.*, microalgae) caused by the sustained increase of the concentration of nutrients like nitrogen and phosphorus. This phenomenon renders water bodies hazardous for aquatic life and compromises their suitability for drinking water purposes (Akinawo, 2023). These insights promptly expanded the goals of wastewater treatment to encompass the removal or reduction of a broader spectrum of contaminants, including organic matter and nutrients. To address these new challenges, modern wastewater treatment plants typically employ a combination of physical (or primary), biological (or secondary), and chemical (or tertiary) unit processes. However, the continuous evolution of technology and the increasing complexity of contaminants in wastewater imposed an enhancement on the efficiency of biological treatment units.

Conventional Activated Sludge

Conventional Activated Sludge (CAS) unit process was first developed for biological wastewater treatment in the early 20th century by combining aerobic conditions and suspended growth of wastewater-borne microorganisms. Since then, CAS has become the dominant biological treatment unit process in municipal and industrial wastewater treatment plants worldwide (Wanner, 2021). In Mexico, the 2021 National Inventory of Municipal Water and Wastewater Plants in Operation showed that CAS systems were present in 818 out of 2872 municipal wastewater treatment plants, treating nearly 75% of wastewater influent (CONAGUA, 2021).

To gain a basic understanding of the CAS systems as a secondary treatment, Figure 2.1 depicts its two pivotal units: the aeration tank and the secondary clarifier. Fundamentally, the primary wastewater effluent is continuously flow into the aeration tank, where oxygen is introduced through air diffusers or impellers. This ensures the maintenance of aerobic conditions that along the organic matter and nutrients derived from the wastewater, stimulate the proliferation of diverse microorganisms, including bacteria, fungi, protozoa, ciliates, rotifers, etc. During growth, these microorganisms not only consume organic matter, nitrogen, and phosphorus but also aggregate with each other and with suspended solids, forming cohesive clumps that resemble sludge. This sludge-like mixture is then directed to the secondary clarifier, where clarification of effluent and thickening of settled solids takes place. The clarified effluent is discharged for further treatment (*i.e.*, tertiary treatment) or disposal. In contrast, a portion of thickened solids (20 – 50%) is recycled back to the aeration tank to maintain a high concentration of active biomass in the aeration tank (Riffat and Husnain, 2022). The remaining portion of the thickened solids are removed from the process as secondary sludge and led to a sludge management and treatment process. This residual sludge could be disposed in landfills or used as feedstock for anaerobic digesters to generate electricity and compost (Ferrentino et al., 2023).

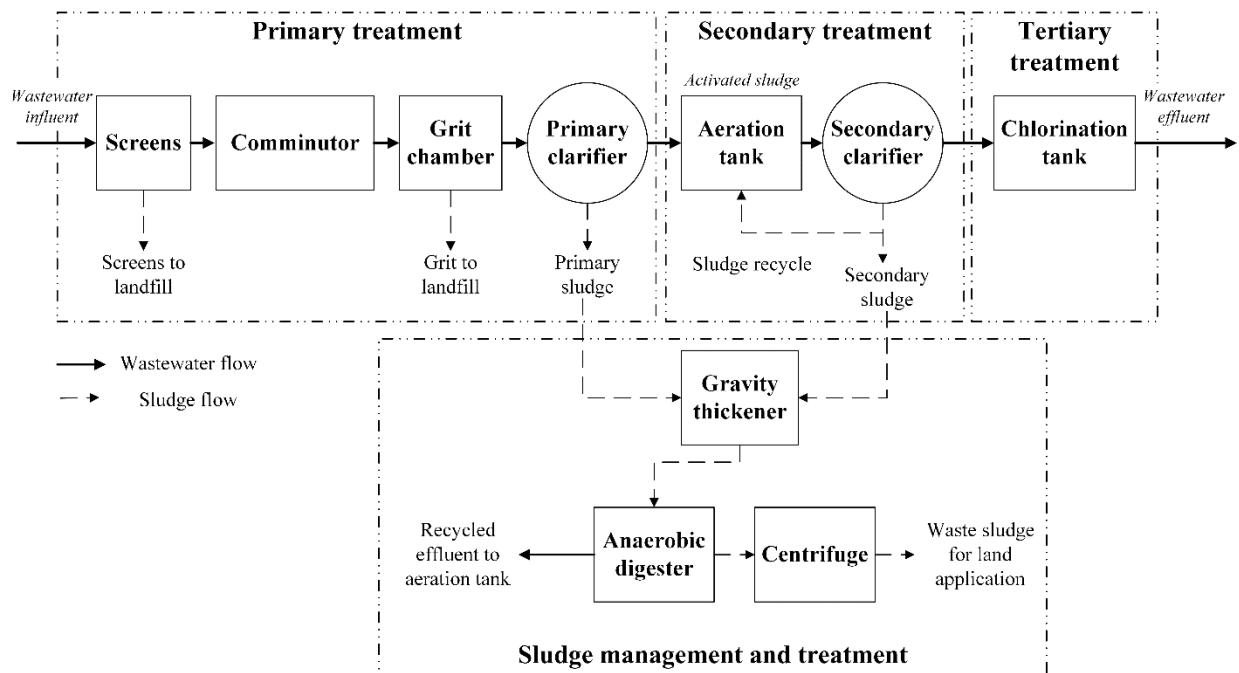


Figure 2.1. Process flow diagram for wastewater treatment using conventional activate sludge process.

Operating parameters play a crucial role in the effectiveness of CAS systems. Their monitoring and control are important to uphold a favorable environment for aerobic, heterotrophic bacteria and ensure an optimal operation of the AS (Shukla and Ahammad, 2022). Table 2.1. explains the typical values for some important operating parameters and their effects on municipal wastewater treatment facilities using CAS systems.

Table 2.1. Operating parameters for activated sludge processes in municipal wastewater treatment facilities.

Parameter	Values	Effect	References
pH	6.5 – 7.5	Improve enzymatic activity of microorganisms. Inhibit fungi growth.	Tchobanoglous et al. (2014)
Temperature	25 °C	Improve enzymatic activity of microorganisms, gas transfer rates, and settling characteristics.	Riffat & Husnain (2022)
Dissolved oxygen (DO)	1.5 – 2.0 mgO ₂ L ⁻¹	Improve nitrification/denitrification and organic matter mineralization.	Tchobanoglous et al. (2014)
Hydraulic retention time (HRT)	3 – 8 h	Improve nitrogen removal and organic matter mineralization rates	Khalaf et al. (2021)
Solids retention time (SRT)	4 – 15 d	Allow aerobic, heterotrophic bacteria dominance. Formation of settleable flocs.	Khalaf et al. (2021)
Food to microorganism ratio (F/M)	0.2 – 0.4	Ensure microorganisms in the sludge are at the end of the stationary phase	Riffat & Husnain (2022)
Volumetric loading rate (V _L)	0.8 – 2.0 kg BOD ₅ m ⁻³ d ⁻¹	Avoid foaming in the aeration tank. Allow constant and predictable outcomes.	Ahnert et al. (2021)

In recent decades, CAS systems have failed to comply with increasingly stringent environmental and water reclamation regulations across the world. A case study in Mexico demonstrated the need of modernizing municipal wastewater treatment facilities with innovative technology to meet the 2030 United Nations Climate Action and Water Agenda (Noyola et al., 2016). The findings of this study projected a scenario where new municipal wastewater treatment

plants that adopted CAS systems would increase carbon dioxide emissions from 726 to 1731 Gg CO₂ eq. due to the power demand. This is problematic since the AS process alone contributes for up to 94% of the total greenhouse gas emissions from wastewater treatment plants (Lu et al., 2022). More importantly, the incorporation of additional steps or processes like nitrification/denitrification, anammox, and chemical precipitation into CAS systems were deemed as needed to address the higher organic load. This render the systems more complex, expensive, and energy-intensive (Aditya et al., 2022). Therefore, moving towards wastewater technologies that also consider resource recovery becomes critical. Water recovery, together with the extraction of added-value bioproducts, appears to be a potential approach to reducing greenhouse gas emissions and increasing wastewater treatment profitability (Chen et al., 2020). In this transformative context, numerous possibilities are emerging, reshaping the landscape of wastewater treatment plants using CAS systems for the near future.

Microalgae-bacteria consortia for wastewater treatment

Microalgae are a diverse group of microorganisms that can assimilate dissolved nutrients through oxygenic photosynthesis. These photosynthetic microorganisms include eukaryotic microalgae as well as photosynthetic prokaryotes (cyanobacteria) which can be found in almost every habitat. In particular, cyanobacteria have gained much attention in recent years for their role in cost-effective and sustainable biological wastewater treatment as well as for a variety of commercial applications like biofuel production and bioplastics (Agarwal et al., 2022). That interest stems from the natural metabolic pathway of some cyanobacteria genera, like *Synechocystis*, *Synechococcus*, *Anabaena*, etc., that results in economically useful value-added compounds like glycogen and PHAs (Arias et al., 2020). Moreover, the benefits of cyanobacteria also extend to their inherent adaptability to a wide diversity of aquatic habitats, where they form associations (consortia) with aerobic, heterotrophic bacteria (Quijano et al., 2017). These consortia provide both cyanobacteria and aerobic, heterotrophic bacteria with essential nutrients for their growth, leading to enhanced removal rates of nitrogen, phosphorus, organic matter, etc.

The concept of incorporating eukaryotic microalgae and cyanobacteria (hereafter simply microalgae) into wastewater treatment has undergone significant redesign to align with increasingly stringent environmental regulations and economic demands (Acién et al., 2017). Like CAS systems, the effectiveness of microalgae-bacteria-based wastewater treatment is contingent

upon various parameters outlined in Table 2.2, which collectively determine their overall treatment efficiency and success. Thus far, the largest commercial-scale demonstration of microalgae-bacteria based wastewater treatment potential is in Chiclana de la Frontera, Spain (Acién et al., 2017). The raw discharges from 60,000 inhabitants (*i.e.*, $\sim 3000 \text{ m}^3 \text{ d}^{-1}$) is treated not only to meet the strict quality standards set by the European Directive 91/271/CE but also to support the production of biogas and biofertilizers. The overall success of that microalgae-bacteria based wastewater treatment plant further expanded the implementation of demo scale facilities in Mexico (Montaño San Agustín et al., 2022) and China (Acién et al., 2017).

Table 2.2. Operating parameters for microalgae-bacteria based wastewater treatment.

Parameter	Values	Effect	References
pH	6.0 – 8.0	Crucial for microalgae metabolism and uptake of ions	Vuppaladadiyam et al. (2018)
Temperature	18 – 30 °C	Improves cellular, physiological, and morphological responses of microalgae cultures	Vuppaladadiyam et al. (2018)
Dissolved oxygen (DO)	$\leq 7.8^b$ $\text{mgO}_2 \text{ L}^{-1}$	Improves photosynthesis and carbon dioxide fixation	Raso et al. (2012)
Light intensity	20 – 400 ^a $\mu\text{mol m}^{-2} \text{ s}^{-1}$	Accelerates growth kinetics of algae cultures	Maltsev et al. (2021)
Nutrient feed	100:49-16:1 molar ratio	Determines growth kinetics of algae cultures and cellular metabolism	Arias et al. (2019)

^a Within the 400-700 nm light spectrum; ^b Representing 100% oxygen-air saturation

The overall effectiveness of microalgae-bacteria wastewater treatment relies on the symbiotic or mutualistic interaction between these microorganisms, as illustrated in Fig. 2.2. During the photoautotrophic growth of microalgae, dissolved nutrients in wastewater are assimilated and transformed into oxygen and new biomass. The evolved oxygen provides chemical energy for bacteria to mineralize organic matter, whose byproducts continue to sustain the photoautotrophic growth of microalgae. Simultaneously, the resulting microalgal biomass becomes a source of high added value products for numerous biotechnological applications, including bioenergy generation, biofertilizer and bioplastics production, etc. (Siddiki et al., 2022).

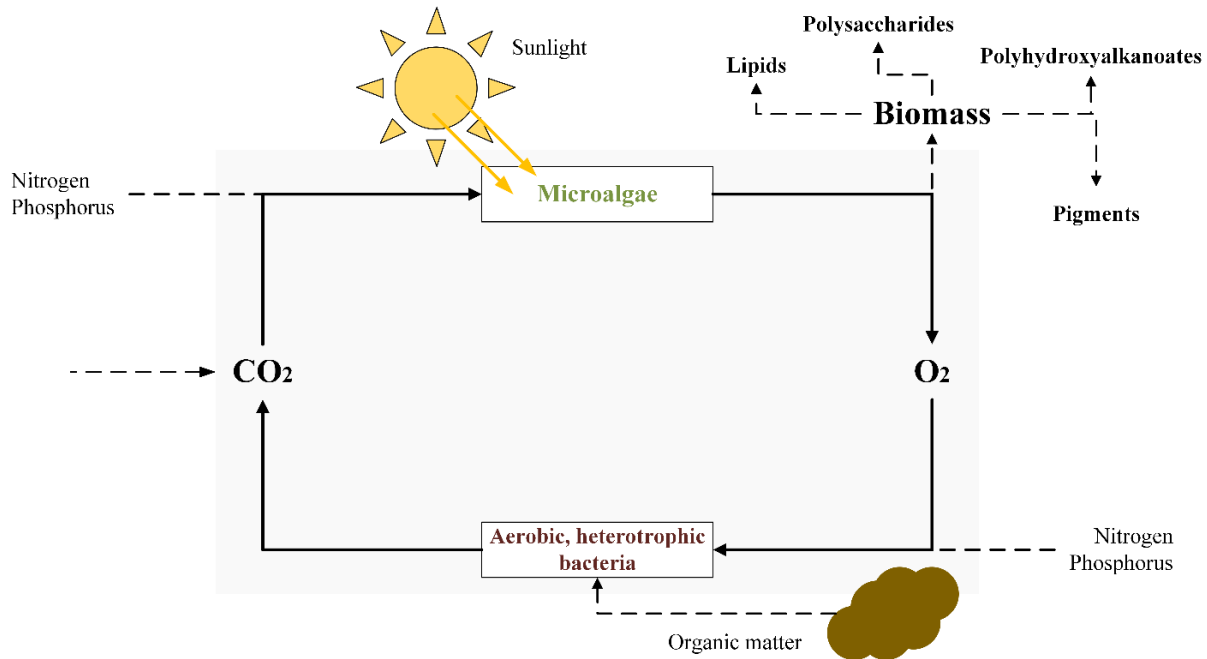


Figure 2.2. Schematic representation of microalgae and bacteria mutualistic interaction.

Remediation of municipal wastewater using microalgae-bacteria consortia has proven to be a complete solution in addressing the complex nature of municipal wastewater. Raw municipal wastewater typically contains 50 to 650 mg L⁻¹ of total nitrogen and 10 to 15 mg L⁻¹ of phosphate (Aditya et al., 2022). These render conventional biological treatment of municipal wastewater particularly challenging. Previous studies have demonstrated the highly efficient removal rates of organic matter (94% as chemical oxygen demand), nitrogen (99% as ammonia, 72% as nitrate), and phosphorus (68% as phosphate) of microalgae-bacteria consortia (Barreiro-Vescovo et al., 2021; Buitrón and Coronado-Apodaca, 2022; dos Santos Neto et al., 2023). These removal efficiencies are superior to those of biological treatment units based on CAS systems, where only up to 90%, 50%, and 30% of organic matter, total nitrogen, and total phosphorus are removed (Güven et al., 2019; Yu et al., 2009). Moreover, microalgae biomass production from wastewater allows to produce up to 1.0 kg per m³ of municipal wastewater at a lower energy consumption and cost when compared to CAS systems (Acién et al., 2016). Despite the evident success of microalgae-bacteria consortia, widespread adoption of microalgae-bacteria based wastewater treatment technologies has been consistently hindered by some key operational challenges. Prioritizing cost-effective transformation of microalgae biomass into high value bioproducts could

increase the overall viability and economic feasibility of microalgae-bacteria consortia (Saratale et al., 2022), thereby broadening their application in wastewater treatment.

2.1.2. Producing biopolymers from microalgae-bacteria consortia

The transformation of microalgae-bacteria biomass into high value bioproducts is dependent on its inherent composition. Biopolymers, which are naturally occurring long chain molecules composed of repeating monomeric units, are the main components of biomass produced from microalgae-bacteria based wastewater treatment. A broad array of biopolymers can be extracted from microalgae biomass, including proteins, carbohydrates, and lipids. The proportions for each of these biopolymers depend on the dominant strains and cultivation conditions (*e.g.*, light intensity, nutrient availability, temperature, etc.). This highly flexible biopolymer content has elevated microalgae-bacteria biomass status as an important feedstock for different industries. Biomass profiles of some microalgae species relevant for wastewater treatment and high value bioproducts generation are compiled in Table 2.3.

Table 2.3. Biomass composition of some microalgae species, expressed as percentage of dry cell weight (% dCW).

Microalga specie	Protein (% dCW)	Carbohydrates (% dCW)	Lipid (% dCW)	References
<i>Chlorella vulgaris</i>	38 – 53	8 – 27	5 – 28	Bernaerts et al. (2019) Razzak et al. (2022)
<i>Scenedesmus obliquus</i>	19 – 21	63 – 69	9 – 14	de Oliveira et al. (2020)
<i>Spirulina platensis</i>	43 – 77	8 – 22	4 – 14	Bernaerts et al. (2019) Razzak et al. (2022)
<i>Synechococcus elongatus</i>	52 – 63	11 – 14	11 – 15	González-Resendiz et al. (2021)
<i>Synechocystis</i> sp.	25 – 66	9 – 35	15 – 27	Paliwal et al. (2015)

Proteins are a family of biopolymers made of an array of amino acids. As seen in Table 2.3, these biopolymers can be found in high amounts for most microalgae species. Proteins play an important role in the catalytic mechanisms that allow microalgae to thrive. These mechanisms

include proteins that are involved in oxygenic photosynthesis like ribulose-1,5-bisphosphate carboxylase/oxygenase (RuBisCO) enzyme, in the pyrenoid of eukaryotic microalgae, and phycobiliproteins, in the thylakoids of cyanobacteria (Safi et al., 2014). Moreover, proteins have also been observed to supply scaffolds for the assembly of chlorophyll molecules and the harvesting chloroplast complexes (Razzak et al., 2022). Regardless of their physiological function, the commercial value of proteins rests on their apparent nutritional value. Becker (2013) observed that microalgae species like *Chlorella vulgaris* and *Spirulina platensis* exhibited favorable amino acid profiles and a good digestibility as a nutrient supplement for human nutrition.

Carbohydrates also constitute another important portion of microalgal biomass. Unlike proteins, these biopolymers are made of different monomeric units of sugars (*i.e.*, monosaccharides). In microalgae, carbohydrates typically exist in various chemical forms and can be categorized according to their physiological function. Storage carbohydrates are located inside the microalgae cell and are used as energy sources to drive the metabolic processes or act as protectants for the survival under stress (Shahid et al., 2020). Starch (in eukaryotic microalgae) and glycogen (in cyanobacteria) are notable examples of storage carbohydrates. On the contrary, structural carbohydrates (*i.e.*, cell wall bound carbohydrates) provide structural support and include monosaccharides, uronic acids, amino sugars, and cellulose (Bernaerts et al., 2019). Bioproducts made from structural carbohydrates are very scarce, likely related to the difficult extractability and low content, *i.e.*, ~ 7% of the total carbohydrate content (Zanchetta et al., 2021). However, starch and glycogen display a versatile functionality as a valuable resource for bioethanol and bioplastics production (López Rocha et al., 2020), with a lot of potential for commercialization.

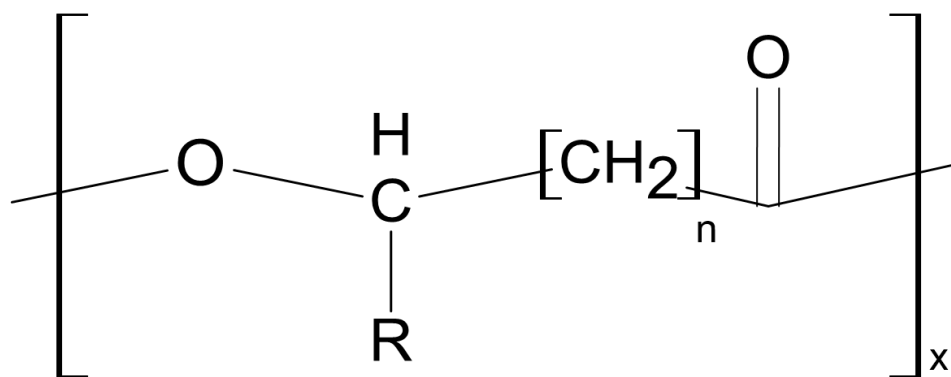
Lipids are a distinct class of biopolymers that are mostly made of fatty acids or their derivatives. These can be divided as polar and non-polar lipids with important physiological roles (Alishah Aratboni et al., 2019). Polar lipids are usually located in the cellular membrane and include phospholipids and glycolipids. These lipids have special roles in the optimal maintenance of membrane fluidity for a variety of metabolic and biosynthetic processes. In contrast, non-polar lipids are found within microalgae cells and are mostly made up of triglycerides, as well as pigments, vitamins, and hydrocarbons (Razzak et al., 2022). Non-polar lipids like triglycerides are typically used as an energy storage molecule within the microalgae cell. These are also key components in the manufacture of biodiesel, eicosapentaenoic acid, and docosahexaenoic acid (Chandra et al., 2019). Microalgae biomass rich in linolenic acid and oleic acid fatty acids can also

be used for nutritional and therapeutic purposes (Aditya et al., 2022). However, the detection of other lipid-like biopolymers has further expanded their application within the bioplastic industry.

2.1.3. Microalgae-bacteria as a platform for polyhydroxybutyrate production

PHAs are a group of naturally occurring polyesters which have received growing attention as an alternative to fossil-based plastics. According to Llewellyn et al. (2019), these polyesters have been commonly been produced using Gram-negative bacteria like *Pseudomonas*, *Ralstonia*, and *Alcaligenes* through heterotrophic fermentation. That method utilizes pure organic carbon sources, which enables fermentative bacteria to produce as much as 80% dCW or 4.0 g L⁻¹ of PHAs (Budde et al., 2011). Moreover, the heterotrophic fermentation is easily scalable for large-scale production due to its minimal infrastructure requirements and well-established process (Hermann et al., 2020). However, challenges remain on the overall sustainability and economic viability of PHAs derived from bacterial fermentation. One major hurdle lies in the high cost of the substrate, which can account for up to 40% of the total production cost for PHAs (Lopez-Arenas et al., 2017). Fermentative bacteria also rely on highly controlled and sterilized environments to produce PHAs, which limits their adaptability to alternative feedstocks and process conditions.

Microalgae-bacteria consortia, particularly those composed mostly of cyanobacteria, are emerging as an alternative host system to address the limitations of traditional PHAs production methods. Essentially, cyanobacteria have minimal nutrient requirements and the ability to accumulate PHAs by oxygenic photosynthesis, giving them the potential to grow in waste effluents (Mastropetros et al., 2022). In cyanobacteria, PHAs are produced as a response to physiological stress, including nitrogen limitation or excess reducing power from oxygen depletion, and are commonly deposited as intracellular granules (Cinar et al., 2020). Depending on the structure and length of carbon atoms that make up the functional group, PHAs can be categorized as long-chain length PHAs (lcl-PHAs) that consist of 15 or more carbon atoms, medium-chain length PHAs (mcl-PHAs), that consist of 6 – 14 carbon atoms, and short-chain length PHAs (scl-PHAs), that consist of 3 – 5 carbon atoms (Zhang et al., 2019a). Figure 2.3 illustrates the general structure of PHAs and showcases some examples of their structural derivatives.



No. of carbon atoms (n)	'R' or alkyl side chain	Type of PHAs	Abbreviation
n = 1	Hydrogen (-H)	poly(3-hydroxypropionate)	[P(3HP)]
	Methyl (-CH ₃)	poly(3-hydroxybutyrate)	[P(3HB)]
	Ethyl (-CH ₂ -CH ₃)	poly(3-hydroxyvalerate)	[P(3HV)]
	Propyl (-(CH ₂) ₂ -CH ₃)	poly(3-hydroxyhexanoate)	[P(3HHx)]
	Pentyl (-(CH ₂) ₄ -CH ₃)	poly(3-hydroxyoctanoate)	[P(3HO)]
	Nonyl (-(CH ₂) ₆ -CH ₃)	poly(3-hydroxydodecanoate)	[P(3HD)]
n = 2	Hydrogen (-H)	poly(4-hydroxypropionate)	[P(4HP)]
	Methyl (-CH ₃)	poly(4-hydroxybutyrate)	[P(4HV)]

Figure 2.3. Molecular structure and main types of polyhydroxyalkanoates based on the number of carbon atom (n = 1 to 2), with R representing possible alkyl functional group and X representing the repeating monomeric units, ranging from 100 to 30,000.

Polyhydroxybutyrate

Polyhydroxybutyrate (PHB) is the most prevalent polyhydroxyalkanoate found in microalgae and aerobic, heterotrophic bacteria (Arora et al., 2023; Cheah et al., 2023; Nanda and Bharadvaja, 2022). The production of PHB using these microorganisms has been extensively investigated following a monoculture approach, fed with sterile growth media (Yashavanth et al., 2021). However, this practice is impractical for further scale-up of the technology and for marketability due to high maintenance cost and elevated polymer production costs. A more promising approach to produce PHB involves utilizing readily available and cost-effective growth media, such as municipal wastewater, using microalgae-bacteria consortia (Arias et al., 2020; Price et al., 2020). Even though microalgae-bacteria have demonstrated their capacity to treat a range of wastewater

effluents, cultivation in such an organic-rich environment involves many operational challenges. These challenges include the risk of contamination by other non-PHB producing heterotrophic microorganisms, which has been extensively reported in the literature (Buitrón and Coronado-Apodaca, 2022; dos Santos Neto et al., 2023). This could be seriously detrimental to biomass production and affect final PHB production yields. Therefore, the incorporation of inorganic carbon could emerge as a favorable option to not only mitigate the bloom of heterotrophs but also to reduce greenhouse gas emissions (carbon dioxide).

The pathway for PHB biosynthesis under photoautotrophic conditions is illustrated in Figure 2.4. In times of light surplus and carbon dioxide, the biosynthesis of PHB competes with the synthesis of storage carbohydrates, *i.e.*, glycogen (cyanobacteria) or starch (eukaryotic microalgae), for glycerate 3-phosphate (GP) metabolic intermediate (Rueda et al., 2020a). This competition is particularly more when growth is limited by nitrogen and results in a great part of the fixed carbon used for storage carbohydrates synthesis instead of PHB production (Singh et al., 2017). When nitrogen limitation is prolonged, storage carbohydrates are oxidized via the oxidative pentose phosphate pathway and their byproducts (Acetyl-CoA) used for PHB synthesis (Kamravamanesh et al., 2019). The biosynthetic pathway for PHB production comprises three reaction steps where i) acetyl-CoA acetyltransferase (PHA-A) catalyzes the condensation of Acetyl-CoA precursors to Acetoacetyl-CoA, ii) Acetoacetyl-Co is then reduced to 3-hydroxybutyryl-CoA (3-HB-CoA) by action of a NADPH-linked acetoacetyl-CoA reductase (PHA-B), and iii) 3-HB-CoA is finally polymerized to PHB via PHA synthase (PHA-C) driven esterification.

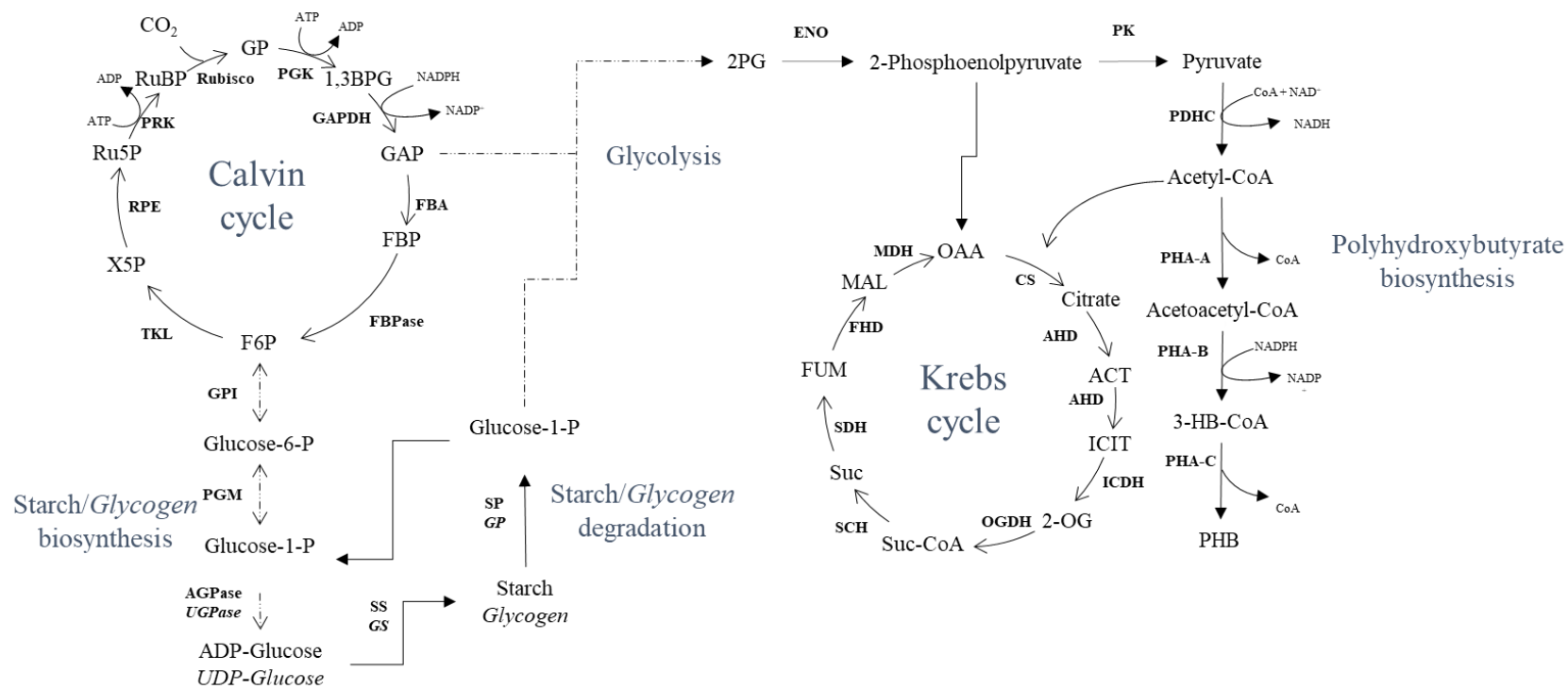


Figure 2.4. Fundamental pathways related to starch, glycogen, and polyhydroxybutyrate biosynthesis in eukaryotic microalgae and cyanobacteria under nitrogen limitation. Solid arrows represent one step reactions, while dotted arrows represent stepwise reactions. **Metabolites:** GP, Glycerate 3-phosphate; 1,3BPG, 1,3-Bisphosphoglycerate; GAP, 3-phosphoglyceraldehyde; FBP, Fructose 1,6-biphosphate; F6P, Fructose 6-phosphate; X5P, Xylulose 5-phosphate; Ru5P, Ribulose 5-phosphate; RuBP, Ribulose 1,5-biphosphate; 3-HB-CoA, (S)-3-Hydroxybutyryl Coenzyme A; ACT, aconitate; ICIT, isocitrate; 2-OG, α -ketoglutarate; Suc-CoA, Succinyl-CoA; Suc, Succinyl; FUM, fumarate; MAL, malic acid; OAA, oxaloacetic acid. **Enzymes:** Rubisco, ribulose 1,5-bisphosphate carboxylase; PGK, 3-phosphoglycerate kinase; GAPDH, glyceraldehyde 3-phosphate dehydrogenase; FBA, Fructose-bisphosphate aldolase; FBPase, fructose 1,6-bisphosphatase; TKL, transketolase; RPE, ribulose 5-phosphate 3-epimerase; PRK, phosphoribulokinase. GPI, phosphoglucose isomerase; PGM, phosphoglucomutase; AGPase, ADP-glucose pyrophosphorylase; UDPase, UGP-glucose pyrophosphorylase; SS, starch synthases; GS, glycogen synthases; SP, starch phosphorylase; GP, glycogen phosphorylase; ENO, enolase; PK, pyruvate kinase; PDHC, pyruvate dehydrogenase complex; PHA-A Acetyl-CoA acetyltransferase; PHA-B Acetoacetyl-CoA reductase; PHA-C PHA synthase; CS, citrate synthase; AHD, aconitate hydratase; ICDH, isocitrate dehydrogenase; OGDH, 2-oxoglutarate dehydrogenase; SDH, succinate dehydrogenase; FHD, fumarate hydratase; MDH, malate dehydrogenase.

Properties of polyhydroxybutyrate

The main properties that make PHB a promising alternative for fossil-based plastics are their similar mechanical and physical properties to polypropylene derived from fossil fuels (Table 2.4). These properties are further enhanced by environmental benefits like full biodegradability, biocompatibility, and functionality (Bugnicourt et al., 2014). Moreover, PHB is water-insoluble and resistant to hydrolytic degradation, making it suitable for medical and food packaging applications. In the field of medicine, this polymer is used mainly for sutures, surgical implants, parts of bones and replanted veins, microencapsulation, chemo-preventive, etc. (dos Santos et al., 2017). PHB has also been successfully tested for the fabrication of bottles, latex, and other products plastic packaging with similar rigidity to polypropylene (Garcia-Garcia et al., 2022). Despite the growing demand for PHB-based bioplastics, which is projected to grow by up to 100% annually (Llewellyn et al., 2019), the current market share of PHB is below 2%. The main reason for being the high production and culture-maintenance costs. In this context, the use of municipal wastewater as feedstock may overcome this by offering an inexpensive and readily available substrate for microalgae photoautotrophic growth (Arias et al., 2020).

Table 2.4. Physical and thermal properties of polyhydroxybutyrate and their comparison with petroleum-based plastics.

Polymer	Crystallinity (%)	Tensile strength (MPa)	Melting temperature (°C)	Glass transition temperature (°C)	Breaking strength (%)	References
PHB	52 – 76	12.5 – 43.0	172 – 178	0.6 – 2.0	1.0-5.0	Shishatskaya et al. (2020) Singh & Mallick (2017)
PP	50 – 70	1700	174 – 176	-10	400	Balaji et al. (2013) Costa et al. (2019)
HDPE	60 – 80	1000	125 – 132	n.r.	12	Costa et al. (2019)

PHB: Polyhydroxybutyrate, PP: Propylene, HDPE: High-density polyethylene, n.r.: Not reported.

Production of polyhydroxybutyrate in microalgae-bacteria consortia

The occurrence of PHB in microalgae-bacteria consortia has predominantly been observed during cultivation in wastewater and other waste streams. Many studies have indicated that the dominant strains associated with photoautotrophic PHB in microalgae-bacteria consortia are cyanobacteria, belonging to *Synechocystis*, *Synechococcus*, and *Nostoc* genera, or eukaryotic microalgae, belonging to *Chlorella* or *Botryococcus* genera (Mastropetros et al., 2022; Sirohi et al., 2021). In most cases, the average PHB content under these conditions ranges between 1 – 10% dCW (Table 2.5), which is relatively lower than that obtained with bacteria (Sirohi et al., 2021). Nevertheless, the PHB-from-wastewater approach offers a second advantage which is treated, or at least cleaner, wastewater (Arias et al., 2020). Cultivation in dynamic environments like wastewater often leads to contamination by other species, which could be detrimental to biomass production and further affect PHB production. Therefore, monitoring and control of operating and cultivation parameters like light-dark cycles, temperature, pH, and gas exchange limitation are critical for an enhanced PHB production in microalgae-bacteria consortia (Ray et al., 2022). A better understanding of the complex process that takes place during PHB formation is needed to fully elevate the yield of this economically valuable byproduct in microalgae-bacteria consortia cultivated in wastewater.

Table 2.5. Dominant species and average polyhydroxybutyrate production in microalgae-bacteria consortia cultivated in waste streams under photoautotrophic conditions.

Dominant species	Type of wastewater	Days of incubation	Content		References
			% dCW	mg L ⁻¹	
<i>Synechococcus leopoliensis</i>	Aquaculture ponds	10	1.0	60	Mariotto et al. (2023)
<i>Synechocystis</i> sp.	Municipal secondary effluent	8	4.8	69	Senatore et al. (2023)
<i>Synechococcus</i> sp.	Agricultural runoff	31	4.5	15	Rueda, García-Galán, Ortiz, et al. (2020b)
<i>Synechocystis salina</i>	Digestate supernatant	40	5.5	20	Meixner et al. (2016)

2.1.4. Valorization of microalgae-bacteria biomass as biofertilizers

The aim of cultivating microalgae-bacteria consortia in municipal wastewater is to obtain a clean effluent while concurrently transforming biomass into valuable organic resources, such as biofuels, animal feed, pigments, and bioplastics (PHB). The selection of any of these bio-based products depends on the biopolymer composition and the targeted services. Transforming microalgae-bacteria biomass into biofuels (*e.g.*, bioethanol, biodiesel, biohydrogen, etc.) for energy production has become challenging on an industrial scale. The major bottleneck for this is in the heterogenic, complex cellular wall of eukaryotic microalgae, which need to be disrupted or weakened for biopolymers extraction (Safi et al., 2017). Different cell disruption methods have been devised to weaken or destroy the cell wall in microalgae, like bead milling, ultrasonication, acid/alkaline pretreatment, etc. Yet, most of these pretreatment methods are either energy intensive or generate pollutant byproducts that decrease the environmental benefits of microalgae-bacteria consortia (Jothibasud et al., 2022).

The multifaceted composition of microalgae-bacteria biomass has led its valorization towards other expedient uses, including fertilization of agricultural soils (Ayre et al., 2021; González et al., 2020; Mückschel et al., 2023), as it can be directly used without any pretreatment and even in combination with treated wastewater for irrigation. Before soil fertilization, microalgae-bacteria biomass is typically subjected to controlled soil incubation under aerobic conditions and plant growth experiments for about 120 days to determine their agronomic value as a biofertilizer (Álvarez-González et al., 2022; Dineshkumar et al., 2020). These experiments take time and resources and could lead to false positives or selection of poor strategies for soil fertilization. Therefore, novel methods are constantly being developed to determine the agronomic value of organic material more expediently and in less time.

In recent years, Jimenez et al. (2015b) observed that complexity (*i.e.*, molecular structure) and bioaccessibility (*i.e.*, availability to soil microorganisms) were valuable parameters in diagnosing the agronomic value of organic materials. These parameters could determine any organic material fate as a source of organic matter, nitrogen, and phosphorus. As a result, they developed a stability and bioaccessibility prediction model (ISBAMO) based on the biochemical profile of organic materials (Jimenez et al., 2017; Muller et al., 2014). For this purpose, sequential chemical extraction was to be carried out, where the strength of the extractants increase progressively, to recover certain biochemical compounds of decreasing accessibility. Then, a three-

dimensional liquid-phase fluorescence spectroscopy would be used to detect all the fluorophores in each extracted fraction based on commercial standards (Muller et al., 2014). The resulting fractions, along with its composition, are depicted in Figure 2.5. ISBAMO has proven effective in characterizing the accessibility and complexity of organic wastes and residues from various sources, including wastewater treatment plants, composting plants, farms, agrifood industries, and municipal solid waste plants (Jimenez et al., 2015a).

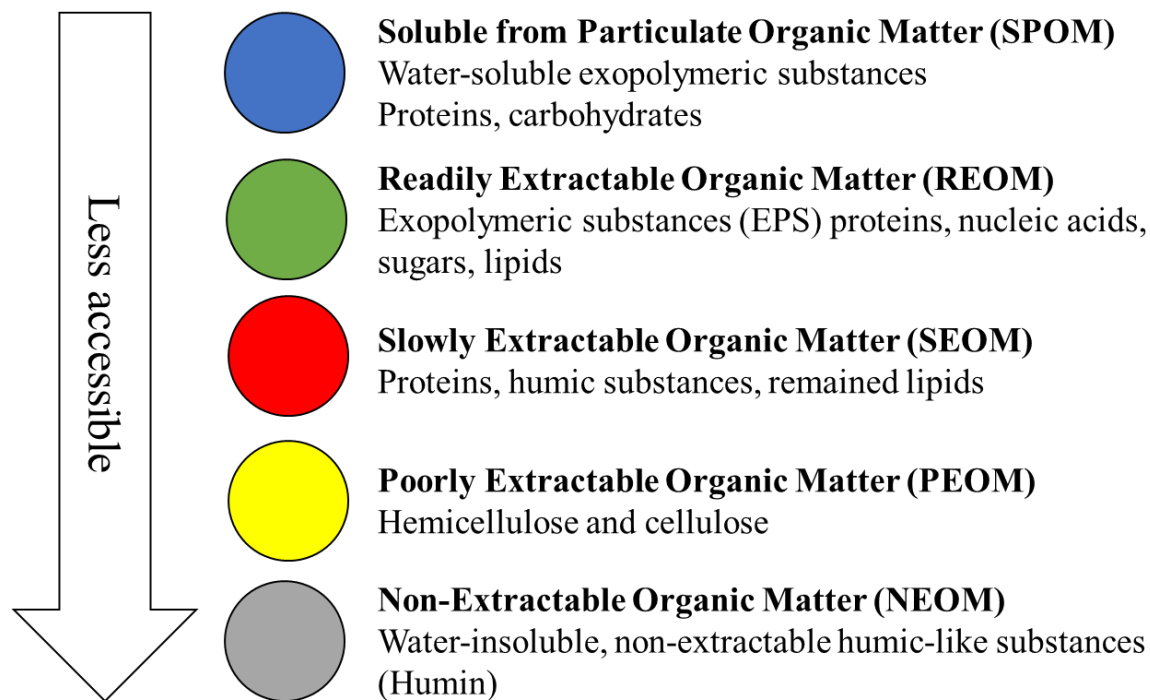


Figure 2.5. Extracted chemical fractions and their common biochemical composition from the stability and bioaccessibility prediction model (ISBAMO).

2.2. Postulates

- Polyhydroxyalkanoate production from photoautotrophic microorganisms like eukaryotic microalgae and cyanobacteria is performed altering the growth conditions (Fradinho et al., 2019; Mastropetros et al., 2022). First, photoautotrophic microorganisms are subjected to conditions for favorable photosynthetic activity, *e.g.*, light intensity, temperature, and nutrient availability, for biomass accumulation. Then, the production of polyhydroxyalkanoates is triggered through the manipulation of abiotic factors, *e.g.*, nitrogen limitation, generating stress conditions.
- Activated sludge is an ideal inoculum of polyhydroxyalkanoate-producing microalgae-bacteria consortia as the fluctuations of carbon and nutrients availability during the aeration process results in nutrient stress conditions that ultimately favors microorganisms that store storage macromolecules as sources of energy and carbon, *e.g.*, polyhydroxyalkanoates (Jayakrishnan et al., 2021).
- Growth conditions, *e.g.*, dissolved oxygen concentration, light intensity, photoperiods (Kazbar et al., 2019; Raso et al., 2012) and abiotic stress, *e.g.*, transient availability of nitrogen or phosphorus (Sirohi et al., 2021) are fundamental aspects to obtain microalgae-bacteria biomass rich in polyhydroxyalkanoates. Moreover, the mutualistic interactions between microalgae and bacteria also enhances nutrients recovery and enriches the biomass with essential elements, *e.g.*, nitrogen and phosphorus (Yan et al., 2022), used for agriculture or soil fertilization (Álvarez-González et al., 2022).

2.3. Hypothesis

2.3.1. General hypothesis

The production of polyhydroxyalkanoates in microalgae-bacteria consortia will be enhanced through a nitrogen-limited and oxygen-deficient condition in primary effluent wastewater under environmental conditions.

2.3.2. Specific hypotheses

- Nile red fluorescent staining and micromanipulation are adequate methods for the efficient identification and selection of polyhydroxyalkanoate-producing microalgae from activated sludge.
- Low dissolved oxygen and nitrogen availability reduce oxidative stress and competition for nutrients between photoautotrophic and heterotrophic bacteria, improving the production of biomass and polyhydroxyalkanoates in microalgae-bacteria consortia.
- Nitrogen limitation in floccular microalgae-bacteria consortia improve the production of storage macromolecules like polysaccharides, proteins, and lipids, improving the extractability (bioaccessibility) of microalgae-bacteria biomass as organic matter, nitrogen, and phosphorus source for soil microorganisms.

2.4. Objectives

2.4.1. General objective

To increase the production of polyhydroxyalkanoates in microalgae-bacteria consortia biomass through the application of abiotic stress factors (nitrogen limitation and low dissolved oxygen concentration) using municipal wastewater under environmental conditions and to evaluate the nutrients biomass bioaccessibility for a possible use as soil fertilizer.

2.4.2. Specific objectives

- To screen and identify polyhydroxyalkanoate-producing microalgae from municipal activated sludge.
- To maximize the production of polyhydroxyalkanoates in selected microalgae by manipulating nutrients and dissolved oxygen concentration in mineral medium.
- To assess the efficacy of selected microalgae and bacteria for polyhydroxyalkanoates production and nutrient removal simulating best performing nutrients and dissolved oxygen concentrations in municipal wastewater.
- To characterize the molecular complexity and bioaccessibility of organic matter, nitrogen, and phosphorus from microalgae-bacteria aggregates with different morphologies (flocs and granules) grown under nutrient-abundant and starvation conditions.

2.5. Work strategy

The proposed scheme of work was divided into four experimental parts (Fig. 2.6), each related to the different specific objectives defined in section 2.4.2. The first experimental part consisted of screening and identifying PHA-producing photoautotrophic biomass from activated sludge and primary effluent. To this end, these waste effluents were collected from a municipal wastewater treatment plant located in Santa Rosa Jauregui, Queretaro, Mexico and analyzed for physicochemical parameters, *e.g.*, nitrogen, organic carbon, phosphorus, suspended solids, etc. Biomass rich in photoautotrophic microorganisms was obtained by mixing activated sludge, as inoculum, and primary effluent, as substrate, in a 1:10 v/v proportion at ambient temperature and under continuous illumination. PHA-producing strains were morphologically identified in the generated photoautotrophic biomass following the Nile red fluorescent staining method and separated using serial dilution and micromanipulation. After proliferating PHA-producing strains in nutrient abundant mineral medium, the cultures were harvested, washed, and transferred to nitrogen-limited mineral medium to trigger polymer production. The polymer production in selected strains was quantified in terms of PHA and polysaccharides using the acid methanolysis/gas chromatography and phenol-sulfuric methods, respectively.

In the second experimental part, nutrient availability and dissolved oxygen concentration were manipulated to maximize the production of PHA in microalgae. Given the rather low PHA production obtained in the previous experimental part, a PHA-producing species, *Synechocystis* sp., was acquired and tested. The strain was first grown in nutrient abundant mineral medium for biomass accumulation. Afterwards, *Synechocystis* sp. cultures were harvested, washed, and transferred in nitrogen-limited mineral medium and phosphorus limited mineral medium. PHA production was assessed using acid methanolysis/gas chromatography. After corroborating the efficacy of nitrogen limitation for PHA production, *Synechocystis* sp. cultures were again harvested, washed, and transferred in nitrogen-limited mineral medium at different dissolved oxygen concentrations. To this end, nitrogen sparging, air sparging, and no sparging were used to achieve low, saturated, and oversaturated oxygen-air levels, respectively. In these cultures, PHA production was also assessed using acid methanolysis/gas chromatography.

The third experimental part consisted in imitating the best performing conditions from the previous experimental part for simultaneous PHA production and removal of nutrients and organic matter in municipal wastewater. To this end, primary effluent from Santa Rosa Jauregui municipal

wastewater treatment plant was collected and analyzed again for physicochemical parameters. *Synechocystis* sp. was cultured in this primary effluent at ambient temperature and following a 12 h light/dark cycles for biomass accumulation and nitrogen removal. These conditions were maintained until a nitrogen-limited condition was achieved (12 d). From this point onward, oxygen evolution from microalgae was inhibited by damaging the light harvesting complex through short photo-dense pulses of light ($\geq 2000 \mu\text{mol m}^{-2} \text{s}^{-1}$). Dissolved oxygen concentration was then reduced by allowing wastewater-borne bacteria to consume dissolved organic matter. Cultures without oxygen management and with no inoculum (only primary effluent) were used as a control and blank, respectively. Nutrient removal, in the form of chemical oxygen demand, ammonia nitrogen, and phosphorus as orthophosphates, as well as PHA production were assessed following Hach colorimetric methods and acid methanolysis/gas chromatography, respectively.

Finally, in the fourth experimental part, the resulting microalgae-bacteria biomass from the first experimental part was used to evaluate its potential for soil fertilization. The organic matter, nitrogen, and phosphorus content was quantified in the obtained biomass. For this purpose, samples of the harvested selected microalgae-bacteria biomass grown in nutrient abundant mineral medium and in nitrogen-limited mineral medium from the first experimental part were lyophilized and milled. Then, the content of the samples was fractionated using ISBAMO (Index of Stability and Bioaccessibility of Organic Matter) and modified Olsen methods. Each fraction, sequentially less bioaccessible and complex, was characterized in terms of organic matter, nitrogen, and phosphorus using Hach and Aqualytic colorimetric methods. The complexity in each fraction was determined through 3D fluorescence spectroscopy. Other microalgae-bacteria structures from photobioreactors fed with wastewater and mineral medium were also evaluated with these methods to rule out important changes in organic matter, nitrogen, and phosphorus content as result of morphology or nutrient limitation.

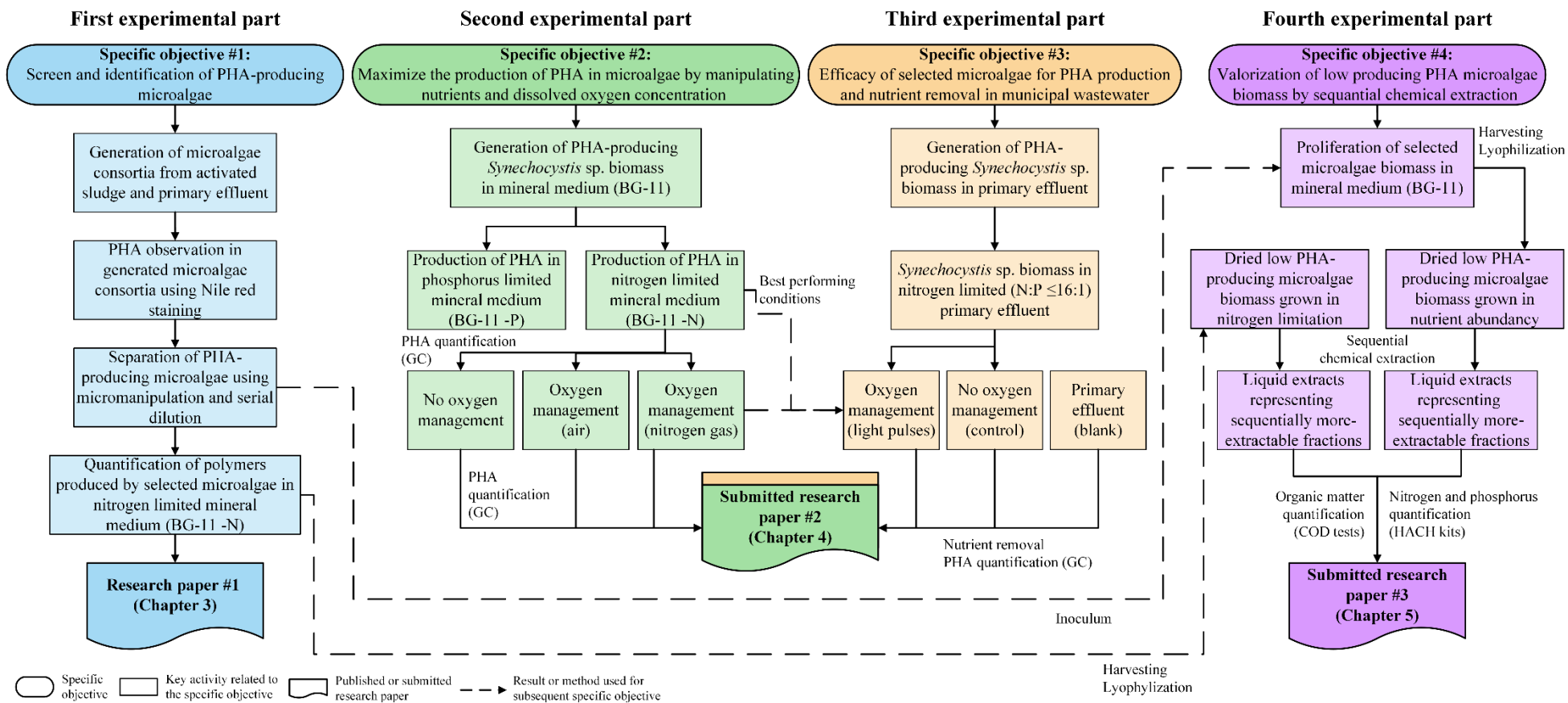


Figure 2.6. Work strategy diagram.

3. Assessment of polyhydroxyalkanoates and polysaccharides production in native phototrophic consortia under nitrogen and phosphorous-starved conditions

Reference to published paper:

Romero-Frasca, E., Buitrón, G. (2023). Assessment of polyhydroxyalkanoates and polysaccharides production in native phototrophic consortia under nitrogen and phosphorous-starved conditions. *International Journal of Environmental Science and Technology*.

<https://doi.org/10.1007/s13762-023-05332-7>

Abstract

Growing demand for sustainable and eco-friendly alternatives to petroleum-based polymers has increased the interest in the microalgae-based production of polymers, specifically polyhydroxyalkanoates and polysaccharides. While most studies in microbial polymer production have primarily focused on axenic or genetically engineered cultures of cyanobacteria and eukaryotic algae, little is known about the potential of mixed phototrophic consortia. This study aimed to obtain and evaluate mixed photosynthetic consortia of different origins (natural and residual) as a novel approach for polyhydroxyalkanoates and polysaccharides accumulation. Activated sludge and freshwater samples were collected and inoculated in lab-scale photobioreactors to generate mixed photosynthetic consortia. After preliminary screening for polymer-accumulating strains under nutrient-unbalanced conditions, the selected strains were subjected to a biphasic strategy (biomass accumulation and nutrient stress) to evaluate their polyhydroxyalkanoates and polysaccharide accumulation. First, cultures were subjected to a nutrient-rich phase to increase the biomass content and then deprived of nutrients (known as the polymer accumulation phase) to evaluate polyhydroxyalkanoates and polysaccharide yield. Findings in this study revealed that the highest polysaccharide yield for activated sludge biomass and freshwater consortia was 460 ± 16 and 320 ± 24 mg glucose g dried biomass⁻¹, respectively. In contrast, the highest polyhydroxyalkanoates accumulation levels for both cultures were calculated at 5 mg polyhydroxyalkanoates g dried biomass⁻¹. The efficacy of nutrient stress as a selective pressure strategy to develop mostly polysaccharides-accumulating consortia was demonstrated.

Keywords: Activated sludge; Bioproducts; Polymers; Microalgae; Polyhydroxyalkanoates

3.1. Introduction

Widespread utilization of fossil-based products, including plastics and fossil fuels, is leading to a significant increase in environmental pollution and health-related problems worldwide. In particular, plastics disposal has become a considerable challenge due to the material's non-biodegradable nature and the lack of adequate recycling infrastructure (OECD, 2022), while fossil fuels combustion contributes significantly to greenhouse gas emissions and climate change, exacerbating the already pressing global environmental issues (Keramidas et al., 2021). Thus, an urgent need to explore and implement innovative solutions that can help mitigate the harmful effects of fossil-based products and promote environmentally friendly practices has arisen.

Microalgae-bacteria consortia represent a viable option for generating sustainable and renewable bioproducts (Arimbrathodi et al., 2023; Ray et al., 2022) and wastewater treatment (Aditya et al., 2022). Fundamentally, these microorganisms form symbiotic associations in which i) microalgae provide bacteria with organic carbon and O₂ through photosynthesis, and ii) bacteria aid in the mineralization of organic matter producing in return CO₂ for microalgae photosynthesis. As a result of this exchange and assimilation of dissolved nutrients, biomass rich in various valuable metabolites is produced.

In this context, PHAs and polysaccharides have attracted much attention in recent years (Cinar et al., 2020; Rajpoot et al., 2022). These algae-based polymers are accumulated intracellularly and physiologically employed as carbon and energy reserves during metabolic unbalance. PHAs and polysaccharides are attractive materials for bioplastic production as they exhibit mechanical and chemical properties that are relatively similar to traditional plastics (Dalton et al., 2022). They are also adaptable to well-known plastic manufacturing processes, such as injection molding and extrusion, which makes them suitable for large-scale production (Mathiot et al., 2019).

Considering polysaccharides' and PHA's carbon and energy role in microalgae, a stress condition is needed to trigger their accumulation. One of the most common strategies to achieve that is limiting nutrients (Madadi et al., 2021). The limited availability of nitrogen and, to a lesser extent, phosphorous generates an imbalance in the metabolic turnover, which triggers the production of these biopolymers in search of redox balance. It has been demonstrated that the overall lack of nitrogen in the growth medium leads to an increase of both PHA (up to 200 mg g dried biomass⁻¹) and polysaccharides content (up to 480 mg g dried biomass⁻¹) in mixed microalgae

consortia (Almeida et al., 2021; Phalanisong et al., 2021). Most recently, the genus *Chlorella* was suggested as an interesting strain for PHA and starch photoautotrophic accumulation (Das et al., 2018; Selvaraj et al., 2021).

Nutrient limitation is a species-dependent enhancement strategy that relies on the prevalence of photoautotrophic microorganisms that produce polymers in mixed consortia. The microbial population in these associations is highly dynamic (Quijano et al., 2017; Zhang et al., 2020), which makes them susceptible to contamination with fast-growing cells that do not produce polymers. That poses a challenge when trying to generate high-quality biopolymers from waste effluents, as non-polymer-producing cells can dilute the overall polymer content and reduce the quality of the final product. One approach to address this issue is to sterilize the media and implement highly controlled processes to limit the growth of unproductive microorganisms. However, this strategy can be expensive and may need to be more economically feasible to compete with its petroleum-based counterpart (Arias et al., 2018). Alternatively, selecting a resilient and adaptable inoculum source can increase the feasibility of producing photosynthetic polymers from mixed consortia without compromising their economic and environmental benefits.

AS derived from municipal wastewater treatment plants offers a promising source of microorganisms that accumulate polymers (Guleria et al., 2022; Jayakrishnan et al., 2021). Previous research indicates that the intermittent availability of carbon and nitrogen during AS process favors the growth of microorganisms that store polymers. That can result in a net production of 900 mg PHA g dried biomass⁻¹ (Tamis et al., 2014). However, it has also been reported that AS can form predominantly phototrophic consortia taking advantage of dissolved nutrients in the growth medium when exposed to continuous illumination (Milferstedt et al., 2017b; Quijano et al., 2017). Considering this information, subjecting an AS inoculum to a two-step enrichment scheme that promotes i) the formation of phototrophic biomass (nutrient-rich) and ii) polymer accumulation (nutrient-limitation) would exert an improved selective pressure on the photoautotrophic consortium that stores polymers.

Therefore, this study aims to evaluate the potential of mixed phototrophic consortia from activated sludge and freshwater, to produce PHA and polysaccharides under a combined nitrogen and phosphorous-limited condition. To the authors' knowledge, this study represents one of the first attempts to evaluate the efficacy of this strategy in sludge-borne eukaryotic algae and cyanobacteria. This study was developed between February and June 2022 in the Laboratory for

Research on Advanced Processes for Water Treatment of the Universidad Nacional Autónoma de Mexico, Santiago de Queretaro, Queretaro, Mexico.

3.2. Materials and methods

3.2.1. Source of photoautotrophic biomass

Different inoculum sources were evaluated for obtaining polymer-producing photoautotrophic biomass in samples of different ecological origins. First, wastewater treatment plant samples were collected from Santa Rosa Jauregui in Queretaro, Mexico. The sampling points for primary effluent and AS were restricted to the upper (clarified) layer of the primary settling tank and a well-mixed segment of the aeration tank, respectively. The procedure reported by Abouhend et al. (2019) with minor modifications was utilized to generate phototrophic biomass from AS. AS (inoculum) and primary effluent (substrate) were mixed in a 1:10 v/v proportion and transferred into laboratory-scale glass photobioreactor (PBR). Mean concentrations for selected parameters in wastewater effluent and AS mix are shown in Table 3.1. The growth of sludge-based eukaryotic algae and cyanobacteria was initiated by continuously illuminating PBR with four 54W fluorescent-light lamps. The illumination provided a photosynthetically active radiation (PAR) of $140 \mu\text{mol m}^{-2} \text{s}^{-1}$ on the inner surface of the reactor. Reactors were kept at ambient temperature and stirred at 120 rpm with a StableTemp™ stirring hotplate to ensure complete mixing.

Identification and separation of polymer-storing strains were carried out with a non-axenic *Chlorella sorokiniana* 211/8 K dominant consortium as a reference, provided by the Department of Civil and Environmental Engineer of the São Paulo State University (UNESP). This photoautotrophic consortium of freshwater origin was initially obtained from the Culture Collection of Algae and Protozoa (CCAP) and cultured in PBR fed with BG-11 growth medium, as it has been found to be the most economical and efficient for *Chlorella* species (Sharma et al., 2016). BG-11 medium composition was the same as in Rueda et al. (Rueda et al., 2020a). The protocol for the consortium maintenance prior this study is detailed elsewhere (Silva et al., 2021; Slompo et al., 2020).

Table 3.1. Characteristics of growth medium used for photoautotrophic biomass generation. All values are the means of independent replicates (n=2) \pm standard deviation.

Parameter	Concentration, mg L ⁻¹
Dissolved total organic carbon (DOC)	71.2 \pm 5.3
Dissolved inorganic carbon (DIC)	147.8 \pm 0.5
Total suspended solids (TSS)	170 \pm 8.5
Volatile suspended solids (VSS)	20 \pm 1.7
Nitrogen, ammonia (NH ₄ ⁺ -N)	70.8 \pm 0.1
Nitrogen, nitrates (NO ₃ ⁻ -N)	n.d.
Nitrogen, nitrites (NO ₂ ⁻ -N)	n.d.
Phosphorus, orthophosphates (PO ₄ ³⁻ -P)	22.9 \pm 3.5

n.d.: Not detected.

3.2.2. Obtention of polymer-storing photoautotrophic consortia

Identification of polymer-storing strains

Generated sludge-based and freshwater-based photoautotrophic biomass in the PBR of the previous section were harvested by centrifugation (3000 g, 20 min, 5 °C). After the supernatant was discarded, cell pellets were rinsed with distilled water to remove residual nutrients. Afterward, these were inoculated in PBR fed with BG-11 limited in nitrogen and phosphorous (BG-11 -NP) as Singhon et al. (2021) described at an initial biomass concentration of 77 \pm 7.5 mg VSS L⁻¹ to trigger polysaccharides and PHA accumulation. Cultures were grown and periodically monitored for three weeks maintaining operating conditions (stirring, temperature, and light intensity) as previously described.

The presumptive polymer-accumulating species were identified following a modified Nile red staining procedure described by Mourão et al. (2020). A volume of 1.0 mL of each NP-limited culture suspension was centrifuged weekly. After discarding the supernatant, cell pellets were resuspended in 1.0 mL of Nile red dye (100 μ g mL⁻¹ dissolved in Dimethyl Sulfoxide (DMSO)) and incubated for 10 min at room temperature. Then, 20 μ L of this solution was heat-fixed in glass slides and gently rinsed with distilled water to remove excess dye. PHA, more specifically polyhydroxybutyrates (PHB), granules, and other lipid bodies were visualized at 40X using a

fluorescence microscope equipped with an excitation filter (450–490 nm), emission filter (515 nm), and a dichroic beam splitter (500 nm). Morphological identification of polymer accumulating strains was carried out in bright field microscopy and printed (Wehr et al., 2015) and online (Hauer and Komárek, 2022) taxonomic databases. Both bright field and fluorescence microscopy were performed using a Nikon ECLIPSE 90i widefield fluorescent microscope.

Separation into polymer-storing consortia

Separation of presumptive polymer accumulating strains was done through serial dilution and micromanipulation. First, samples from each PBR fed with BG-11 -NP were subjected to a fluorescence excitation spectrum of 510-560 nm to facilitate the observation of chlorophyll under a widefield fluorescent microscope (Nikon ECLIPSE 90i). Photoautotrophs were then directly counted using a 0.1 mm improved Neubauer counting chamber and progressively diluted in autoclaved distilled water until a final suspension of 100 cells mL⁻¹ was obtained. Polymer-accumulating algae were then sought based on their identified morphology and aspirated through a micromanipulator made by joining the heated tips of glass Pasteur pipettes and pulling them apart while molten. Finally, these were deposited in test tubes containing 1 mL of BG-11 and cultured as previously described. Cultures were successively transferred in PBR with a working volume of 250 mL and 1 L.

3.2.3. Evaluation of growth and enhancement of polymer production in enriched mixed consortia

Experiments were conducted indoors in square methacrylate Flat Panel Photobioreactors (FP-PBR) at room temperature, with a total volume of 15 L and a working volume of 13 L. All FP-PBR were operated in duplicates under batch conditions for 10 d. The reactors were continuously mixed by filtered compressed air injections enriched with 2.0% CO₂ at 0.3 VVM for the duration of the experiment. Illumination was continuously supplied using four 54W fluorescent-light, providing a PAR of 140 μmol m⁻² s⁻¹. The pH was continuously measured using a Vernier Tris-Compatible Flat pH Sensor and maintained within an 8.0 to 9.0 range using either 1.0 M NaOH or 1.0 M HCl.

Growth curves, as well as PHA and polysaccharides accumulation kinetics, were evaluated following a two-phase approach. First, inoculums were subjected to a nutrient-rich phase to increase the biomass concentration. FP-PBR fed with BG-11 were inoculated with 70 mg VSS L⁻¹

of homogenized samples of each consortium. The duration of this phase was carried out until a final concentration of approximately 1.0 g VSS L⁻¹ was reached. The second phase consisted of enhancing PHA and polysaccharides production through N-limitation, P- limitation and DIC abundance. Biomass from the nutrient-rich phase was harvested by centrifugation, rinsed with distilled water, and centrifuged once more. After removing residual nutrients from biomass pellets, these were transferred to FP-PBR fed with BG-11 -NP maintaining operating conditions for 29 d as previously described.

3.2.4. Analytical measurements

Nutrients analysis

DIC and DOC concentration was determined using a Shimadzu TOC Model 5050 analyzer, whereas dissolved PO₄³⁻-P, NO₃⁻-N, and NO₂⁻-N were measured using a Thermo Scientific DIONEX ICS1500 ion chromatography. NH₄⁺-N was determined using the 10031 Hach colorimetric method. Samples for analyzing these nutrients were previously filtered through 0.45µm pore-size filters. Biomass concentration (X) was monitored periodically as Volatile Suspended Solids (VSS) following the standard APHA 2540E (American Public Health Association, American Water Works Association, Water Environment Federation., 2023). The maximum specific growth rate (μ) was calculated via linear regression applied to the logarithmic growth rate obtained from plotting $\ln X$ vs. time (days). Biomass productivity (r) was also determined by dividing the difference between X at time t minus time 0 and time t minus time 0.

PHA and polysaccharides analysis

PHA and polysaccharides were extracted and measured in duplicates from lyophilized biomass pellets from the FP-PBR used for PHA and polysaccharides production. A volume of 50 mL of mixed liquor samples were collected three days per week, centrifuged, and spread in plastic trays. After freezing for at least 4 h at -2 °C, samples were freeze-dried in a Labconco Freezone 6 freeze dryer at -85°C and 0.05 hPa for 24 h.

Extraction and quantification protocol for PHA content was determined utilizing acid methanolysis and gas chromatography (Agilent Technologies 6890B), as reported by Rueda et al. (2022a) with minor modifications. A 2.0 mL volume of acidified (15 % v/v H₂SO₄) methanol and 2.0 mL of chloroform were added to 10 mg of dried biomass in a glass test tube with a Teflon liner

screw cap. After vortexing for 1 min, the resulting solution was incubated in a dry bath (Labnet International AccuBlock™) for 2.5 h at 100 °C and cooled at room temperature. Next, 1.0 mL of deionized water was added to each tube and vortexed to facilitate the separation of different solvents by density. The bottom layer (chloroform) was retrieved through a glass Pasteur pipette and filtered through a 0.45µm pore-size nylon membrane filter. A volume of 1.0 mL from the filtrate was collected, and 1.0 µL was injected into the chromatograph. PHB and PHV (polyhydroxyvalerate) concentrations were determined through a standard curve generated from natural origin Poly[(R)-3-hydroxybutyric acid-co-(R)-3-hydroxyvaleric acid].

Polysaccharides were extracted and measured following a modified phenol-sulfuric method first described by Romero-Frasca et al. (2021). A 1 mL of 1.0 M HCl was added to 1-2 mg of lyophilized biomass in a glass test tube with a Teflon liner screw cap and vortexed for 1 min. After incubating the mixture for 2 h at 100 °C in a dry bath (AccuBlock™ Labnet International, USA), samples were cooled at room temperature, and polysaccharides were determined as glucose (mg glucose g dried biomass⁻¹) from acid hydrolysis with phenol (5% w/v) and concentrated sulfuric acid.

3.3. Results and discussion

3.3.1. Culturing of photosynthetic biomass

The non-axenic *Chlorella sorokiniana* consortium was grown under photoautotrophic conditions in BG-11 upon arrival to the lab. This initial culture developed a green color after 10 d and was populated by two morphologically different strains. Microscopic observations (Fig. 3.1a) confirmed that these had a morphological resemblance to *Chlorella* (dominant) and *Scenedesmus* genera. *Chlorella* specimens are commonly described as green-colored, often spherical (3 to 8 µm in diameter) single cells which lack a flagellum and have a parietal, cup-shaped chloroplast with an easily observable pyrenoid (Ma et al., 2019). On the other hand, *Scenedesmus* are depicted as elongated, cylindrical (10 to 20 µm length; 3 to 6 µm in width) cells with protruding spines or bristles in their poles (Kumar et al., 2021). Strains belonging to this genus are commonly found as single cells or coenobiums consisting of 4 and 8 cells in their exponential and stationary phase, respectively. Overall, recovery of *Chlorella -i.e., C. sorokiniana-* and *Scenedesmus* strains from freshwater sources has been extensively described (Gomaa et al., 2019; Kim et al., 2016; Ruangsomboon et al., 2013; Xin et al., 2010) and ultimately confirmed in this study. A

predominantly photoautotrophic consortium from AS was obtained after 14 d of constant illumination. Observations on the microscope revealed that different eukaryotic algae and diatoms strains were obtained with morphological resemblance to *Scenedesmus*, *Nitzschia*, *Chlorella*, *Oscillatoria*, and *Phormidium* (Fig. 3.1b). Morphologically undistinguishable algae, regarded as unicellular cyanobacteria owed to their spherical small cell size ($\leq 1 \mu\text{m}$ diameter) and bright autofluorescence pattern under green light excitation (500-570 nm, image not shown), were also observed. These photosynthetic taxa are commonly prone to survive in polluted aquatic ecosystems due to their intrinsic tolerance to various organic contaminants (Arias et al., 2020). Previous reports have observed that both unicellular (*i.e.*, *Synechocystis* and *Synechococcus*) and motile filamentous (*i.e.*, *Oscillatoriales*) cyanobacteria, as well as *Scenedesmus* and *Chlorella* eukaryotic microalgae, could be successfully obtained from AS and wastewater effluents (Arcila and Buitrón, 2016; Arias et al., 2019; Buitrón and Coronado-Apodaca, 2022; Milferstedt et al., 2017b; Rueda et al., 2020a).

3.3.2. Enrichment of consortia with polymer-accumulating algae

An initial qualitative screening (Nile red) of polymer accumulators confirmed that a selected number of strains were present in both experimental inoculums upon transferal to BG-11 -NP medium. Due to the absence of an organic matter source within the culturing medium, the presence of polymer-accumulating heterotrophic bacteria could be excluded. *Chlorella*-like single cells (Fig. 3.1c) and unicellular cyanobacteria (Fig. 3.1d) emitted a bright red fluorescence within 1-2 weeks of nutrient stress in both photoautotrophic consortia, respectively. Samples of non-axenic *Chlorella* microalgae and predominantly photoautotrophic consortium samples before transferal to BG-11 -NP were also processed and observed under fluorescence to rule out false positives. Microscopic imaging of these resulted in no observable fluorescence emission (*i.e.*, completely black) for Nile red dye and a dim, barely visible red emission for non-stressed experimental inoculums (Fig. S3.1).

Results provided evidence of Nile red dye's staining efficiency for detecting PHA - specifically polyhydroxybutyrates (PHB)- granules. It can be deduced that Nile red stained strains can also accumulate polysaccharides, as their catabolism during nutrient stress has been associated with synthesizing PHB granules (Koch et al., 2019). It has been reported that the non-polar oxazone molecules present in Nile red allow this dye to quickly and strongly bind to the non-polar phospholipidic membrane that covers PHB granules compared to Nile blue and Sudan black (Rumin et al., 2015). The Nile red dye can stain all intracellular lipid-rich bodies in

photoautotrophic (Meixner et al., 2022; Mourão et al., 2020) and heterotrophic (Narayanan et al., 2020; Trakunjae et al., 2021) species, including PHA granules. In addition, the total fluorescence emitted during this step could be correlated to the amount of PHB present in the cell culture through analytical methods.

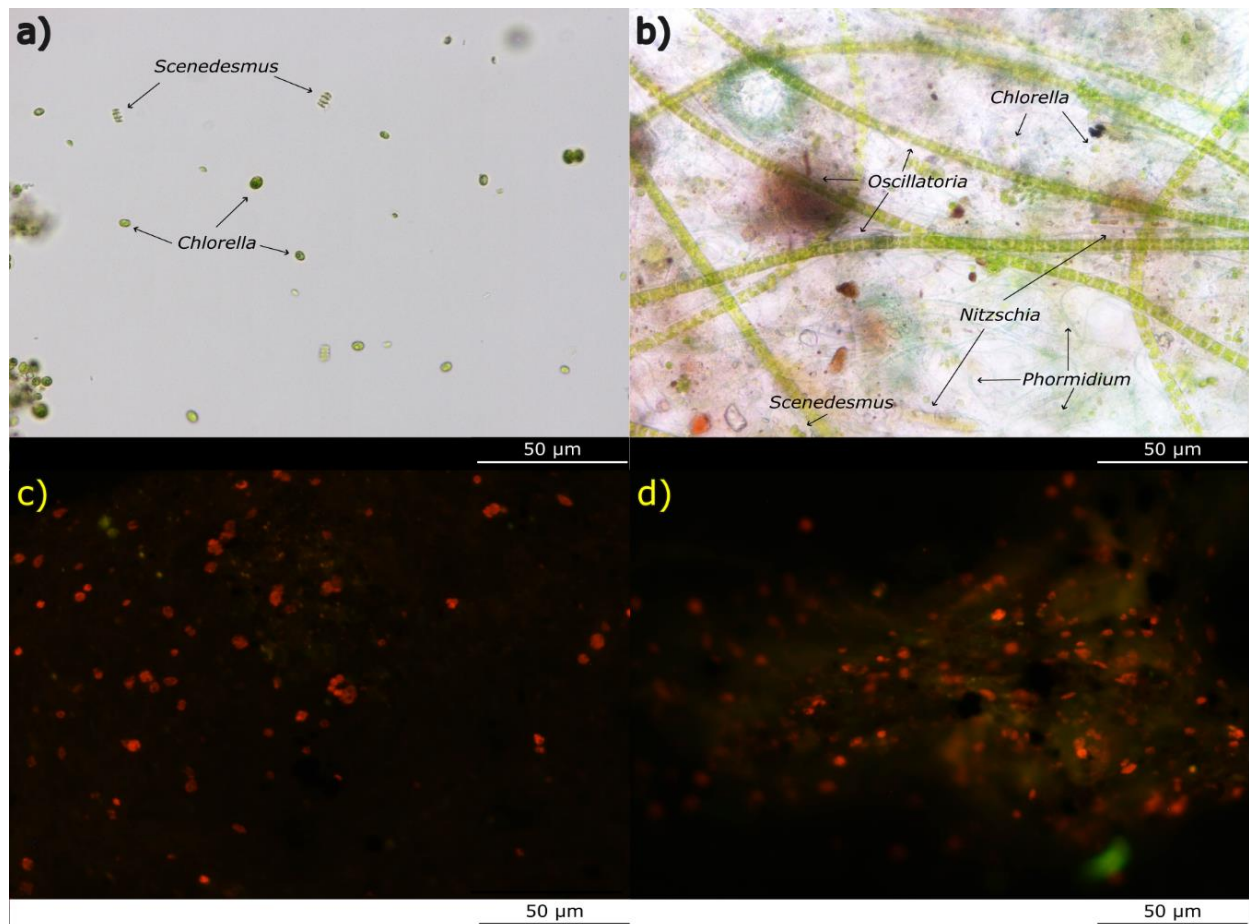


Figure 3.1. Microscopic images illustrating the microbial composition of (a) non-axenic *Chlorella* consortium observed in bright field visible light microscope at 40X; (b) the microbial composition of predominantly photoautotrophic consortium observed in bright field visible light microscope at 40X; (c) polymer accumulating *Chlorella* strains in non-axenic *Chlorella* consortium observed under fluorescence microscope at 40X after straining with Nile red dye; (d) polymer accumulating *Chlorella* and unicellular cyanobacteria strains in predominantly photoautotrophic consortium observed under fluorescence microscope at 40X after straining with Nile red dye.

A quantitative analysis of PHA and polysaccharides was performed to confirm the production and accumulation of polymers in these consortia. Separating potentially polymer-accumulating strains was first performed based on the morphology of stained cells via serial

dilution and micromanipulation techniques. Cultures were accordingly labeled and referred to from here on as *Chlorella sorokiniana* dominant consortium (CDC) and mixed photoautotrophic consortium (MPC). Before this test, CDC and MPC were successfully grown in BG-11 for 3-4 weeks and transferred once more to BG-11 -NP medium. The most notable outcome of this experimental test was that polysaccharides accumulation peaked in week 1 with 198 ± 3 mg glucose g dried biomass⁻¹ and 262 ± 4 mg glucose g dried biomass⁻¹ for CDC and MPC, respectively. On the other hand, PHA accumulation peaked after week 2, in which both consortia accumulated 6.7 mg PHA g dried biomass⁻¹ (CDC) and 19 mg PHA g dried biomass⁻¹ (MPC). As a reference, PHA accumulation was also calculated for non-axenic *Chlorella* consortium and predominantly photoautotrophic consortium before selection in BG-11 -NP, in which no PHA was detected (≤ 0.1 mg PHA g dried biomass⁻¹) for up to 3 weeks.

Separating unicellular algae and cyanobacteria is a complicated procedure that often requires skilled lab personnel and expensive equipment (Vu et al., 2018). This study showed that high-purity cultures for polymer accumulation could be obtained by combining an enrichment strategy (nitrogen and phosphorous limitation) and serial dilution and micromanipulation techniques. Overall, the N and P limitation allowed the dominance of cells with an intrinsic survival mechanism to store carbon and energy molecules (*i.e.*, starch and glycogen), which could be further used to produce PHA (Koch and Forchhammer, 2021). As a result, the abundance of non-accumulating strains was gradually reduced. Continuously diluting a sample of these stressed cultures made the physical extraction of dominant, polymer-accumulating strains more efficient. Similar conclusions were drawn by previous studies, which also isolated unicellular and filamentous cyanobacteria (Meixner et al., 2022) for PHA production, as well as *Chlorella* for biodiesel production (Huang et al., 2019) and microbial ecology investigations (Soares et al., 2022).

3.3.3. Evaluation of growth and polymer production enhancement in enriched mixed consortia

Biomass growth and microbial evolution

FP-PBR inoculated with CDC and MPC started with a biomass concentration of nearly 70 ± 12 mg VSS L⁻¹ during the biomass accumulation or nutrient-rich phase. Both cultures grew until reaching values of 1.0 ± 0.2 g VSS L⁻¹ by day 12 due to the synergistic actions of photosynthesis and nutrient assimilation. Interestingly, CDC and MPC cultures could grow (Fig. 3.2) and achieve significant

growth kinetics even under nutrient-unbalanced conditions. Biomass concentration, growth rate, and biomass productivity during the PHA accumulation phase in each consortium are shown in Table 3.2. The observed μ for CDC achieved a similar value to nutrient-limited *Chlorella* consortia from previous studies, which usually ranged from 0.053 to 0.077 d⁻¹ (Chu et al., 2013). Likewise, μ in MPC was somewhat in range to those observed for wastewater-borne mixed photosynthetic cultures (0.135 to 0.215 d⁻¹, (2018) used for PHA production under permanent illumination and nutrient stress. Findings in this study further suggest that nutrient concentration is a critical factor that influences both biomass yield and productivity and, subsequently, polymer yield.

Table 3.2. Biomass concentration growth rate and biomass productivity in each culture. All values are mean of independent replicates ($n=2$) \pm standard deviation.

Parameter	Nutrient-limited phase	
	CDC	MPC
X (g VSS L ⁻¹)	1.6 \pm 0.1	2.7 \pm 0.1
r (g VSS L ⁻¹ d ⁻¹)	0.066 \pm 0.010	0.133 \pm 0.030
μ (d ⁻¹)	0.072 \pm 0.007	0.240 \pm 0.024

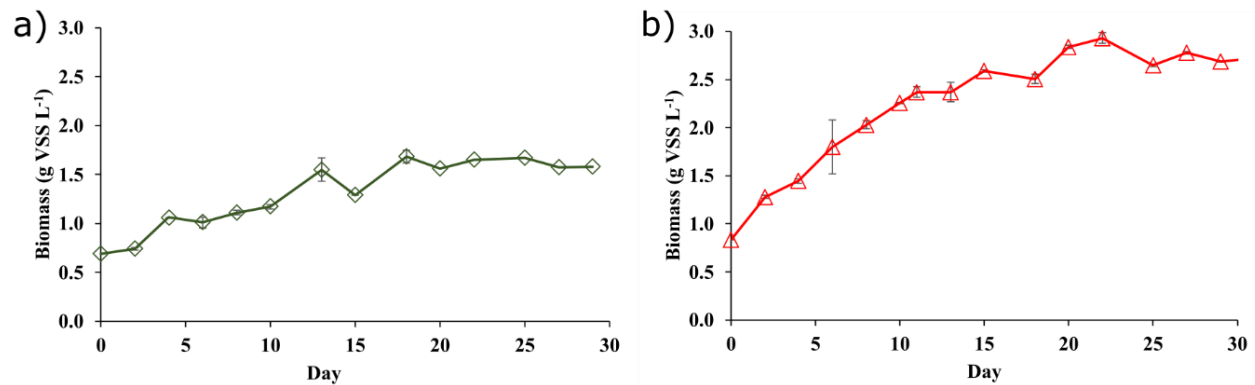


Figure 3.2. Biomass concentration during *Chlorella sorokiniana* dominated consortium (a) and mixed photosynthetic consortium (b) cultures in nutrient unbalanced growth medium. Error bars represent standard deviation of the mean value.

Finally, it should be noted that a yellowish-brown color was observed from day 10 in nutrient-starved FP-PBR inoculated with CDC and MPC (Fig S3.2). This quiescence mechanism, called nitrogen chlorosis or bleaching, is a survival strategy commonly triggered during unbalanced

nutrient conditions (Koch and Forchhammer, 2021; Kumari et al., 2021; Neumann et al., 2021) and a side effect of polymer accumulation. Light harvesting complexes are degraded during nutrient limitation to reduce the photosynthetic activity associated with ATP and NADPH production. Cells favor the synthesis of polysaccharides as a new energy sink for newly fixed CO₂ to maintain a redox balance. Eventually, as nutrient limitation becomes persistent over time, cells look for new sources of ATP to maintain a minimum survival level. In some strains, this results in the degradation of polysaccharides and the conversion of the glucose-phosphates intracellular pool into PHA, allowing the cell to stay on standby until nutrients are replenished.

Effect of N-starvation and P-limitation on polymer production

The evolution of polymer accumulation values in nutrient-stressed CDC and MPC cultures are shown in Fig. 3.3. Polysaccharides content gradually increased in CDC (320 ± 24 mg glucose g dried biomass⁻¹) and MPC (460 ± 16 mg glucose g dried biomass⁻¹) during the first 15 d of nutrient stress. Likewise, PHA content also increased and became stable (4.8 mg PHA g dried biomass⁻¹) in MPC at day 13, suggesting that the accumulation of PHA and polysaccharides in *Chlorella* dominant consortia could not be mutually exclusive. By contrast, CDC showed a somewhat inconsistent PHA accumulation during the operation of nutrient-stressed FP-PBR, reaching up to 3.7 mg PHA g dried biomass⁻¹ after 15 d. To the authors' best knowledge, this is one of the first studies to assess the photoautotrophic PHA production in *C. sorokiniana*-dominated consortium. Previous reports on this strain have had somewhat contradicting results under mixotrophic conditions, achieving from 4 to 295 mg PHA g dried biomass⁻¹ (Alcántara et al., 2015; Kumari et al., 2022). Results emphasized future studies to develop a photo-mixotrophic mode of operation to assess *C. sorokiniana* PHA production.

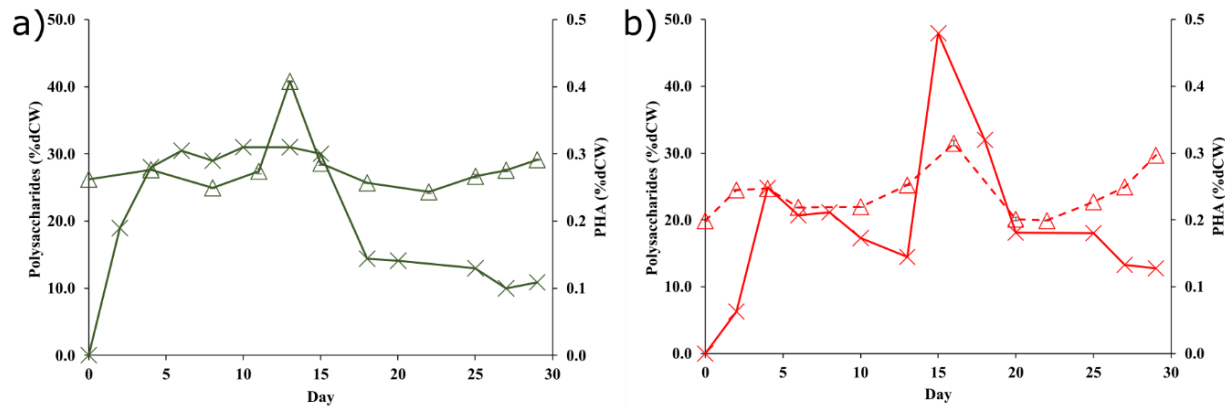


Figure 3.3. Changes in PHA (X) and polysaccharides (Δ) values *Chlorella sorokiniana*-dominated consortia (a) and mixed photosynthetic consortium (b) cultures in nutrient unbalanced growth medium. Error bars represent standard deviation of the mean value.

The consensus is that polysaccharides and, eventually, PHA synthesis and accumulation are positively triggered and stabilized over time by removing N sources (Koch and Forchhammer, 2021; Sirohi et al., 2021). Nonetheless, findings in our study are a valuable addition to the expanding body supporting the idea that certain P levels lead to a relative reduction in the PHA content, even under N stress. Kamravamanesh et al. (2019) reported that after introducing 9.6 mg P L^{-1} in polymer accumulating PBR fed with BG-11 N-limited, a 10% decrease in the PHA accumulation yield was observed. Their results suggest that the availability of P prompted the dominant cyanobacterial species (*Synechocystis* sp.) to prioritize polysaccharides (*i.e.*, glycogen) synthesis over PHA synthesis to sustain cell maintenance. More recent studies further evidenced that even under P concentrations in the range of 1.4 to 3.0 mg P L^{-1} , PHA production stops altogether and decreases to less than $10 \text{ mg PHA g dried biomass}^{-1}$ (Rueda et al., 2022b; Singhon et al., 2021).

Finally, an analogous study was carried out by Rueda et al. (2020a) in mixed consortia using an N and P feast and famine strategy for polymer production. Their research reported an average accumulation of $20 \text{ mg PHA g dried biomass}^{-1}$ and $400 \text{ mg glucose g dried biomass}^{-1}$. They also suggested that different C (inorganic for PHA production and organic for PHA/Polysaccharides production) stimulate the accumulation of different polymers under unbalanced nutrient conditions. Although the preparation of BG-11 -NP in the present study does not involve adding organic C sources, and DIC was continuously sparged into the growth medium (Fig. 3.4), an enhanced accumulation of PHA was not observed. Given our improved polysaccharides production, the

supplementation of exogenous organic C by cellular death (due to extended culturing under nutrient stress) and the semi-open operation of FP-PBR are also crucial to control the PHA production process.

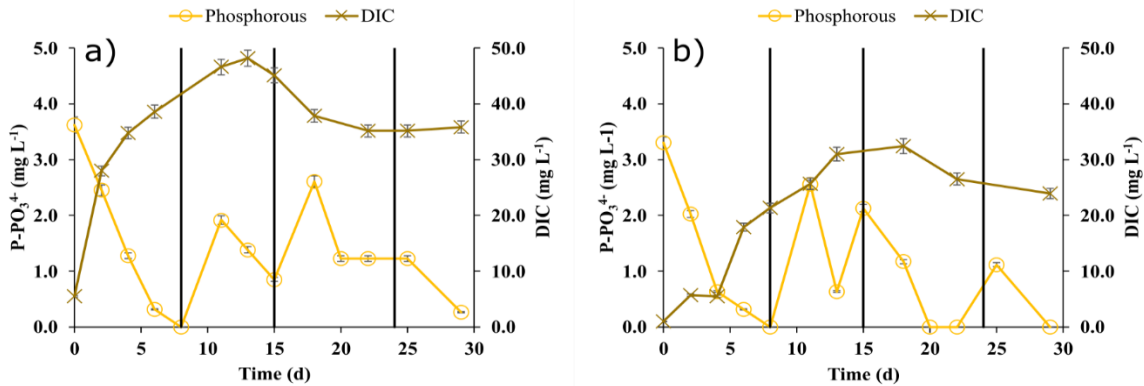


Figure 3.4. Phosphorous and dissolved inorganic carbon (DIC) dynamics for (a) *C. sorokiniana*-dominated consortium and (b) mixed photosynthetic consortium cultures under nutrient stressed conditions. Bold lines represent time intervals were phosphorous was added. Error bars represent standard deviation of the mean value.

3.4. Conclusion

A mixed photosynthetic and *Chlorella* dominant consortia were prospected for the first time for photoautotrophic production of polysaccharides and polyhydroxyalkanoates under nutrient stress. Maximum polysaccharides and polyhydroxyalkanoates accumulation values in the *Chlorella* consortium were 320 ± 24 mg glucose g dried biomass⁻¹ and 4 mg PHA g dried biomass⁻¹ after 15 d of nitrogen starvation, phosphorous limitation, and constant inorganic carbon availability. Conversely, under these conditions, the mixed sludge photosynthetic consortium achieved 460 ± 16 mg glucose g dried biomass⁻¹ and 5 mg PHA g dried biomass⁻¹ after 15 d and 13 d, respectively. Findings in this study highlight the potential of mixed phototrophic consortia from waste effluents and contaminated sources as a novel and sustainable approach for polyhydroxyalkanoates and polysaccharide accumulation. Although our knowledge of polysaccharide metabolism in algae has expanded considerably in the last years, further studies are needed to fully understand the specific kinetics of starch and glycogen conversion into polyhydroxyalkanoates to sustain a long-term production and ultimately combine waste effluent treatment and bioplastic production.

4. Municipal wastewater treatment and polyhydroxybutyrate production using *Synechocystis* sp. under oxygen-controlled conditions

Reference to be submitted:

Romero-Frasca, E., Buitrón, G., González-Sánchez, A., Etchebehere, C. (2024). Municipal wastewater treatment and polyhydroxybutyrate production using *Synechocystis* sp. under oxygen-controlled conditions.

Abstract

The use of photosynthetic microorganisms to produce polyhydroxybutyrate (PHB) at the same time as treating wastewater is a very promising alternative for the sustainable production of bioplastics. Oxygen concentration is a key parameter as it is needed for biomass growth, but an excess of oxygen can lead to futile metabolic processes decreasing the PHB production. This study examined the effect of different dissolved oxygen concentrations on the production of polyhydroxybutyrate by *Synechocystis* sp. grown in mineral medium and municipal wastewater. The experimental setup consisted of a two-stage process: i) growth stage, to maximize biomass production through nutrient abundance, and ii) accumulation stage, to induce polyhydroxybutyrate production through nitrogen limitation. During the accumulation stage in the mineral medium, *Synechocystis* sp. was subjected to three dissolved oxygen concentrations, 8.0, 6.5, and 1.2 mgO₂ L⁻¹. The production of polyhydroxybutyrate in municipal wastewater was evaluated using the best dissolved oxygen concentration that had been previously determined. Results showed that lowering dissolved oxygen concentration in mineral medium to 1.2 mgO₂ L⁻¹ maximized polyhydroxybutyrate content in *Synechocystis* sp. up to 12% dCW (95 mg L⁻¹). Moreover, adding *Synechocystis* sp. in municipal primary effluent led to high removal rates of chemical oxygen demand (92%), ammonia nitrogen (99%), and phosphorus as orthophosphates (88%), resulting in a nitrogen-limited state after 12 days of cultivation. The nitrogen limitation and a low dissolved oxygen concentration (5.7 mgO₂ L⁻¹) achieved a polyhydroxybutyrate content of 10% dCW (80 mg L⁻¹) in municipal primary effluent. These results provide a first insight into nitrogen limitation and dissolved oxygen management as a combined strategy to maximize the photoautotrophic polyhydroxybutyrate production by *Synechocystis* sp.

Keywords: Biopolymers; Cyanobacteria; Nitrogen; Oxygen; PHB; Photorespiration; Wastewater

4.1. Introduction

The growing sustainability concerns surrounding non-degradable, fossil-based plastic waste have prompted an extensive search for biodegradable, bio-based sources for plastic manufacturing. Aliphatic polyesters like polyhydroxyalkanoates (PHAs) have emerged as outstanding candidates (Kannah et al., 2022). PHAs are distinguished from other bio-based polymers because of their i) excellent biodegradability and biocompatibility, ii) similar thermoplastic and mechanical properties to fossil-based polymers, and iii) procurement from biomass (Cheah et al., 2023). Among the over 150 types of PHAs currently known, polyhydroxybutyrate (PHB) stands out as the most prevalent alternative, given its wide range of industrial applications and occurrence in microorganisms. These include certain prokaryotic bacteria species like Gram-negative bacteria *Cupriavidus necator* and cyanobacteria like *Synechocystis* sp. (Koch et al., 2020b). While *C. necator* can produce nearly 90% of PHB as dry cell weight (dCW), its substrate and maintenance costs are relatively higher than those of fossil-based plastics (Bellini et al., 2022). Consequently, *Synechocystis* sp. has become a promising platform for PHB production due to their minimum nutrient requirements, carbon dioxide fixation, and ability to grow using waste effluents (Mastropetros et al., 2022).

Photoautotrophic production of PHB from *Synechocystis* sp. follows a two-stage cultivation method. First, these microorganisms are grown under nutrient-abundant conditions (growth stage) and then exposed to stress conditions, like nitrogen limitation, to stimulate PHB production (accumulation stage) (Lee et al., 2021). This approach has led to a relatively moderate content ($\leq 10\%$ dCW or 69 mg L^{-1}) in *Synechocystis* sp. when compared to Gram-negative bacteria (Sirohi et al., 2021). As a result, extensive efforts have been made to improve the PHB content in these microorganisms. During the growth stage, the dissolved oxygen (DO) concentration frequently exceeds oxygen-air saturation conditions (7.1 to $19 \text{ mgO}_2 \text{ L}^{-1}$) as a result of photoautotrophic growth (Arias et al., 2018; Rueda et al., 2022b). This excess in the DO concentration persists into the accumulation stage, triggering futile metabolic processes such as photorespiration, which is used to decrease oxidative stress (Gao et al., 2022). Photorespiration is known to impair the efficiency of ribulose-1,5-bisphosphate carboxylase/oxygenase (RuBisCO) carboxylase activity by increasing its specificity for oxygen, *i.e.*, oxygenase activity. The resulting RuBisCO oxygenase activity produces 2-Phosphoglycolate (2PG), an inhibiting metabolite for the most crucial carbon pathway for PHB production, *i.e.*, Embden-Meyerhof-Parnas (EMP) pathway (Koch et al., 2019).

The elevated 2PG concentration further results in increased energy (ATP) and reducing equivalents (NADPH) demand and the loss of up to 50% of the carbon that is fixed during photosynthesis (Toro-Huertas et al., 2019). Given that NADPH also participates in the production of PHB during nitrogen limitation (Koch et al., 2020a; Sukkasam et al., 2022), RuBisCO oxygenase activity possibly interferes with PHB production due to competition for this reducing equivalent under DO concentration above oxygen-air saturation levels.

Thus far, the impact of oxygen concentration during the production of PHB in *Synechocystis* sp. has been explored by gas exchange limitation. Panda and Mallick (2007) were among the first to observe that oxygen concentration played a vital role in the production of PHB. These authors reported that PHB content in *Synechocystis* sp. cultured in a mineral medium was maximized from 7.1 % dCW to more than 10% dCW under a combined nitrogen-limitation, organic carbon addition, and gas exchange limitation. These conditions also decreased oxygen concentration from 13 mgO₂ L⁻¹ (control) to 5.1 mgO₂ L⁻¹. However, further studies failed to replicate these findings for photoautotrophic production of PHB. Kamravamanesh et al. (2017) reported that *Synechocystis* sp. grown under a photoautotrophic mode of cultivation in a gas-exchanged and nitrogen-limited environment resulted in a reduced PHB concentration (less than 2.2% dCW). Although the oxygen concentration was not directly measured, the authors suggested that gas exchange limitation alone was insufficient to avoid oxygen build-up during photoautotrophic production of PHB, and other experimental conditions that could have sustained oxygen evolution. Therefore, strategies that affect the oxygen-evolving system are needed to decrease oxygen concentration and maximize photoautotrophic production of PHB. Previous studies have effectively inhibited the oxygen-evolving system of eukaryotic algae through high light intensities, *i.e.*, above 2000 μmol m⁻² s⁻¹, for brief periods, resulting in oxygen-limited conditions (Degrenne et al., 2011; Markov et al., 2006). The present study aims to systematically evaluate the effect of different concentrations of oxygen on the growth performance, photosynthetic activity, and PHB content of nitrogen limited *Synechocystis* sp. cultures. To this end, various concentrations of DO were maintained through physical (sparging with nitrogen gas and with air) oxygen stripping protocols during the accumulation stage. The present study also tested simultaneous wastewater treatment and PHB production in *Synechocystis* sp. cultures using photoinhibition as an oxygen-control strategy.

4.2. Materials and methods

4.2.1. Strain and inoculum preparation

Experiments were conducted using *Synechocystis* sp. strain 2470 (hereafter referred to as *Synechocystis* sp.) obtained from the University of Texas at Austin Culture Collection of Algae (UTEX, USA). A fresh inoculum was generated under controlled laboratory conditions in agar slant tubes with BG11 mineral medium (Vital-Jácome et al., 2020), adding 2% agar (solid medium). The inoculum was incubated at room temperature (25 ± 5 °C) and continuously illuminated using cool-white, fluorescent lamps, providing a Photosynthetically Active Radiation (PAR) of $45 \mu\text{mol photons m}^{-2} \text{ s}^{-1}$. A sample of *Synechocystis* sp. was taken and transferred to a fresh solid BG11 mineral medium every four weeks to keep the cultures under exponential growth.

4.2.2. Experimental setup and cultivation conditions

Trials in mineral medium

To investigate the effect of different DO concentrations on the PHB content of *Synechocystis* sp., a two-stage cultivation method was employed where cultures would be i) subjected to nutrient-abundant conditions to grow biomass (growth stage) and ii) limited in nitrogen to induce PHB production (accumulation stage). A constant pH (7.1 ± 0.2) was maintained in both stages by introducing a 20 mM HEPES-NaOH buffer solution. All cultures were incubated at room temperature (25 ± 5 °C), exposed to a PAR of $45 \mu\text{mol photons m}^{-2} \text{ s}^{-1}$ following 12 h light/dark cycles, and agitated using a magnetic stirrer set at 220 rpm. The concentration of DO in *Synechocystis* sp. cultures during mineral medium trials is presented in Figure 4.1.

For the growth stage, fresh inoculum of *Synechocystis* sp. was transferred into 1-L Erlenmeyer flasks containing 800 mL (working volume) of modified BG11 mineral medium (BG11+N), consisting of the following components: 1.0 mg L^{-1} Na_2MgEDTA , 6.0 mg L^{-1} $(\text{NH}_4)_5[\text{Fe}(\text{C}_6\text{H}_4\text{O}_7)_2]$, 1500 mg L^{-1} NaNO_3 , 6 mg L^{-1} $\text{C}_6\text{H}_8\text{O}_7 \cdot \text{H}_2\text{O}$, 36 mg L^{-1} $\text{CaCl}_2 \cdot 2\text{H}_2\text{O}$, 75 mg L^{-1} $\text{MgSO}_4 \cdot 7\text{H}_2\text{O}$, 40 mg L^{-1} K_2HPO_4 , 20 mg L^{-1} Na_2CO_3 , 4000 mg L^{-1} NaHCO_3 , and 1.0 mL L^{-1} of A5 trace metals. Carbon (Na_2CO_3 , NaHCO_3) and phosphorous (K_2HPO_4) sources were modified to achieve a C:N:P molar ratio of 106:34:1 (Redfield ratio), recommended to sustain prolonged cultivation of this cyanobacterium (Arias et al., 2019). These cultures were maintained in nutrient-abundant conditions for 11 days. For the accumulation stage, biomass from the growth stage was harvested by centrifugation (3000 g, 20 min, 5 °C) and washed with distilled water to remove traces

of BG11+N mineral medium. Washed biomass pellets were then transferred to 250-mL Erlenmeyer flasks equipped with vented caps at an initial optical density OD_{680} of 0.150 ± 0.050 , containing 200 mL of modified BG11 mineral medium without $NaNO_3$ (BG11-N) at different concentrations of DO. A first set of four Erlenmeyer flasks was prepared as a positive control for PHB production, for which no gas sparging was provided. DO concentration reached oxygen-air oversaturation conditions ($8.0 \pm 2.1 \text{ mgO}_2 \text{ L}^{-1}$). In contrast, a second set of four Erlenmeyer flasks was continuously sparged with filtered air to ensure a constant DO concentration at oxygen-air saturation conditions ($6.5 \pm 0.4 \text{ mgO}_2 \text{ L}^{-1}$). Finally, a third set of four Erlenmeyer flasks was sparged with filtered, ultrapure nitrogen gas ($\geq 99.9\%$, CRIOGAS, Mexico) to maintain a DO concentration below oxygen-air saturation conditions, corresponding to $1.2 \pm 0.4 \text{ mgO}_2 \text{ L}^{-1}$. A constant inorganic carbon concentration was kept at a 106:1 C:P ratio by adding 2 mL of sodium bicarbonate salt with a 4 g C L^{-1} concentration.

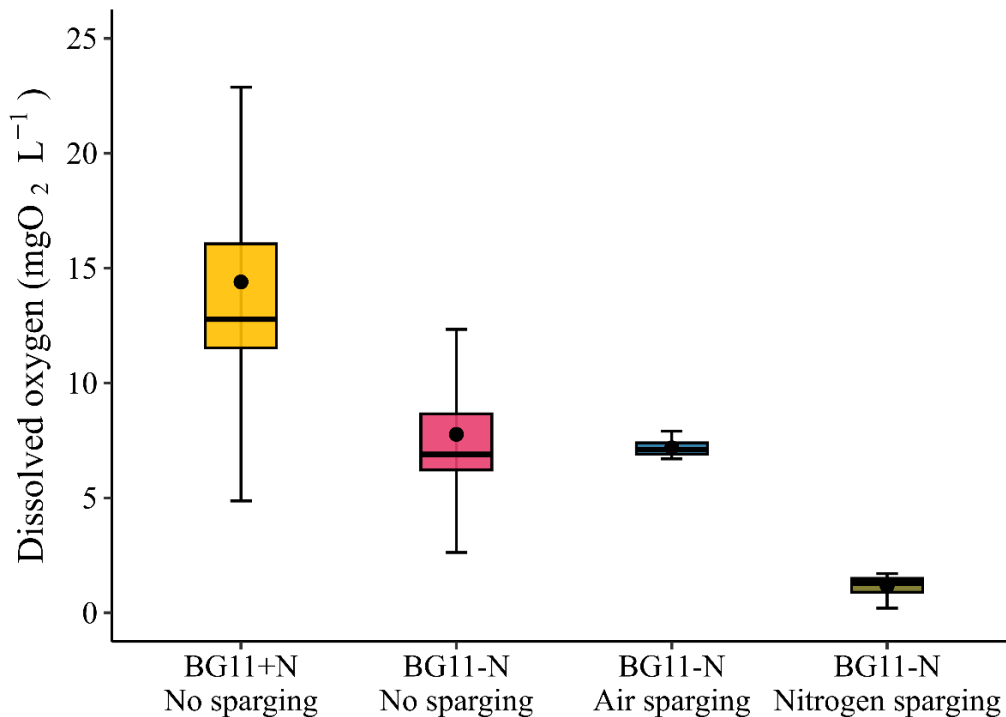


Figure 4.1. Boxplot showing the dissolved oxygen concentration measured in *Synechocystis* sp. cultures during mineral medium trials. The lower boundary of the box indicates the 25th percentile, a line within the box marks the median, and the upper boundary of the box indicates the 75th percentile. Whiskers (error bars) above and below the box indicate the 90 and 10th percentiles, respectively. Black circles indicate the mean value. Nitrogen addition (+N) and nitrogen-limited (-N).

Trials using wastewater effluent

To investigate the effect of DO on simultaneous wastewater treatment and PHB content in *Synechocystis* sp., the effluent from a primary sedimentation tank of a municipal wastewater treatment plant located in Queretaro, Mexico, was selected. The DO concentration that presented the highest PHB accumulation yield in the previous experiment was reproduced for the wastewater trial. Fresh inoculums of *Synechocystis* sp. were transferred to two 1-L Erlenmeyer flasks containing 800 mL of effluent from the primary sedimentation tank (growth stage) following the two-stage cultivation method previously described. The average composition of the municipal wastewater used in this study is summarized in Table 4.1. Nutrients were periodically monitored to detect when the culture had depleted all the nitrogen, and the accumulation stage began. Once nitrogen became limited, *i.e.*, when the N:P ratio below 16:1 mole basis was achieved, a high photo-dense PAR ($\geq 2000 \mu\text{mol m}^{-2} \text{s}^{-1}$) was maintained during brief photoperiods of 30 min to control the DO concentration. The previous conditions were also applied to a control consisting only of wastewater.

Table 4.1 Characteristics of the wastewater effluent from the primary sedimentation tank of a municipal wastewater treatment plant.

Parameter	Concentration, mg L ⁻¹
Dissolved Organic Carbon (DOC)	306 ± 1.1
Dissolved Inorganic Carbon (DIC)	150 ± 3.8
Chemical Oxygen Demand (COD)	789 ± 13
Nitrogen, ammonia (NH ₄ ⁺ -N)	108 ± 1.4
Nitrogen, nitrates (NO ₃ ⁻ -N)	6.3 ± 0.1
Phosphorous, orthophosphates (PO ₄ ³⁻ -P)	16 ± 0.3
N:P ^a	16:1

^a Ratio in mole base

4.2.3. Analytical procedures

The growth of *Synechocystis* sp. biomass was determined as optical density OD₆₈₀ following the 2120 C spectrophotometric method described by APHA-AWWA-WPCF (2023) using a VE-

5600UV UV-VIS spectrophotometer (Velab, USA). The growth rate was calculated via linear regression plotting $\ln OD_{680}$ vs. time. Photosynthetic activity yield, measured in terms of Photosystem II quantum yield (QY), was determined using an AquaPen AP 110-C PAM fluorometer (Photon Systems Instruments, Czech Republic). Samples for analyzing nutrients in wastewater trials were filtered through 0.45 μ m pore-size filters. DIC and DOC concentration was determined using a TOC 5050 total organic carbon analyzer (Shimadzu, Japan), whereas soluble COD, NH_4^+ -N, and PO_4^{3-} were measured using the 8000, 10031, and 10127 Hach colorimetric methods, respectively. NO_3^- -N was measured using a DIONEX ICS1500 ion chromatography (Thermo Scientific, USA).

PHB was digested, extracted, and quantified through Agilent 6890B gas chromatograph (Agilent Technologies, USA) following the method described in Montiel-Corona and Buitrón (2022), with minor modifications. Mixed liquor samples were collected, centrifuged, and spread in glass trays. Samples were dried at 60 °C for 24 h and 15-20 mg of dried biomass were placed in a glass test tube with a Teflon liner screw cap. 2.0 mL volume of acidified (2 % v/v H_2SO_4) methanol and 2.0 mL of chloroform were added. After vortexing for 1 min, the solution was incubated in an AccuBlock digital dry bath (Labnet International, USA) for 24 h at 120 °C and then cooled at room temperature. 1.0 mL of deionized water was added to each tube and vortexed. The bottom layer (chloroform) was retrieved through a glass Pasteur pipette and filtered through a 0.45 μ m pore-size nylon membrane filter. A volume of 1.0 mL from the filtrate was collected, and 1.0 μ L was injected into the gas chromatograph. PHB and PHV (polyhydroxyvalerate) concentrations were determined through a standard curve generated from natural origin Poly[(R)-3-hydroxybutyric acid-co-(R)-3-hydroxyvaleric acid].

4.2.4. Statistical analysis

Analytical measurements were performed in duplicates. All statistical analyses were conducted using the RStudio open-source software package (RStudio PBC, Boston, U.S.A.) under the R version 4.3.1 (R Core Team, USA) environment. Data presented in tables and figures were calculated as mean values, with corresponding standard deviation values, using the `get_summary_stats` function of the `rstatix` (Kassambara, 2023) package. Statistically significant differences ($p \leq 0.05$) were determined through a one-way analysis of variance followed by a Tukey's honestly significant difference post-hoc test, using the functions `aov` and `HSD.test` of the

rstatix (Kassambara, 2023) and agricolae (Mendiburu, 2023) packages, respectively.

4.3. Results and discussion

4.3.1. Growth performance and photosynthetic activity of *Synechocystis* sp. in mineral medium

An exponential growth of *Synechocystis* sp. was observed during the growth stage (Fig. 4.2a), indicating that cells were proliferating. However, the calculated growth rate for this stage was $0.305 \pm 0.011 \text{ d}^{-1}$, notably lower than the standard value (2.160 d^{-1}) expected for this strain in mineral medium at below (60 to 100%) oxygen-air saturation levels (van Alphen et al., 2018). Interestingly, the observed photosynthetic activity yield for *Synechocystis* sp. during the growth stage (Fig. 4.2b) fell within the optimal QY range (0.5-0.7) for photoautotrophic growth, suggesting that cells were metabolically active and under nutrient-sufficient conditions (Rohit and Venkata Mohan, 2018). These results demonstrate the detrimental effect of high DO concentrations on *Synechocystis* sp. growth, given their above oxygen-air saturation levels ($14 \text{ mgO}_2 \text{ L}^{-1}$). Similar findings were reported by Raso et al. (2012), where the growth rate of *Nannochloropsis* sp. grown in the mineral medium was decreased from 0.500 d^{-1} to 0.180 d^{-1} when DO concentration increased from 100% oxygen-air saturation level to 250 % oxygen-air saturation level. Their results were correlated to an increasing oxygenase activity in RuBisCO as the DO concentration increased. Marquez et al. (1995) reported a 36% reduction in the growth rate of *Spirulina platensis* when DO increase from $2 \text{ mgO}_2 \text{ L}^{-1}$ to $40 \text{ mgO}_2 \text{ L}^{-1}$, associated with a deterioration of photosynthetic pigments caused by photooxidative inhibition.

Similar biomass concentrations and growth rates were obtained during the accumulation stage for all *Synechocystis* sp. cultures (Fig. 4.2a). *Synechocystis* sp. cultures subjected to no sparging ($8.0 \text{ mgO}_2 \text{ L}^{-1}$), air sparging ($6.5 \text{ mgO}_2 \text{ L}^{-1}$), and nitrogen sparging ($1.2 \text{ mgO}_2 \text{ L}^{-1}$) presented a growth rate of $0.154 \pm 0.006 \text{ d}^{-1}$, $0.195 \pm 0.019 \text{ d}^{-1}$, and $0.144 \pm 0.008 \text{ d}^{-1}$, respectively. Likewise, the photosynthetic activity for *Synechocystis* sp. cultures significantly decreased from 0.6 to less than 0.2 on day 5 for all cases (Fig. 4.2b). Statistical analysis showed that the growth rate and photosynthetic activity during the accumulation stage were significantly lower ($p \leq 0.05$) than their corresponding values during the growth stage. Nonetheless, no significant differences in biomass growth and photosynthetic activity were observed between the different DO concentrations tested during the accumulation stage. These findings suggest that *Synechocystis* sp.

biomass growth and photosynthetic activity were not affected by oxygen stripping, and their low values could be attributed to the deprivation of nitrogen sources during the accumulation stage, *i.e.*, $\leq 1.0 \text{ mgNO}_3^- \text{-N L}^{-1}$. Nitrogen is the second most abundant element in any microalgae biomass, reaching up to 10% in dry mass, and it is essential to produce several biochemical compounds, including photosynthetic pigments (Morales-Plasencia et al., 2023). Thus, a partial or total lack of nitrogen supply results in limited photosynthetic activity and decreased growth performance (Singhon et al., 2021). Further studies aimed at monitoring the photosynthetic activity of *Synechocystis* sp. during nitrogen limitation also revealed that QY notably reduced because of the degradation and reorganization of light-harvesting systems to avoid photoinhibition (Lakatos et al., 2021).

It is essential to mention that from day 5 onward, *Synechocystis* sp. cultures in the accumulation stage subjected to non-sparged ($8.0 \text{ mgO}_2 \text{ L}^{-1}$) and air-sparged ($6.5 \text{ mgO}_2 \text{ L}^{-1}$) conditions increased their photosynthetic activity yield once more (Fig. 4.2b). In contrast, *Synechocystis* sp. cultures under gaseous nitrogen sparging ($1.2 \text{ mgO}_2 \text{ L}^{-1}$) continued to maintain a low photosynthetic activity yield ($\text{QY} \leq 0.1$). These differences could be linked to a limited futile electron-consuming processes that below oxygen-air saturation conditions and nitrogen limitation caused in stressed microalgae cells. At high DO concentrations, photorespiration is normally activated as alternative electron sinks that use the flux of energy and electrons from the photosynthetic electron transport chain to maintain cellular homeostasis (Kazbar et al., 2019). However, this photorespiratory activity can be avoided through suitable oxygen stripping or carbon-to-oxygen adjustment methods. Gao et al. (2022) reported that adding inorganic carbon salts during *Monoraphidium minutum* 26B-AM and *S. obliquus* UTEX393 growth increased their biomass productivity by up to 37%. These authors associated their results with the fact that inorganic carbon salts were converted to carbon dioxide and increased the carboxylase activity of RuBisCO, thus overcoming photorespiratory activity. Toro-Huertas et al. (2019) also reported that photorespiratory activity in outdoor photobioreactors used for biogas upgrading could be controlled by managing irradiance and temperature. In their study, maintaining an average temperature between $24 \text{ }^\circ\text{C}$ and $30 \text{ }^\circ\text{C}$ with irradiances ranging from $50 \text{ } \mu\text{mol m}^{-2} \text{ s}^{-1}$ to $2000 \text{ } \mu\text{mol m}^{-2} \text{ s}^{-1}$ allowed a better carbon dioxide fixation from biogas sparging.

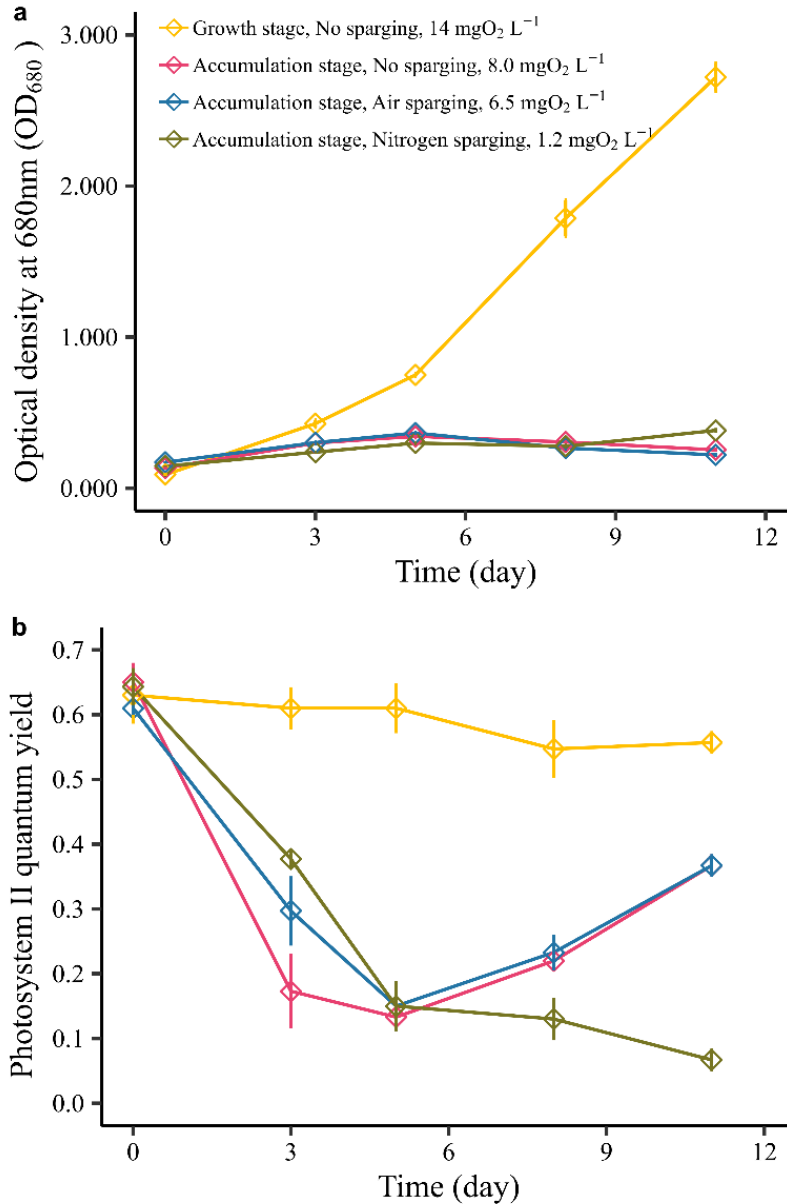


Figure 4.2. Changes in the (a) biomass concentration and (b) photosynthetic activity of *Synechocystis* sp. cultures during the growth stage and the accumulation stage.

4.3.2. PHB analysis in the cultures of *Synechocystis* sp. grown in mineral medium

During the growth stage, *Synechocystis* sp. cultures presented a negligible PHB content (Fig. 4.3). These observations further prove that unbalanced growth conditions (nitrogen limitation) initiate the production of PHB in *Synechocystis* sp. (Koch and Forchhammer, 2021). The persistent nitrogen limitation during the accumulation stage caused a significant increase ($p \leq 0.05$) in the

PHB content of *Synechocystis* sp. Cultures of *Synechocystis* sp. subjected to non-sparged ($8.0 \text{ mgO}_2 \text{ L}^{-1}$) and air-sparged ($6.5 \text{ mgO}_2 \text{ L}^{-1}$) conditions exhibited a similar PHB content of $9.4 \pm 0.4\%$ dCW (23 mg L^{-1}) and $9.7 \pm 0.2\%$ dCW (25 mg L^{-1}) after 11 days of operation, respectively. The obtained PHB yields fall within the range previously reported for *Synechocystis* sp. (4.0 to 8.0% dCW) when cultured under nitrogen-limited and without DO control (Rueda et al., 2020a; Singhon et al., 2021).

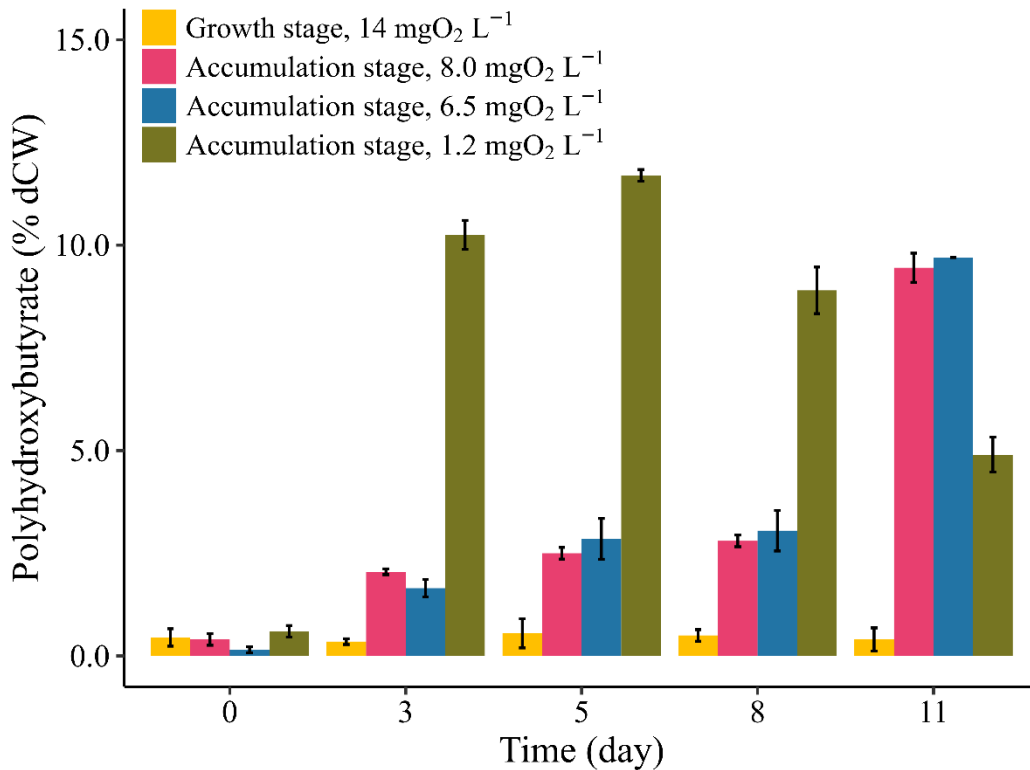


Figure 4.3. PHB content in *Synechocystis* sp. cultures during growth and accumulation stages in the mineral medium.

Synechocystis sp. cultures subjected to nitrogen sparging ($1.2 \text{ mgO}_2 \text{ L}^{-1}$) exhibited the statistically highest PHB content on day 5, reaching a maximum value of $12 \pm 0.1\%$ dCW or 95 mg L^{-1} , respectively. As previously discussed, these results could be attributed to the successful limitation of electron-consuming processes, like photorespiration, given their low DO concentration and inorganic carbon addition. Previous studies have observed that regulating RuBisCO activity successfully maximized PHB content in nitrogen limited *Synechocystis* sp. PCC 6803. Tharasirivat and Jantaro (2023) reported a higher PHB content because of the overexpression of rbc LXS operons. That operon encodes the small subunits of proteins that assemble into carbon

dioxide-fixing enzymes. The sodium bicarbonate supplementation allowed the photosynthetic electron transport chain to flow continuously, yielding an increased NADPH pool. Given that the RuBisCO oxygenase activity was suppressed due to inorganic carbon addition, the flux of intermediate metabolites from carbon dioxide fixation was mostly diverted to PHB production. Although the proteins or metabolic activity related to the RuBisCO enzyme were not directly monitored in this study, it could be argued that their oxygenase activity was negligible given the low DO concentration, excess of bicarbonate salts, and highly reduced state observed in cultures subjected to nitrogen sparging (1.2 mgO₂ L⁻¹). The strategic combination of nitrogen limitation and oxygen stripping during the accumulation stage exhibited higher PHB productivities compared to other research works (Table 4.2), indicating the benefits of this approach.

Table 4.2 Comparison of the maximum polyhydroxybutyrate (PHB) values obtained in this study with the results obtained in other studies using *Synechocystis* sp. cultures.

Nutrient limited	Oxygen stripping	Dissolved oxygen concentration	Time of incubation	Maximum PHB		References
		mgO ₂ L ⁻¹	Days	% dCW	mg L ⁻¹	
Nitrogen	Yes	1.2	5	12	95	This study
Nitrogen	No	8.0	11	10	25	This study
Nitrogen Phosphorous	No	≥ 8.0*	21	11	n.r.	Meixner et al. (2022)
Phosphorous	No	≥ 8.0*	35	6.8	n.r.	Singhon et al. (2021)
Nitrogen	No	≥ 8.0*	14	5.0	16	Rueda et al. (2020a)

n.r.: Not reported.; * Approximate value.

4.3.3. Evaluation of *Synechocystis* sp. performance grown in municipal wastewater

A new set of experiments was conducted below oxygen-air saturation conditions to check whether DO concentration would also affect the production of PHB in *Synechocystis* sp. in municipal primary effluent. These conditions were selected based on the PHB content results from section 3.2. In the below-oxygen-air saturation conditions, wastewater was used for the accumulation

stage. Tests were not sparged with nitrogen gas to avoid transforming nitrogen gas into bioavailable forms by diazotrophs (Saidu et al., 2022). Instead, an oxygen stripping protocol based on high, short pulses of photo-dense PAR ($\geq 2000 \mu\text{mol m}^{-2} \text{s}^{-1}$) was selected because the inhibition of the Photosystem II (oxygen evolution) activity and maintenance of a stable the Photosystem I activity, in charge of photosynthetic electron transport chain (Jokel et al., 2019). The average DO concentration during the accumulation stage of the wastewater trial by using the high, short pulses of photo-dense PAR oxygen stripping protocol was $5.7 \text{ mgO}_2 \text{ L}^{-1}$ (Fig. 4.4).

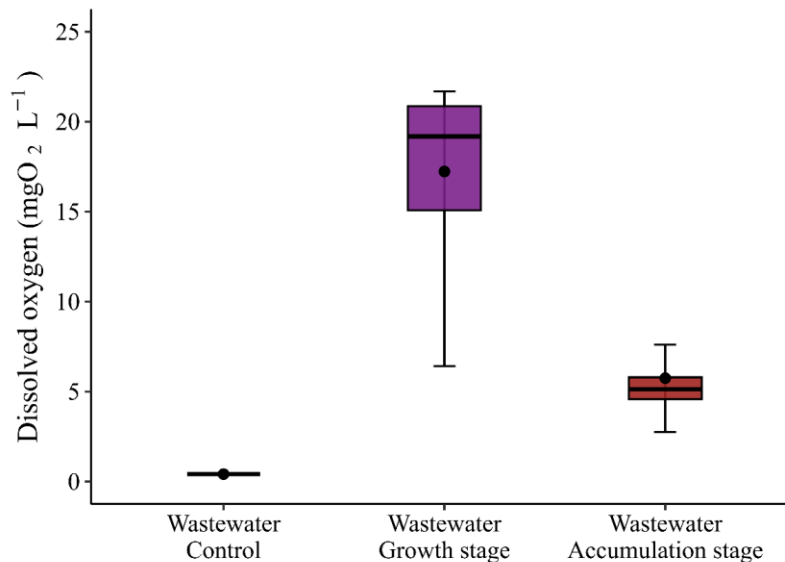


Figure 4.4. Boxplot showing the dissolved oxygen concentration in wastewater and in cultures of *Synechocystis* sp. in wastewater during growth and accumulation stages. The lower boundary of the box indicates the 25th percentile, a line within the box marks the median, and the upper boundary of the box indicates the 75th percentile. Whiskers (error bars) above and below the box indicate the 90 and 10th percentiles, respectively. Black circles indicate the mean value.

The results for nutrient concentration on wastewater at the end of the growth stage (12 d) and accumulation stage (11 d) are presented in Table 4.3. Removal of DOC varied between 49% (end of growth stage) and 52% (end of accumulation stage) in Erlenmeyer flasks containing only primary effluent (blank). Similarly, COD and $\text{PO}_4^{3-}\text{-P}$ also presented notable removal rates of 85% and 76%, respectively, at the end of the accumulation stage. This behavior suggests that bacteria from domestic wastewater primary effluent can remove organic matter and nutrients (Posadas et al., 2013). Cultivating *Synechocystis* sp. in primary effluent maximized the removal of nutrients in wastewater, resulting in a condition of nitrogen limitation (N:P molar ratio of 14:1) at the end of

the growth stage (12 d), compared to the results obtained for the blank. The removal of nutrients in cultures of *Synechocystis* sp. in primary effluent continued even under the nitrogen limitation state (accumulation stage), where DOC, DIC, COD, NH₄⁺-N, and PO₄³⁻-P reached a maximal removal of 71%, 97%, 92%, 99%, and 88%, respectively. This superior nutrient removal rate could be associated with the mutualistic interaction between microalgae, which encompass cyanobacteria, and heterotrophic bacteria from wastewater. This interaction has been extensively reported in the literature, where the oxygen provided by microalgae improves the assimilation of nutrients and organic matter oxidation carried out by bacteria (Aditya et al., 2022; Sayara et al., 2021).

Table 4.3 Nutrient concentration in the effluent obtained after growth and accumulation stages in primary effluent (blank) and in the cultures of *Synechocystis* sp. in primary effluent. Values represent the mean ± standard deviation, and parenthesis shows the average percentage removal according to the influent characterization.

Parameter	End of growth stage		End of the accumulation stage	
	Primary effluent (Blank)	Primary effluent <i>Synechocystis</i> sp.	Primary effluent (Blank)	Primary effluent <i>Synechocystis</i> sp.
	Concentration, mg L ⁻¹ (%)		Concentration, mg L ⁻¹ (%)	
Dissolved Organic Carbon (DOC)	155 ± 1.1 (49%)	148 ± 3.6 (51%)	146 ± 14 (52%)	89 ± 2.6 (71%)
Dissolved Inorganic Carbon (DIC)	111 ± 2.8 (26%)	86 ± 4.0 (42%)	43 ± 3.4 (71%)	4.5 ± 2.2 (97%)
Chemical Oxygen Demand (COD)	265 ± 5.1 (66%)	85 ± 16 (89%)	118 ± 10 (85%)	63 ± 1.0 (92%)
Nitrogen, ammonia (NH ₄ ⁺ -N)	104 ± 3.0 (3%)	28 ± 2.3 (74%)	100 ± 1.9 (8%)	1.5 ± 0.2 (99%)
Nitrogen, nitrates (NO ₃ ⁻ -N)	2.6 ± 1.6	3.1 ± 2.4	3.6 ± 2.5	1.6 ± 1.4
Phosphorous, orthophosphates (PO ₄ ³⁻ -P)	5.0 ± 1.6 (69%)	4.5 ± 0.9 (72%)	3.8 ± 1.5 (76%)	1.6 ± 0.8 (88%)
N:P ^a	46:1	14:1	59:1	4:1

^a Ratio in molar base

Biomass growth and photosynthetic activity in cultures containing primary effluent (blank) and *Synechocystis* sp. in primary effluent are presented in Figure 4.5. Insignificant biomass growth was observed in the blank cultures. However, photosynthetic activity notably increased on the last day of operation, suggesting that some microalgae were present. Milferstedt et al. (2017b) reported that microalgae could become the majority of the microbial community under temperature-controlled and illuminated conditions (90 to 200 $\mu\text{mol photons m}^{-2} \text{ s}^{-1}$). Further studies confirmed that these microalgae cells were, in fact, primarily filamentous cyanobacteria, which are harbored by sludge aggregates during wastewater treatment (Ansari et al., 2019). Maximum *Synechocystis* sp. biomass concentration, measured as the optical density at 680 nm during growth and accumulation stages in wastewater, were 0.706 ± 0.007 and 0.100 ± 0.001 g/L, respectively (Fig. 4.5a). Compared to mineral medium, the overall lower values could be attributed to an adaptation period. Meixner et al. (2016) reported the same extended acclimatization for *Synechocystis salina* upon transferring from nutrient-rich BG11 mineral medium to nutrient-diluted liquid digestate. The growth rates observed during the growth stage for both culture media were relatively similar: 0.305 d^{-1} in mineral medium and 0.388 d^{-1} in primary effluent. The same is true for the accumulation stage: 0.144 d^{-1} in mineral medium and 0.111 d^{-1} in primary effluent. Photosynthetic activity remained unchanged during the growth stage in primary effluent, *i.e.*, QY between 0.5 and 0.6 (Fig. 4.5b), when compared to the same stage in the mineral medium. As previously discussed, this could be attributed to the nutrient abundance in the growth medium. However, a similar decreasing photosynthetic activity was observed during the accumulation stage between *Synechocystis* sp. grown in mineral medium and municipal primary effluent, providing further evidence of the persistent nitrogen limitation effect on low photosynthetic activity. PHB content notably increased during the accumulation stage for *Synechocystis* sp. grown in municipal primary effluent (Fig. 4.6). A maximum value of $9.8 \pm 0.4\%$ dCW or 80 mg L^{-1} was observed on day 5 under nitrogen-limited, low dissolved oxygen ($5.7 \text{ mgO}_2 \text{ L}^{-1}$) conditions. That represents about 81% of the PHB value obtained in the mineral medium using nitrogen sparging. Compared to the literature, PHB content in *Synechocystis* sp. cultured in wastewater is superior to that obtained for *Synechocystis salina* when using nutrients from waste effluents without oxygen stripping (Kovalcik et al., 2017; Meixner et al., 2016).

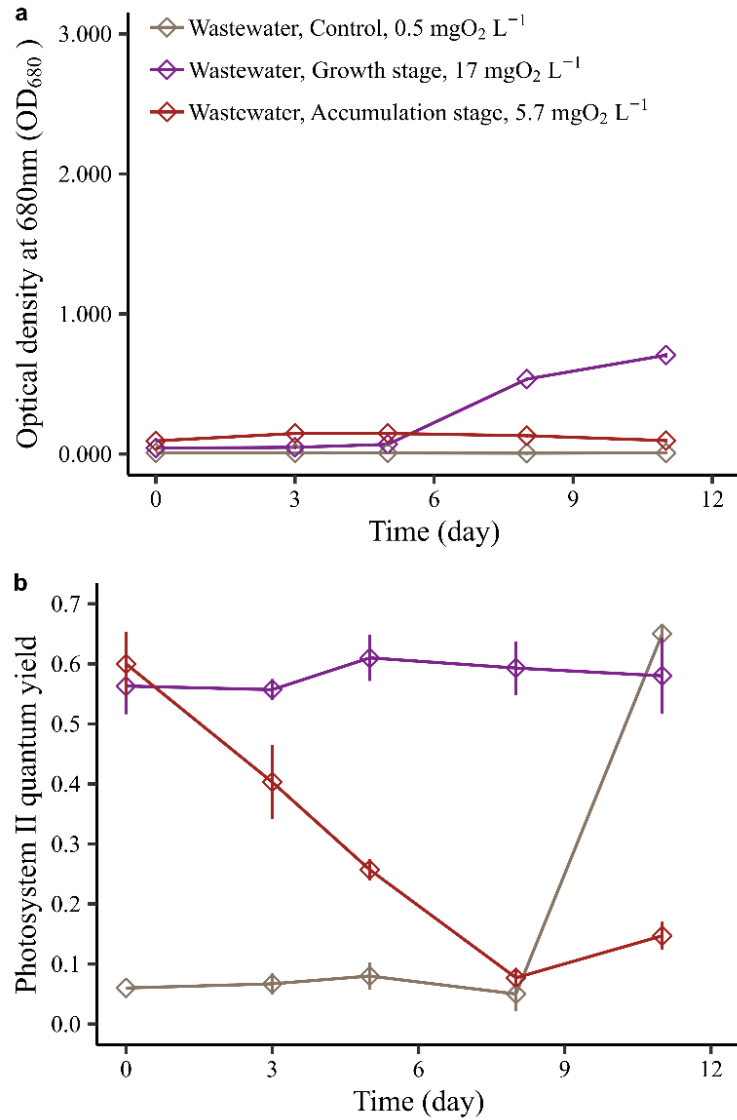


Figure 4.5. Monitoring of (a) biomass growth and (b) photosynthetic activity in *Synechocystis* sp. cultures performed in municipal primary effluent during growth and accumulation stages.

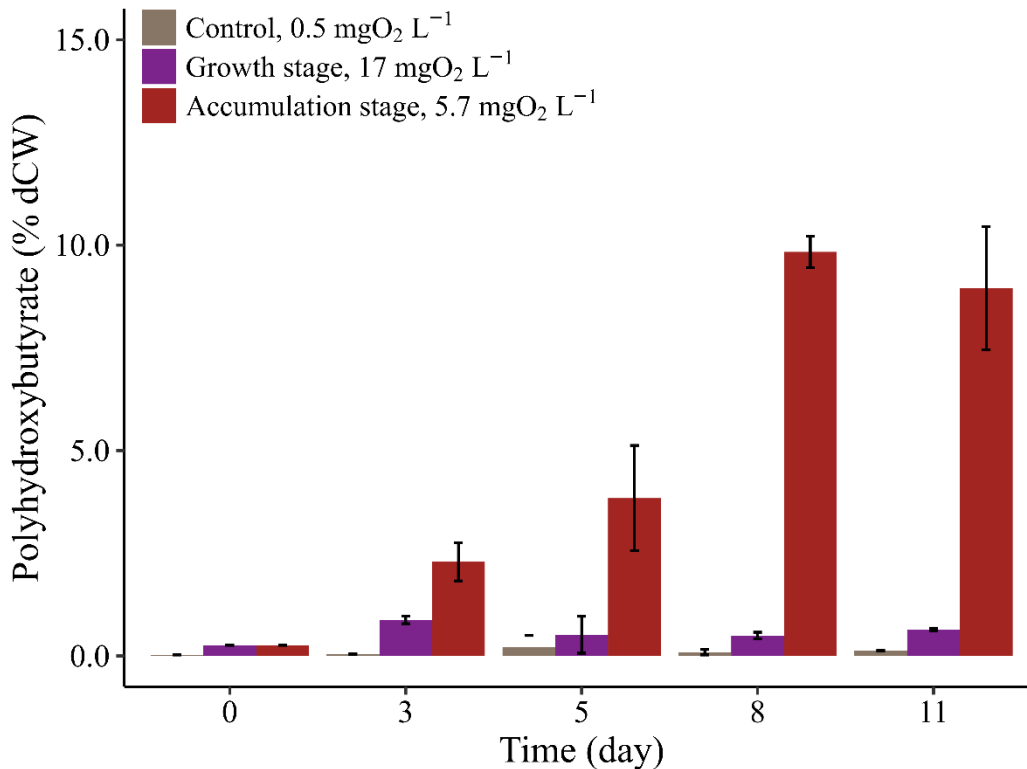


Figure 4.6. PHB content in *Synechocystis* sp. cultures during growth and accumulation stages using municipal wastewater.

4.4. Conclusion

Our results showed that the content of polyhydroxybutyrate was maximized by decreasing dissolved oxygen concentration under nitrogen limitation. It was found that changes in the photosynthetic activity occurred at a dissolved oxygen concentration of 1.2 mgO₂ L⁻¹, indicating that electron-consuming activities were limited. This allowed a higher polyhydroxybutyrate content (12% dCW or 95 mg L⁻¹) than other dissolved oxygen concentrations. In the experiment carried out using primary municipal effluent, it was observed that short photo-dense pulses of light achieved notable removal rates of chemical oxygen demand (92%), ammonia nitrogen (99%), and phosphorus as orthophosphates (88%) that resulted in a treated wastewater effluent. Moreover, the short photo-dense pulses of light also led to a dissolved oxygen concentration of 5.7 mgO₂ L⁻¹ owed to the inhibition of the Photosystem II activity, as observed by the decreasing quantum yield. Polyhydroxybutyrate content in *Synechocystis* sp. cultured in wastewater was about 9.8% dCW or 80 mg L⁻¹, superior to previous studies where no oxygen stripping was applied.

5. Bioaccessibility characterization of organic matter, nitrogen, and phosphorus from microalgae-bacteria aggregates

Reference to published paper:

Romero-Frasca, E., Galea-Outón, S., Coronado-Apodaca, K.G., Milferstedt, K., Jimenez, J., Hamelin, J., Buitrón, G. (2024). Bioaccessibility characterization of organic matter, nitrogen, and phosphorus from microalgae-bacteria aggregates. *Waste and Biomass Valorization*.

<https://doi.org/10.1007/s12649-024-02495-3>

Abstract

The quality of microalgae-bacteria biomass as an organic soil fertilizer may depend on the microbial composition, morphology, and growth history of the biomass. This study aims to characterize the molecular complexity and bioaccessibility of organic matter, nitrogen, and phosphorus from microalgae-bacteria aggregates with different morphologies (flocs and granules) grown under nutrient-abundant and starvation conditions. A biochemical fractionation method based on sequential chemical extraction and fluorescence spectroscopy was used. Microalgae-bacteria aggregates were cultured and collected from photobioreactors using contrasting growth conditions to generate i) loose flocs, ii) consolidated flocs, iii) smooth granules, and iv) filamentous granules. The organic matter, nitrogen, and phosphorus from consolidated flocs were mostly extractable, accounting for up to 94% of their total content, whereas the organic matter from loose flocs was up to 50% non-extractable. The extractability of loose flocs was improved under starvation conditions. All microalgae-bacteria aggregates showed a low structural complexity, corresponding to an abundance of simple microbial-related constituents like tyrosine, tryptophane, etc. Differences between the gradients of bioaccessibility for each microalgae-bacteria structure were related to the abundance of microorganisms and their metabolic products. The findings of this study have implications for the development of sustainable and environmentally friendly organic fertilizers.

Keywords: Biochemical fractioning; Biomass valorization; Fluorescence spectroscopy; Nutrients bioaccessibility; Oxygenic photogranule; Soil fertilization

5.1. Introduction

Modern agriculture is driven by the energy-intensive synthesis of fertilizers (*i.e.*, the Haber-Bosch process) and extraction of mineral ore deposits (*e.g.*, phosphate rock). With a projected global growth of the human population from eight to nine billion by 2050, a similar increase in food demand and utilization of these fertilizers can be expected. However, synthetic fertilizers negatively affect the environment and soil quality over the long term. Current manufacturing practices of the fertilizing industry are energy-intensive and responsible for 2.5% or 1203 Tg of global carbon dioxide emissions (Herrera et al., 2022), and the continuous depletion of mineral deposits worldwide (Tian et al., 2020). The limited retention capacity of nutrients in soils has resulted in their excessive application, which has been linked to the eutrophication of ground and surface bodies and the limited growth of endemic soil microorganisms (Nadarajan and Sukumaran, 2021). A need for more sustainable and innovative organic fertilizers that minimize energy consumption and dependency on fossil resources while maintaining crop growth and yield is evident.

Microalgae, including eukaryotic microalgae, diatoms, and cyanobacteria, may be used as organic fertilizers because of their ability to convert nutrients into biomass rich in essential elements for soil fertilization, namely, nitrogen and phosphorus (Lu and Xiao, 2022). Furthermore, microalgae biomass has shown a notable contribution to plant growth through several mechanisms, including phytohormone production, root association formation, and protection against phytopathogens and pests (Alvarez et al., 2021). These promising attributes have resulted in improvements in crop performance that are equal to or even superior to those achieved using synthetic fertilizers. Álvarez-González et al. (2022) reported a significant increase in shoot and leaf weight, as well as the number of leaves of basil (*Ocimum basilicum* L.) by harnessing the high nitrogen content of the eukaryotic microalga *Scenedesmus* sp. biomass cultivated in municipal wastewater. Similar enhancements in the growth, development, and nitrogen assimilation of potato plants (*Solanum tuberosum*) were reported using spray-dried eukaryotic microalga *Asterarcys quadricellulare* biomass (Cordeiro et al., 2022). Height, leaves, and other essential aspects of onion plants (*Allium cepa* L.) were also improved by mixing soil with cow manure and the cyanobacterium *Spirulina platensis*, compared to cow manure alone (Dineshkumar et al., 2020).

Recently, growing heterotrophic and phototrophic microorganisms in syntrophy was recognized as a promising strategy to boost bioproduct yields (Khoo et al., 2021). The key to

syntrophic interactions is the production of oxygen by microalgae through photosynthesis. In return, heterotrophic bacteria oxidize organic matter and produce carbon dioxide to sustain the growth of microalgae. Compared to pure microalgae monocultures, co-culturing microalgae and heterotrophic bacteria has improved nutrient assimilation and biomass yield, tolerance against pollutants, and stability against competing microorganisms (Yan et al., 2022). Moreover, combining these microorganisms has also been reported to promote biomass aggregation, allowing efficient and inexpensive harvesting by gravity settling (Arcila and Buitrón, 2016). Studies describing the mechanisms of microalgae-bacteria aggregation have been reported. Aggregates can be in the form of flocs, compact granules (Quijano et al., 2017), and filamentous granules (Milferstedt et al., 2017a), dominated by different genera of eukaryotic microalgae or cyanobacteria.

The feasibility of using microalgae-bacteria aggregates as feedstock for organic fertilizer production has previously been discussed (González et al., 2020). However, their fertilizing value has yet to be systematically determined. Previous studies have established that organic substrates can be categorized into different fractions, each defined by i) their complexity (molecular structure) and ii) their bioaccessibility (availability as a source of organic matter, nitrogen, and phosphorus to soil microorganisms) (Jimenez et al., 2015b). This categorization has proven to be a valuable approach for a better diagnosis of the fertilizing value of organic materials, as it delivers a more comprehensive prediction of the fate of nitrogen, phosphorus, and organic matter after soil amendment (Jimenez et al., 2020). Assessing the complexity and bioaccessibility of microalgae-bacteria aggregates offers valuable insights into their composition and serves as a foundation for the potential optimization of fertilizer production.

This study provides a comprehensive characterization of morphologically distinct microalgae-bacteria aggregates in terms of molecular complexity and organic matter, nitrogen, and phosphorus bioaccessibility as potential organic soil fertilizers. Biochemical fractionation methods were employed based on sequential chemical extraction and fluorescence spectroscopy (Fernández-Domínguez et al., 2023). This investigation also compared the molecular complexity and organic matter, nitrogen, and phosphorus bioaccessibility between selected microalgae-bacteria aggregates grown under nutrient-abundant and nutrient-reduced conditions to analyze changes in their composition during starvation. The underlying hypothesis is that the morphology of microalgae-bacteria aggregates influences the molecular complexity and the bioaccessibility of

organic matter, nitrogen, and phosphorus. Microalgae-bacteria flocs, being more fragile structures, may present more bioaccessible nutrients, whereas in the more compact microalgae-bacteria granules, the nutrients may be less bioaccessible.

5.2. Materials and methods

5.2.1. Origin, morphology, and preparation of microalgae-bacteria aggregates samples

Four morphologically distinct samples of microalgae-bacteria aggregates used for wastewater treatment or biomass production were collected from three photobioreactors (PBRs) operated under different conditions. Sample A consisted of microalgae-bacteria aggregates and was collected from flat-panel PBRs with a working volume of 13 L (total volume of 15 L). The culture was grown in fresh BG-11 medium (Vital-Jácome et al., 2020) in which the phosphorus concentration was increased from 0.23 mM (39 mg $\text{K}_2\text{HPO}_4 \text{ L}^{-1}$) to 1.1 mM (192 mg $\text{K}_2\text{HPO}_4 \text{ L}^{-1}$). Phosphorus was increased to obtain a nitrogen-to-phosphorus molar ratio of 38:1. This ratio is within the optimum range (16:1–49:1) for sustaining the growth of eukaryotic microalgae and cyanobacteria (Arias et al., 2019). Cultures were grown at $25 \pm 5 \text{ }^\circ\text{C}$ and pH between 7.0 and 8.0. Illumination was induced using cool-white LED lights at a photosynthetically active radiation (PAR) of $120 \mu\text{mol m}^{-2} \text{ s}^{-1}$. An airflow of $0.15 \text{ L}_{\text{air}} \text{ L}_{\text{culture}}^{-1} \text{ min}^{-1}$ was always kept, maintaining a continuous mixture of the cultures.

Sample B and Sample C consisted of two morphologically distinct microalgae-bacteria aggregates found in a high-rate algae pond (HRAP) used to treat wastewater. The HRAP has a working volume of 50 L (total volume 80 L), 0.26 m^2 of surface area, and a consistent liquid velocity of 0.2 m s^{-1} . This pond was continuously fed with primary effluent from a municipal wastewater treatment plant in Santa Rosa Jauregui, Queretaro, Mexico. The composition of the primary effluent was as follows: $517 \pm 133 \text{ mg COD L}^{-1}$, $86 \pm 15 \text{ mg N-NH}_4^+ \text{ L}^{-1}$, $43 \pm 4 \text{ mg N-NO}_3^- \text{ L}^{-1}$, $25 \pm 10 \text{ mg N-NO}_2^-$, and $43 \pm 4 \text{ mg P-PO}_4^{3-} \text{ L}^{-1}$. More on the design and operating conditions of the HRAP can be found in Buitrón & Coronado-Apodaca (2022).

Sample D was obtained from sequencing batch PBRs with a working volume of 4 L and fed with nitrate mineral salt (NMS) growth medium containing 246 mg $\text{CH}_3\text{COONa L}^{-1}$, 5.4 mg $\text{KH}_2\text{PO}_4 \text{ L}^{-1}$, 11 mg $\text{Na}_2\text{HPO}_4 \cdot 12\text{H}_2\text{O L}^{-1}$, 100 mg $(\text{NH}_4)_2\text{SO}_4 \text{ L}^{-1}$, 2.5 mg $\text{Na}_2\text{EDTA} \cdot 2\text{H}_2\text{O L}^{-1}$, 0.001 mg $\text{Na}_2\text{MoO}_4 \cdot 2\text{H}_2\text{O L}^{-1}$, 0.01 mg $\text{FeSO}_4 \cdot 7\text{H}_2\text{O L}^{-1}$, 0.02 mg $\text{H}_3\text{BO}_3 \text{ L}^{-1}$, 0.004 mg

ZnSO₄·7H₂O L⁻¹, 0.001 mg MnCl₂ L⁻¹, 0.01 mg CoCl₂·6H₂O L⁻¹, 0.014 mg CuSO₄·5H₂O L⁻¹, 0.2 mg FeCl₃ L⁻¹ and 0.001 mg NiCl₂·6H₂O L⁻¹. Cultures were grown at an average temperature of 25 °C, pH of 8.5 ± 0.5, and hydraulic retention time (HRT) of 8 h. Illumination was constantly provided using cool-white LED lights at a PAR of 62 μmol m⁻² s⁻¹. Overhead stirring at 100 rpm was used to continuously mix the biomass.

The settling velocity and size distribution of the four different aggregate types were determined using the APHA 2710 E method (American Public Health Association, American Water Works Association, Water Environment Federation., 2023) and stereomicroscopy (Vital-Jácome et al., 2020), respectively. Genus identification of eukaryotic microalgae and cyanobacteria was carried out according to the guidelines by Wehr and Sheath (2015) using an ECLIPSE 90i microscope (Nikon, Japan) equipped with an NIS-Elements V.4.30 image acquisition system (Nikon, Japan). Collected microalgae-bacteria aggregates were harvested through centrifugation (3000 g, 20 min, 5 °C), frozen at -20 °C for at least 3 h, lyophilized overnight (-80 to -85 °C, 0.05 hPa), and ground using 4.8-mm stainless steel beads in a bead mill. Dry matter was determined gravimetrically using the APHA 2540 B method (American Public Health Association, American Water Works Association, Water Environment Federation., 2023).

5.2.2. Assessment of total organic matter, total nitrogen, and total bioavailable phosphorus content

Total organic matter (TOM), total nitrogen (TN), and total bioavailable phosphorus (TBP) content for each freeze-dried and ground type of microalgae-bacteria aggregate were measured. For TOM, 250 mg of freeze-dried, ground microalgae-bacteria aggregates were placed in a propylene vessel containing 10 mL of 96% w w⁻¹ H₂SO₄. After 24 h, the mixture was diluted with distilled water until a final weight of 250 g was reached, and TOM was measured in the liquid extract using Aqualytic Vario COD tubes for a range of 0 – 1500 mg COD L⁻¹ (Tintometer GmbH, Germany). For TN, 2 – 3 mg of freeze-dried, ground microalgae-bacteria aggregates were analyzed using a CHNS/O FlashSmart Elemental Analyzer (ThermoFisher, USA). TBP was determined by placing 300 mg of freeze-dried, ground microalgae-bacteria aggregates in 30 mL of distilled water. Samples were shaken for 24 h in an orbital shaker at 280 rpm and then centrifuged (18600 g, 20 min, 4 °C). The liquid extract was recovered, filtered (0.45 μm), and stored for analyses. The same procedure was repeated using residual pellets from the previous step but in a 0.5 M NaHCO₃ (pH

8.5) solution. Phosphorus concentration in each liquid extract was determined using Hach LCK 348 (Hach GmbH, Germany) kits, summed, and considered as the TBP content as described in Jimenez et al. (2020).

5.2.3. Sequential chemical extraction for organic matter, nitrogen, and phosphorus fractions characterization

A biochemical fractionation method based on sequential chemical extraction of organic matter and nitrogen bioaccessibility was carried out following the ISBAMO fractionation protocol described by Fernández-Domínguez et al. (2023). For each type of freeze-dried, ground microalgae-bacteria aggregates, 1.0 g was weighed and subjected to four different extraction solvents: 1) 10 mM CaCl₂, 2) 10 mM NaCl + 10 mM NaOH, 3) 100 mM NaOH, and 4) 72% w w⁻¹ H₂SO₄) using an Accelerated Solvent Extractor DIONEX ASE-350 (Thermo Fisher, USA). Each solvent, sequentially more aggressive to organic substrates (Fernández-Domínguez et al., 2023), allowed the recovery of the resulting four liquid ISBAMO fractions. These fractions contain the organic matter and nitrogen within microalgae-bacteria aggregates according to their degree of bioaccessibility. The four ISBAMO fractions were defined as (1) soluble (extracted with 10 mM CaCl₂), (2) readily extractable (extracted with 10 mM NaCl + 10 mM NaOH), (3) slowly extractable (extracted with 100 mM NaOH), and (4) poorly extractable (extracted with 72% w w⁻¹ H₂SO₄). The organic matter and nitrogen concentrations of each ISBAMO fraction were determined using Aqualytic Vario COD tubes for a range of 0 – 1500 mg COD L⁻¹ (Tintometer GmbH, Germany) and Hach LCK 338 kit (Hach GmbH, Germany), respectively. Finally, a fifth non-extractable fraction was calculated by subtracting the organic matter or nitrogen content of each ISBAMO fraction from the TOM or TN values determined in section 5.2.2.

Inorganic and organic phosphorus fractions of the TBP in microalgae-bacteria aggregates were determined following a modified Olsen-phosphorus methodology (Jimenez et al., 2020). Liquid extracts from distilled water and 0.5 M NaHCO₃ extractions were obtained for TBP estimation from section 4.2.2. were analyzed for inorganic phosphorus using a Hach LCK 348 kit (Hach GmbH, Germany). In this study, the inorganic phosphorus determined for liquid extracts from distilled water and 0.5 M NaHCO₃ extractions were summed and considered as inorganic phosphorus in the TBP content. Organic phosphorus was determined by subtracting inorganic phosphorus from TBP content with TBP values obtained in section 5.2.2.

5.2.4. Fluorescence spectroscopy analysis for molecular complexity characterization

Following the methodology described by Fernández-Domínguez, Yekta, et al. (2023), the fluorescence spectra of the ISBAMO fractions of the microalgae-bacteria aggregates were acquired using an LS55 luminescence spectrometer (Perkin Elmer, USA). For the analysis, each fraction was filtered using a 1.6 μm pore-size glass fiber filter, mounted on a 1 cm path-length quartz cuvette, and exposed to excitation wavelengths between 200 and 600 nm at fixed increments of 10 nm. The scanning monochromator speed was set at 1200 nm s^{-1} , and the fluorescence emission values were recorded each 0.5 nm using the FL Winlab V.4.00.03 software (Perkin Elmer, USA). These records aimed to obtain a comprehensive fluorescence excitation-emission matrix per 10 nm increment.

The matrices were then integrated to determine the structural complexity of microalgae-bacteria aggregates (Muller et al., 2014). The integration algorithm interpolates the measured data with known fluorescence values of molecular intermediates (*e.g.*, proteins, cellulose, etc.) and converts the fluorescence matrices to a grey-level bitmap. These images were then split into seven fluorescence zones, each corresponding to a group of molecules with similar structural complexity (Fernández-Domínguez et al., 2021). Zones I-III correspond to simple proteins, amino acid-like molecules, or soluble sugars. In contrast, more complex, polymer-like molecules (*e.g.*, humic acid-like substances) give a strong signal in zones IV-VII. The zone fluorescence volume (Eq. 4.1), the fluorescence proportion (Eq. 4.2), and the fluorescence complexity index (Eq. 4.3) were calculated per liquid fraction (Fernández-Domínguez et al., 2021).

$$V_f(x) = \frac{V_{f_{raw}}(x)}{OM_S} \times \frac{\sum_1^7 S(x)}{S(x)} \quad (4.1)$$

$$P_f(x) = \frac{V_f(x)}{\sum_1^7 V_f(x)} \times 100 \quad (4.2)$$

$$\text{Fluorescence Complexity Index} = \frac{\sum_4^7 V_f(x)}{\sum_1^3 V_f(x)} \quad (4.3)$$

where $V_f(x)$ is the normalized fluorescence volume of zone x , $V_{f\text{ raw}}(x)$ is the raw volume of zone x , OM_S is the organic matter (mg COD L⁻¹) concentration of the ISBAMO fraction, $S(x)$ is the area of zone x , and $P_f(x)$ is the proportion of fluorescence in zone x (%).

5.2.5. Statistical analyses

Experiments were conducted in duplicate. All statistical analyses were performed using R version 4.2.2 (R Core Team, USA). Data presented in tables and figures were calculated as mean values with corresponding standard deviations using the `get_summary_stats` function of the `rstatix` (Kassambara, 2023) package. Statistically significant differences ($p \leq 0.05$) were determined through a one-way analysis of variance followed by Tukey's honestly significant difference post-hoc test, using the functions `aov` and `HSD.test` of the `rstatix` (Kassambara, 2023) and `agricolae` (Mendiburu, 2023) packages, respectively.

5.3. Results and discussion

5.3.1. Morphology of microalgae-bacteria aggregates samples

The collected microalgae-bacteria aggregates samples were characterized by settling velocity, diameter, and genus-level identification (Table 5.1). Samples were considered as floccular biomass in the form of loose flocs (Sample A) and consolidated flocs (Sample B) and granular biomass in the form of smooth granules (Sample C) and filamentous granules (Sample D), considering an increasing degree of granulation. An increased settling velocity reflects a higher degree of granulation. Fundamentally, the aggregates consistently contained unicellular eukaryotic microalgae, like *Scenedesmus*, and filamentous cyanobacteria, like *Oscillatoria*, which are commonly found in freshwater environments (Chandel et al., 2023). Notably, microalgae-bacteria aggregates also included various other non-phototrophic microorganisms. Representative images of the different types of microalgae-bacteria aggregates used in this study are shown in Figure 5.1.

Table 5.1. Physical and morphological characteristics of microalgae-bacteria aggregates. See Figure 5.1 for representative images of the different sample types.

	Sample type	Settling velocity (m h ⁻¹)	Diameter (mm)	Identified microalgae and cyanobacteria
Floccular biomass	A) loose flocs	≤ 1.0	≤ 0.1	<i>Chlorella</i> <i>Scenedesmus</i> <i>Nitzschia</i> <i>Oscillatoria</i> <i>Phormidium</i>
	B) consolidated flocs	4.7 ± 0.1	2.2 ± 0.9	<i>Chlorella</i> <i>Stigeoclonium</i>
Granular biomass	C) smooth granules	6.4 ± 0.4	4.0 ± 1.4	<i>Chlorella</i> <i>Stigeoclonium</i> <i>Nitzschia</i>
	D) filamentous granules	≥ 13.0	2.0 ± 1.4	<i>Oscillatoria</i>

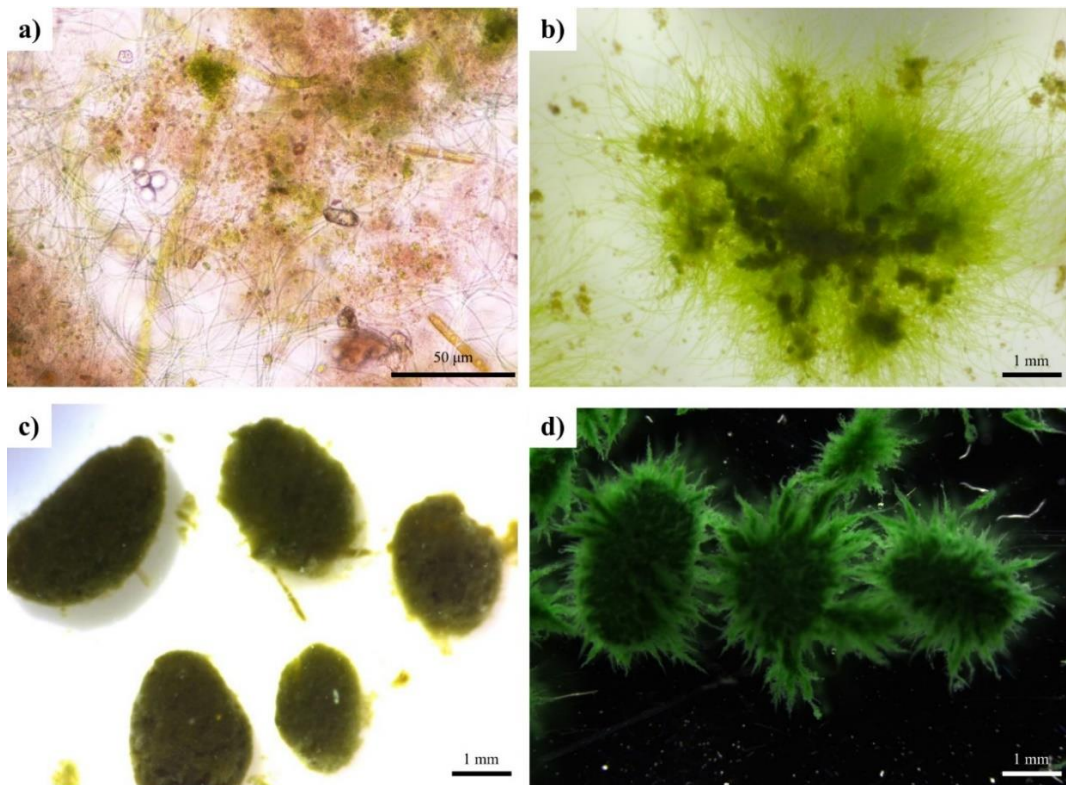


Figure 5.1. Representative images of (a) loose flocs, (b) consolidated flocs, (c) smooth granules, and (d) filamentous granules.

5.3.2. Total organic matter, total nitrogen, and total bioavailable phosphorus content in microalgae-bacteria aggregates

The initial hypothesis proposed that the morphology of microalgae-bacteria aggregates could influence the bioaccessibility of organic matter, nitrogen, phosphorus content, and molecular complexity. TOM (expressed as COD), TN, and TBP content of freeze-dried, ground microalgae-bacteria aggregates were determined. The results of this characterization are presented in Table 5.2. Statistically significant differences ($p \leq 0.05$) were observed when comparing TOM, TN, and TBP values between analyzed samples. The results between the microalgae-bacteria aggregate samples with the highest TOM, TN, and TBP values led to the consideration that factors other than morphology, *i.e.*, microbial diversity distribution and extracellular polymeric substances (EPS) secretion, could have influenced these values. The following paragraphs address the individual explanations for each parameter to further understand these outcomes.

Table 5.2. Total organic matter (TOM), total nitrogen (TN), and total bioavailable phosphorus (TBP) in different microalgae-bacteria aggregates. Lowercase letters indicate significant differences ($p \leq 0.05$) between samples for each parameter.

	Sample type	TOM (mg COD g dry matter ⁻¹)	TN (mg TN g dry matter ⁻¹)	TBP (mg TBP g dry matter ⁻¹)
Floccular biomass	A) loose flocs	1004 ± 2 ^c	93 ± 3 ^a	14 ± 1 ^b
	B) consolidated flocs	1097 ± 17 ^b	88 ± 4 ^a	17 ± 1 ^a
Granular biomass	C) smooth granules	1208 ± 71 ^a	59 ± 3 ^c	17 ± 1 ^a
	D) filamentous granules	1223 ± 1 ^a	73 ± 2 ^b	13 ± 1 ^b

Granular biomass (smooth granules and filamentous granules) had a higher TOM content than floccular biomass (loose flocs and consolidated flocs). TOM across all microalgae-bacteria aggregates samples ranged between the theoretical COD values for microalgae biomass and bacteria biomass, calculated as 952 mg COD g dry matter⁻¹ and 1420 mg COD g dry matter⁻¹, respectively (Ahnert et al., 2021). It has been suggested that differences between theoretical COD

values could be attributed to the inherent carbon, oxygen, hydrogen, and nitrogen ratio, *i.e.*, the elemental ratio, of each type of biomass (Ahnert et al., 2021). For microalgae, the common biomass elemental ratio is $\text{CH}_{2.48}\text{O}_{1.04}\text{N}_{0.15}\text{P}_{0.01}$ (Chai et al., 2021). In contrast, the elemental ratio of bacteria is $\text{CH}_{1.40}\text{O}_{0.40}\text{N}_{0.20}\text{P}_{0.02}$ (Chen et al., 2020). The significantly higher TOM content observed in granular biomass could be attributed to a higher bacteria proportion over the microalgae biomass when compared to floccular biomass. These findings agree with those of previous studies, where the overall bacteria biomass accounted for approximately 30% of the total biomass concentration in floccular microalgae-bacteria aggregates (Shriwastav et al., 2015). In contrast, non-phototrophic and phototrophic bacteria gene sequence types in photogranules were found at maximum abundances of 17% and 67%, respectively (Milferstedt et al., 2017b). Considering these proportions and assuming that the prevailing population in floccular microalgae-bacteria aggregates and photogranules were made up of microalgae with their respective elemental ratio, the theoretical COD values could be calculated at $1086 \text{ mg COD g dry matter}^{-1}$ and $1340 \text{ mg COD g dry matter}^{-1}$, which are like the data reported in Table 5.2.

Granular biomass had a significantly lower TN content than that of loose flocs. The TN content in all microalgae-bacteria aggregates was within the theoretical TN range for microalgae biomass and bacteria biomass. Based on the above-mentioned biomass elemental ratios of microalgae and bacteria, the theoretical TN content was calculated to be $63 \text{ mg TN g dry matter}^{-1}$ and $124 \text{ mg TN g dry matter}^{-1}$, respectively. Differences in the theoretical TN content could be attributed to the lower proportion of nitrogen per microalgae biomass compared to bacteria biomass. Granular biomass had a lower TN content than floccular biomass, even lower than the theoretical TN value calculated to be $114 \text{ mg TN g dry matter}^{-1}$ based on the microalgae and bacteria proportions mentioned in Milferstedt, Kuo-Dahab, et al. (2017b). These observations indicate that factors other than microalgae and bacteria could have contributed to the low TN content of granular biomass. The overall formation of microalgae-bacteria aggregates depends on the association between these microorganisms and the quality of EPS. EPS are mainly composed of proteins and polysaccharides. The proteins to polysaccharides ratio seems to be linked to the central aggregation mechanism in microalgae-bacteria aggregates (Arcila and Buitrón, 2016). In this context, proteins are the primary reservoir of nitrogen, whereas polysaccharides determine the carbon content (Morillas-España et al., 2022). According to Arcila and Buitrón (2017), high protein and thus nitrogen content in the EPS could be found in microalgae-bacteria granules when the carbon-to-nitrogen ratio in growth

media was below five. In the present study, gas exchange and pH control (8.0 to 9.0) favored the transformation of atmospheric CO₂ into HCO₃⁻ in the growth medium, influencing the carbon-to-nitrogen ratio during granular biomass development, as previously reported by Arcila and Buitrón (2017). This condition likely resulted in a carbon-to-nitrogen ratio equal or greater than five, which negatively affected the protein and thus nitrogen content in the EPS of granular biomass.

TBP content in consolidated flocs and smooth granules was significantly higher than that in loose flocs and filamentous granules. TBP content across all microalgae-bacteria aggregates was also higher than that of microalgae biomass, but lower than that of bacterial biomass. The theoretical phosphorus content for microalgae and bacteria was calculated to be 9 mg TBP g dry matter⁻¹ and 20 mg TBP g dry matter⁻¹, using their respective elemental ratios introduced above. Differences in these theoretical values could be attributed to the lower share of phosphorus per microalgae biomass compared to bacteria biomass. The significantly higher TBP in consolidated flocs and smooth granules could also be attributed to other microorganisms contributing to the phosphorus content of the biomass. Considering that these aggregates were cultivated in wastewater, the growth of polyphosphate-accumulating organisms (PAOs) could have influenced the TBP content of the consolidated flocs and smooth granules. This is supported by Q. Wang et al. (2019), who obtained PAOs from secondary effluent sludge and co-cultured them with the eukaryotic microalga *Chlorella pyrenoidosa*. Moreover, PAOs, known to assimilate substantial amounts of inorganic phosphorus as polyphosphates (up to 38 mg TBP g dry matter⁻¹), were successfully integrated into photogranules (Trebuch et al., 2023). The physicochemical gradients in the granules provided a niche for PAOs. These PAO-enriched photogranules showed a notably higher phosphorus content than non-enriched granules.

5.3.3. Extractable fractions of organic matter, nitrogen, and phosphorus in microalgae-bacteria aggregates

Biomass fractions along a gradient of bioaccessibility of organic matter, nitrogen, and phosphorus in different microalgae-bacteria aggregates were analyzed. The results obtained for organic matter, nitrogen, and phosphorus bioaccessibility are shown in Figure 5.2 and Tables S5.1, S5.2, and S5.3 in the supplementary data. Consolidated flocs, followed by filamentous granules, had the highest amount of extractable organic matter and nitrogen, given by the soluble, readily extractable, slowly extractable, and poorly extractable fractions. Consolidated flocs contained more readily extractable

(*i.e.*, EPS extractions as proteins and lipids) and slowly extractable (*i.e.*, protein-like compounds). In contrast, filamentous granules are rich in poorly extractable fraction, which is associated with carbohydrate-like (*e.g.*, cellulose and hemicellulose) compounds and poorly accessible proteins, given the nitrogen concentration of this fraction. Consolidated flocs and filamentous granules also had the highest proportion of inorganic phosphorus in the TBP.

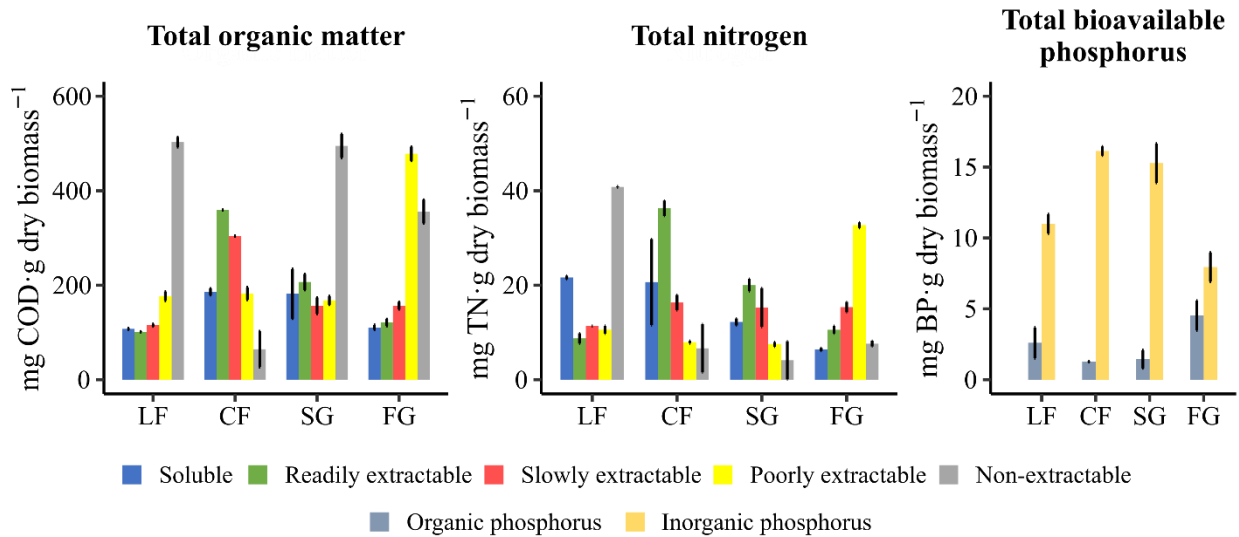


Figure 5.2. Contribution of each extracted biochemical fraction to the total organic matter (TOM), total nitrogen (TN), and total bioavailable phosphorus (TBP) in loose flocs (LF), consolidated flocs (CF), smooth granules (SG), and filamentous granules (FG).

Microalgae-bacteria flocs were initially hypothesized to be fragile, more bioaccessible structures than the compact microalgae-bacteria granules. However, the results show that the morphology of microalgae-bacteria aggregates, whether they were flocs or granules, did not influence the bioaccessibility of organic matter, nitrogen, and phosphorus. Additional events during the formation of the different microalgae-bacteria aggregates, *e.g.*, microbial diversity distribution and EPS secretion, could have played a pivotal role in shaping the observed bioaccessibility profiles.

The higher extractability and, thus, higher bioaccessibility of organic matter and nitrogen in consolidated flocs could be attributed to an abundance of macromolecules like polysaccharides, proteins, and lipids. These macromolecules are typically the main components of the soluble, readily extractable, and slowly extractable ISBAMO fractions (Muller et al., 2014). The contrasting

growth and operating conditions for the development of granular and floccular biomass in this study could have impacted their macromolecular content. Previous studies reported that the occurrence of macromolecules in microalgae-bacteria aggregates was associated with different abiotic factors, including nutrient availability, light intensity, temperature, shear stress, and pH (Li et al., 2021). These environmental perturbations directly affect the cellular integrity and change the intracellular distribution of carbon flux, determining whether one or another macromolecule is produced. For instance, the occurrence of lipids and carbohydrates in the eukaryotic microalga *Scenedemus acuminatus* increased due to limited nitrogen availability (Zhang et al., 2019b). This occurs as these macromolecules are the primary carbon and energy reserves in microalgae that allow them to cope with environmental stress.

Similarly, the protein content in microalgae-bacteria aggregates decreased from 69% dried weight to 58% dried weight when HRT was increased from 6 d to 10 d (Arcila and Buitrón, 2016). Such a decrease was linked to the depletion of nitrogen caused by the growth of microalgae and bacteria. It is possible that operating and process conditions used for growing consolidated flocs (*i.e.*, wastewater growth medium, 6 d HRT, 12 h photoperiods, $200 \mu\text{mol m}^{-2} \text{s}^{-1}$, pH 8.4 ± 0.4 , 22 °C temperature) contributed to their higher nutrient bioaccessibility.

The lower share of extractable fractions and, thus, lower bioaccessibility of organic matter and nitrogen in loose flocs, smooth granules, and filamentous granules could be then attributed to the presence of non-extractable humic-like substances. This is supported by the literature, as the non-extractable ISBAMO fraction contains water-insoluble, non-extractable humic-like substances (Muller et al., 2014). EPS secretion may explain the abundance of these compounds in loose flocs, smooth granules, and filamentous granules. Arcila and Buitrón (2016) observed that the formation of microalgae-bacteria aggregates in the form of granules was related to EPS secretion as the biomass age, or solids retention time, increased. Humic substances are integral components of the EPS matrix (Tang et al., 2020). These authors reported that humic substances, including fulvic acids, humic acids, and water-insoluble humin, could be taken up by the EPS matrix from their surrounding medium, *e.g.*, wastewater effluents or dead cells. Further studies confirmed that syntrophic interactions between eukaryotic microalga *Chlorella pyrenoidosa* and bacteria could decompose humic-like substances in stabilized landfill leachates, thus resulting in water-insoluble humin (Zhao et al., 2014). Given that only smooth granules were grown in wastewater, the origin of water-insoluble, non-extractable humic-like substances in loose flocs and filamentous granules

could be related to other factors, including partially/fully decomposed microbial constituents from dead cells including partially/fully decomposed dead microbial cells (More et al., 2014). These could have come from decaying, slow-growing microorganisms, *e.g.*, diatoms, whose debris has been observed in the core of filamentous granules with large diameters (≥ 3.0 mm) (Abouhend et al., 2019).

The prevalence of inorganic phosphorus in the TBP content of consolidated flocs and filamentous granules is unexpected. In other phototrophic systems, the organic fraction of phosphorus dominated: In the cyanobacterium *Synechocystis* sp. PCC 6803, organic phosphorus accounted for nearly 77% of the total phosphorus content (Zhou et al., 2017). In the eukaryotic microalga *Scenedesmus* sp., 71% of the total phosphorus was stored in an organic form when grown in a synthetic medium (Wu et al., 2021). The high inorganic phosphorus fraction in the bioavailable phosphorus in this study may result from the activity of PAOs. PAO-enriched aerobic granules exhibited an inorganic phosphorus fraction as high as 77% of the total phosphorus content (Huang et al., 2015), similar to the one observed for the different types of microalgae-bacteria aggregates used in this study.

5.3.4. Effect of starvation

Nutrient availability in the growth medium affects the development and biochemical composition of microalgae-bacteria aggregates (Arcila and Buitrón, 2016). Therefore, organic matter, nitrogen, and phosphorus bioaccessibility in loose flocs and filamentous granules were determined before (nutrient abundant) and after a starvation period. Two contrasted biomass types, loose flocs and filamentous granules, were grown under nutrient starvation for over 8 and 3 d, respectively, using the growth media described in the supplementary material (Table S5.4 for loose flocs and Table S5.5 for filamentous granules). The other operating conditions were kept as described in section 5.2.1. As shown in Figure 5.3, the biomass with contrasted spatial structures, loose flocs versus filamentous granules, differed in their shift in biochemical compositions when starved. The amount of poorly extractable organic matter in loose flocs significantly increased from 177 ± 10 mg TN g dry matter⁻¹ in nutrient-abundant conditions to 442 ± 19 mg TN g dry matter⁻¹ after starvation. The non-extractable TOM for this biomass significantly decreased from 502 ± 11 mg COD g dry matter⁻¹ in nutrient-abundant conditions to 55 ± 10 mg COD g dry matter⁻¹ after starvation. Similarly, the

poorly extractable fraction of nitrogen in loose flocs also increased from $11 \pm 1 \text{ mg TN g dry matter}^{-1}$ to $25 \pm 2 \text{ mg TN g dry matter}^{-1}$ before and after starvation conditions, respectively.

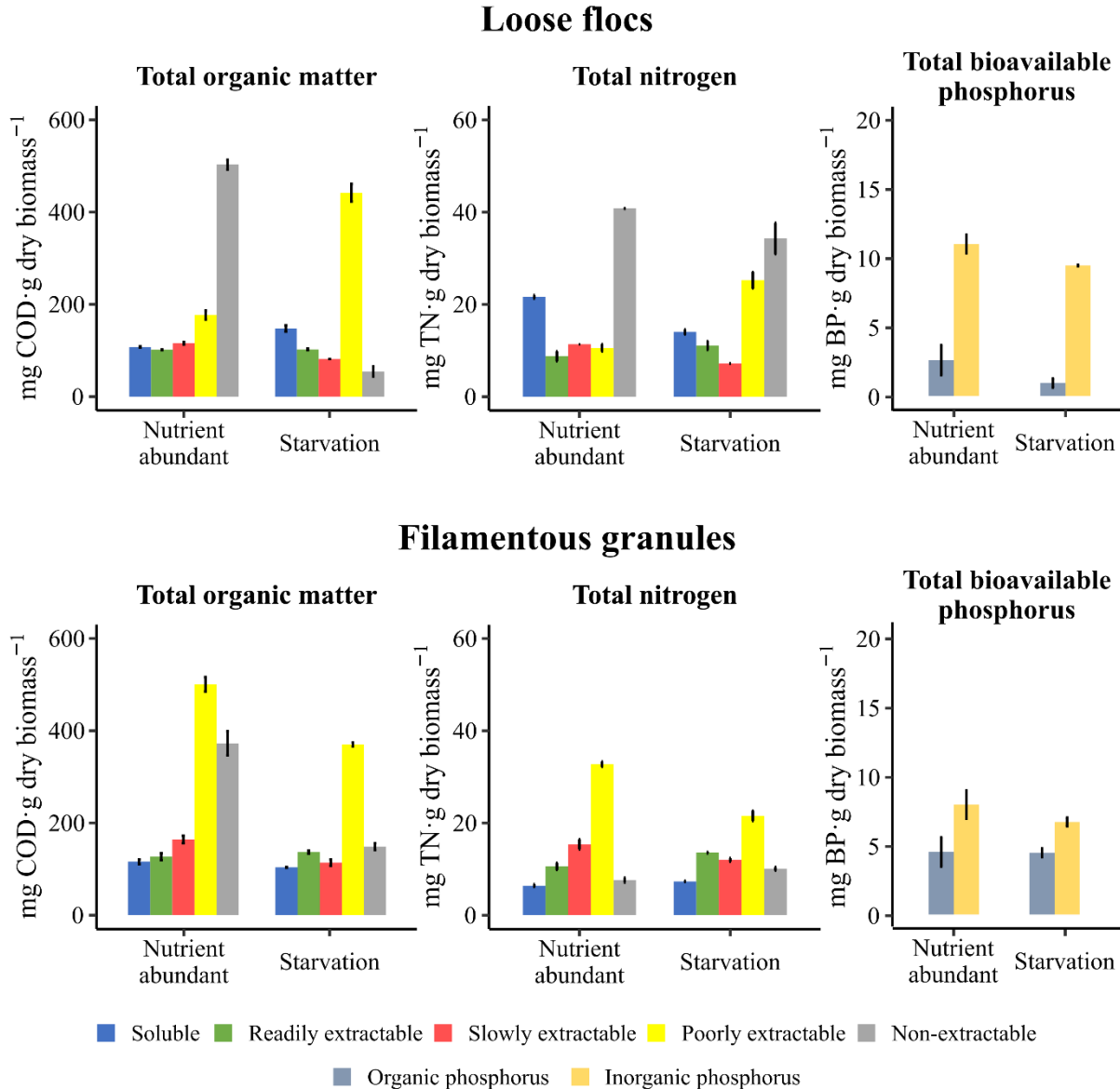


Figure 5.3. Contribution of each extracted biochemical fraction to the total organic matter (TOM), total nitrogen (TN), and total bioavailable phosphorus (TBP) observed for loose flocs and filamentous granules before and after starvation conditions.

The notable increase in the poorly extractable fraction of starved loose flocs correlates with an abundance of cellulose-like and hemicellulose-like key compounds targeted by this fraction

(Muller et al., 2014). Under nutrient-abundant conditions, microalgae store polysaccharides in many ways, including polymeric cellulose-like and hemicellulose-like substances in the inner layer of their cellular wall. These cellular constituents not only provide rigidity and protection against environmental interferences but also represent up to 7.1% (cellulose) and 16.3% (hemicellulose) of their dry matter content in microalgae-bacteria aggregates (Zanchetta et al., 2021). However, previous studies have reported that cellulose and hemicellulose content in microalgae could also be positively influenced by starvation. The eukaryotic microalga *Nannochloropsis salina* grown under nitrogen deficiency experienced a twofold increase in cellulose content compared to growth under nutrient abundance (Jeong et al., 2017). The authors proposed that microalgae channel excess energy and carbon intermediates from photosynthesis toward synthesizing storage molecules, including cellulose-like compounds, as an alternative sink. This redirection was seen as a response to inhibiting anabolic pathways requiring nitrogen, *i.e.*, amino acid and nucleotide synthesis, which usually works as the primary energy and carbon sink in microalgae.

The key components of the non-extractable ISBAMO fraction are water-insoluble, non-extractable humic-like substances that come from EPS or partially/fully degraded microbial constituents. Therefore, decreased non-extractable fractions after starvation could be associated with limited degradation of microbial constituents because of decayed microbial activity. Starvation leads the cell into a dormant-like state with no metabolic activity to synthesize microbial constituents and potentially transform them into water-insoluble, non-extractable humic-like substances (Neumann et al., 2021). Previous studies confirmed these observations, where the lack of one or more nutrients during the formation of microalgae-bacteria aggregates decreased the abundance of humic-like substances in anaerobic digestate effluent (Xie et al., 2018).

5.3.5. Complexity of microalgae-bacteria aggregates

The structural complexity of the ISBAMO fractions was determined to complement the bioaccessibility characterization of the different types of microalgae-bacteria aggregates. This complexity assessment allowed i) the identification of groups of molecules based on their fluorescence excitation and emission wavelengths and ii) the estimation of a complexity index based on all fluorescence information (Jimenez et al., 2015b; Muller et al., 2014). This complexity index is defined by dividing the sum of fluorescence volumes of complex, humic-like substances by the sum of fluorescence volumes of simpler compounds (*e.g.*, tyrosine, tryptophane, and

microbial-related constituents). A fluorescence complexity index (FCI) greater than 1.0 indicates a dominance of complex, humic-like substances whereas an index smaller than 1.0 indicates a dominance of simpler compounds (Fernández-Domínguez et al., 2021).

The fluorescence complexity indices from ISBAMO fractions for the samples from the starvation experiments, *i.e.*, loose flocs and filamentous granules, are presented in Figure 5.4. Most aggregate types had an FCI lower or equal to 1.0, indicating that most bioaccessible fractions are primarily simple constituents, *e.g.*, tyrosine, tryptophane, and microbial-related constituents. These results follow earlier studies in the eukaryotic microalga *Scenedesmus acuminatus* grown under nutrient abundance and starvation, where up to 32% of its dry matter is in the form of amino acids, including tyrosine (Zhang et al., 2019b). Similarly, the *Chlorella* genus commonly contains about 17% and 10% of its total dried biomass in the form of soluble polysaccharides (Gifuni et al., 2018) and triacylglycerides (Andeden et al., 2021), respectively.

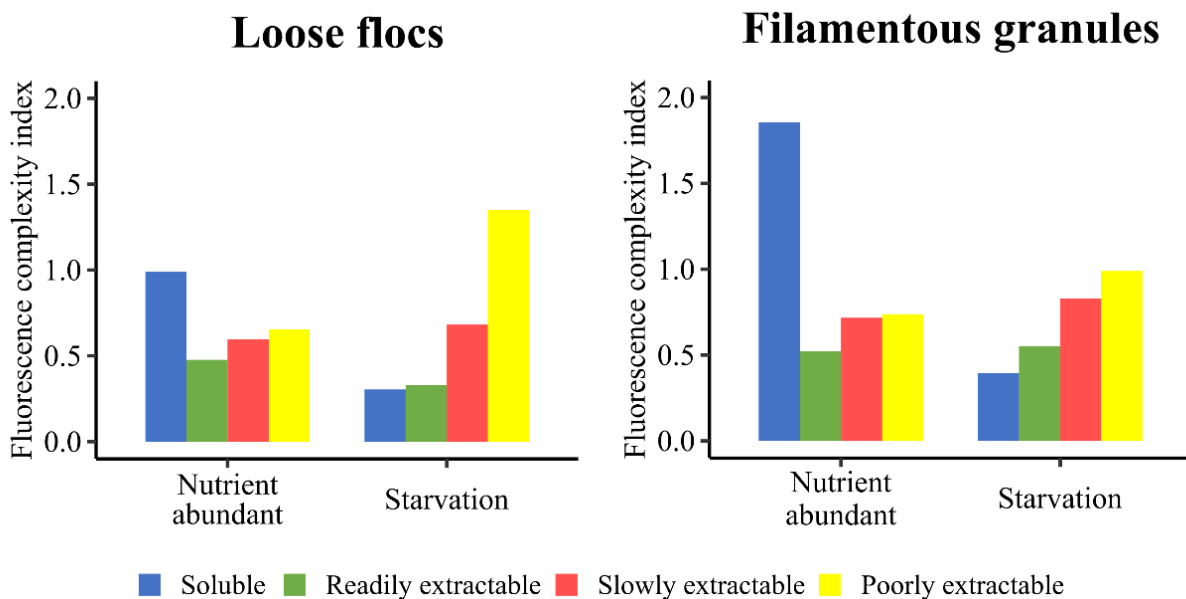


Figure 5.4. Fluorescence complexity index (FCI) for the different biochemical fractions from loose flocs and filamentous granules before and after starvation conditions.

Whatever the spatial structure of the biomass (loose flocs or filamentous granules), two fractions had an FCI greater or equal to 1.0, indicating an abundance of complex, humic-like substances. These specific fractions were the soluble fraction from filamentous granules grown under nutrient-abundant conditions and the poorly extractable fraction from loose flocs grown

under starvation. Even though the discussed results did not distinguish between the contribution of external (*e.g.*, EPS) and internal (*e.g.*, microbial-related constituents) compounds to the complexity of microalgae-bacteria aggregates, the overall complexification of these fractions could be related to the adsorption of humic-like substances by EPS during microalgae-bacteria aggregation (Zhao et al., 2014) or to the partial decay of cells (Xie et al., 2018). These sources of biomass complexity should be considered in future studies.

5.4. Conclusion

Biochemical fractionation methods were applied to morphologically distinct microalgae-bacteria aggregates to characterize their molecular complexity and organic matter, nitrogen, and phosphorus bioaccessibility. This study shows that morphologically distinct microalgae-bacteria aggregates have different total organic matter, total nitrogen, and total bioavailable phosphorus content. Floccular biomass in consolidated flocs contains more bioaccessible fractions of organic matter, nitrogen, and phosphorus than other analyzed structures. This biomass also presents the highest proportions of soluble, readily extractable, and slowly extractable organic matter and nitrogen, as well as bioavailable phosphorus in the form of inorganic phosphorus. After starvation, changes in the poorly extractable and non-extractable fractions of organic matter in floccular biomass were observed, suggesting that humic-like substances mostly accumulate under these conditions. All microalgae-bacteria aggregates presented a low molecular complexity, highlighting their benefits as soil fertilizer. The results indicated that microalgae-bacteria aggregates are a promising source of highly bioaccessible organic matter, nitrogen, and phosphorus.

6. General conclusion and future perspectives

This thesis confirmed that combining abiotic stress factors like nitrogen limitation and low dissolved oxygen concentration improved the production of polyhydroxyalkanoates as polyhydroxybutyrate in microalgae-bacteria consortia biomass. Moreover, this combined stress strategy also increased the removal of dissolved nutrients and mineralization of dissolved organic matter in municipal wastewater, improving the effluent quality. The overall conclusions of this thesis are divided according to the delineated experimental parts of the study and are presented in the specified order.

It was evidenced that polyhydroxyalkanoate-producing microalgae were retrieved from municipal activated sludge and contaminated freshwater samples. Subjecting microalgae cultures from these sources to nitrogen-limited conditions improved polysaccharides content (41% dCW or 460 mg glucose g dried biomass⁻¹) over polyhydroxyalkanoates (0.5% dCW or 5 mg g dried biomass⁻¹). The rather low production of polyhydroxyalkanoates was related to the supplementation of exogenous organic carbon from cellular death and the semi-open method of cultivation, which could have led to the growth of non-accumulating strains.

Polyhydroxyalkanoate production in *Synechocystis* sp. was maximized by manipulating dissolved oxygen concentration in a nitrogen-limited growth medium. Lowering dissolved oxygen concentrations to 1.2 mgO₂ L⁻¹ in nitrogen-limited medium maximized polyhydroxybutyrate concentration of *Synechocystis* sp., achieving up to 12% dCW or 95 mg L⁻¹. A high redox state was observed under these conditions, suggesting that the increased production of polyhydroxybutyrate likely occurred due to the inactivation of electron-consuming processes linked to high dissolved oxygen concentrations (photorespiration).

The syntrophic interactions between *Synechocystis* sp. and wastewater-borne bacteria in primary effluent led to nitrogen-limited conditions. The combination of nitrogen limitation and low dissolved oxygen concentrations (5.7 mgO₂ L⁻¹) in municipal wastewater achieved high polyhydroxybutyrate production yields (9.8% dCW or 80 mg L⁻¹) due to the inhibition of photorespiratory activity. Moreover, that combined strategy was also able to reduce chemical oxygen demand, ammonia nitrogen, and phosphorous content in wastewater from 265 to 63 mgCOD L⁻¹ (92% removal), 104 to 1.5 mgNH₄⁺-N L⁻¹ (99% removal), and 5.0 to 1.6 mgPO₄³⁻-P L⁻¹ (88% removal), respectively.

The bioavailability of organic matter, nitrogen, and phosphorus of microalgae-bacteria biomass with different morphological structures was evaluated. It was observed that nutrients

bioavailability of microalgae-bacteria biomass content varies according to the morphological structure, which is determined by the abundance of microorganisms and their metabolic products. In this context, more than 94% of the total organic matter, nitrogen, and phosphorus content of microalgae-bacteria biomass from consolidated flocs was extractable. These results were attributed to an abundance of macromolecules like polysaccharides, proteins, and lipids, which are more easily accessible to soil microorganisms. Moreover, nitrogen-limited conditions were observed to increase the extractability of microalgae-bacteria biomass flocs. That was linked to the fact that microalgae-bacteria consortia channel energy and carbon intermediates from photosynthesis toward synthesizing more extractable storage molecules, like cellulose, under nitrogen limitation.

Overall, results obtained in this thesis confirmed that microalgae-bacteria biomass is a promising and attractive approach for removing organic matter and nutrients from wastewater while simultaneously producing polyhydroxyalkanoates for potential bioplastic production. However, some challenges are to be overcome to achieve an efficient scale-up of the technology. These include an optimization of the selection and cultivation procedures of polyhydroxyalkanoate-producing microalgae, the automatic control of sensitive operational conditions that could interfere with polyhydroxyalkanoate production (phosphorus availability, inorganic carbon concentration, pH, temperature), integration of optimal oxygen management strategies to lower dissolved oxygen concentration, and valorization of the polymer metabolic pathway in microalgae to develop a biorefinery concept for polymer-based bioproducts (bioplastics, biofertilizers, biofuels, etc.).

References

- Abouhend, A.S., Milferstedt, K., Hamelin, J., Ansari, A.A., Butler, C., Carbajal-González, B.I., Park, C., 2019. Growth Progression of Oxygenic Photogranules and Its Impact on Bioactivity for Aeration-Free Wastewater Treatment. *Environmental Science & Technology*. <https://doi.org/10.1021/acs.est.9b04745>
- Acién, F.G., Gómez-Serrano, C., Morales-Amaral, M.M., Fernández-Sevilla, J.M., Molina-Grima, E., 2016. Wastewater treatment using microalgae: how realistic a contribution might it be to significant urban wastewater treatment? *Applied Microbiology and Biotechnology* 100, 9013–9022. <https://doi.org/10.1007/s00253-016-7835-7>
- Acién, F.G., Molina, E., Fernández-Sevilla, J.M., Barbosa, M., Gouveia, L., Sepúlveda, C., Bazaes, J., Arbib, Z., 2017. Economics of microalgae production, In: Gonzalez-Fernandez, C., Muñoz, R. (Eds.), *Microalgae-Based Biofuels and Bioproducts*, Woodhead Publishing Series in Energy. Woodhead Publishing, pp. 485–503. <https://doi.org/10.1016/B978-0-08-101023-5.00020-0>
- Aditya, L., Mahlia, T.M.I., Nguyen, L.N., Vu, H.P., Nghiem, L.D., 2022. Microalgae-bacteria consortium for wastewater treatment and biomass production. *Science of The Total Environment* 838, 155871. <https://doi.org/10.1016/j.scitotenv.2022.155871>
- Agarwal, P., Soni, R., Kaur, P., Madan, A., Mishra, R., Pandey, J., Singh, S., Singh, G., 2022. Cyanobacteria as a Promising Alternative for Sustainable Environment: Synthesis of Biofuel and Biodegradable Plastics. *Frontiers in Microbiology* 13. <https://doi.org/10.3389/fmicb.2022.939347>
- Ahnert, M., Schalk, T., Brückner, H., Effenberger, J., Kuehn, V., Krebs, P., 2021. Organic matter parameters in WWTP – a critical review and recommendations for application in activated sludge modelling. *Water Science and Technology* 84, 2093–2112. <https://doi.org/10.2166/wst.2021.419>
- Akinnawo, S.O., 2023. Eutrophication: Causes, consequences, physical, chemical and biological techniques for mitigation strategies. *Environmental Challenges* 12, 100733. <https://doi.org/10.1016/j.envc.2023.100733>
- Alcántara, C., Fernández, C., García-Encina, P.A., Muñoz, R., 2015. Mixotrophic metabolism of *Chlorella sorokiniana* and algal-bacterial consortia under extended dark-light periods and nutrient starvation. *Applied Microbiology and Biotechnology* 99, 2393–2404. <https://doi.org/10.1007/s00253-014-6125-5>

- Alishah Aratboni, H., Rafiei, N., Garcia-Granados, R., Alemzadeh, A., Morones-Ramírez, J.R., 2019. Biomass and lipid induction strategies in microalgae for biofuel production and other applications. *Microbial Cell Factories* 18, 178. <https://doi.org/10.1186/s12934-019-1228-4>
- Almeida, J.R., Serrano, E., Fernandez, M., Fradinho, J.C., Oehmen, A., Reis, M.A.M., 2021. Polyhydroxyalkanoates production from fermented domestic wastewater using phototrophic mixed cultures. *Water Research* 197, 117101. <https://doi.org/10.1016/J.WATRES.2021.117101>
- Alvarez, A.L., Weyers, S.L., Goemann, H.M., Peyton, B.M., Gardner, R.D., 2021. Microalgae, soil and plants: A critical review of microalgae as renewable resources for agriculture. *Algal Research* 54, 102200. <https://doi.org/10.1016/j.algal.2021.102200>
- Álvarez-González, A., Uggetti, E., Serrano, L., Gorchs, G., Ferrer, I., Díez-Montero, R., 2022. Can microalgae grown in wastewater reduce the use of inorganic fertilizers? *Journal of Environmental Management* 323, 116224. <https://doi.org/10.1016/j.jenvman.2022.116224>
- American Public Health Association, American Water Works Association, Water Environment Federation., 2023. Standard Methods for the Examination of Water and Wastewater, APHA Press, Washington DC.
- Andeden, E.E., Ozturk, S., Aslim, B., 2021. Effect of alkaline pH and nitrogen starvation on the triacylglycerol (TAG) content, growth, biochemical composition, and fatty acid profile of *Auxenochlorella protothecoides* KP7. *Journal of Applied Phycology* 33, 211–225. <https://doi.org/10.1007/s10811-020-02311-0>
- Ansari, A.A., Abouhend, A.S., Park, C., 2019. Effects of seeding density on photogranulation and the start-up of the oxygenic photogranule process for aeration-free wastewater treatment. *Algal Research* 40. <https://doi.org/10.1016/j.algal.2019.101495>
- Arcila, J.S., Buitrón, G., 2017. Influence of solar irradiance levels on the formation of microalgae-bacteria aggregates for municipal wastewater treatment. *Algal Research* 27, 190–197. <https://doi.org/10.1016/j.algal.2017.09.011>
- Arcila, J.S., Buitrón, G., 2016. Microalgae–bacteria aggregates: effect of the hydraulic retention time on the municipal wastewater treatment, biomass settleability and methane potential. *Journal of Chemical Technology and Biotechnology* 91, 2862–2870. <https://doi.org/10.1002/jctb.4901>

- Arias, D.M., García, J., Uggetti, E., 2020. Production of polymers by cyanobacteria grown in wastewater: Current status, challenges and future perspectives. *New Biotechnology* 55, 46–57. <https://doi.org/10.1016/j.nbt.2019.09.001>
- Arias, D.M., Rueda, E., García-Galán, M.J., Uggetti, E., García, J., 2019. Selection of cyanobacteria over green algae in a photo-sequencing batch bioreactor fed with wastewater. *Science of the Total Environment* 653, 485–495. <https://doi.org/10.1016/j.scitotenv.2018.10.342>
- Arias, D.M., Uggetti, E., García-Galán, M.J., García, J., 2018. Production of polyhydroxybutyrates and carbohydrates in a mixed cyanobacterial culture: Effect of nutrients limitation and photoperiods. *New Biotechnology* 42, 1–11. <https://doi.org/10.1016/j.nbt.2018.01.001>
- Arimbrathodi, S.P., Javed, M.A., Hamouda, M.A., Aly Hassan, A., Ahmed, M.E., 2023. BioH2 Production Using Microalgae: Highlights on Recent Advancements from a Bibliometric Analysis. *Water* 15, 185. <https://doi.org/10.3390/W15010185/S1>
- Arora, Y., Sharma, S., Sharma, V., 2023. Microalgae in Bioplastic Production: A Comprehensive Review. *Arab Journal of Science and Engineering* 48, 7225–7241. <https://doi.org/10.1007/s13369-023-07871-0>
- Ayre, J.M., Mickan, B.S., Jenkins, S.N., Moheimani, N.R., 2021. Batch cultivation of microalgae in anaerobic digestate exhibits functional changes in bacterial communities impacting nitrogen removal and wastewater treatment. *Algal Research* 57, 102338. <https://doi.org/10.1016/j.algal.2021.102338>
- Balaji, S., Gopi, K., Muthuvelan, B., 2013. A review on production of poly β hydroxybutyrates from cyanobacteria for the production of bio plastics. *Algal Research* 2, 278–285. <https://doi.org/10.1016/j.algal.2013.03.002>
- Barreiro-Vescovo, S., González-Fernández, C., de Godos, I., 2021. Characterization of communities in a microalgae-bacteria system treating domestic wastewater reveals dominance of phototrophic and pigmented bacteria. *Algal Research* 59. <https://doi.org/10.1016/j.algal.2021.102447>
- Becker, E.W., 2013. Microalgae for Human and Animal Nutrition, In: Richmond, A., Hu, Q. (Eds.), *Handbook of Microalgal Culture*. John Wiley & Sons, Ltd., pp. 461–503. <https://doi.org/10.1002/9781118567166.ch25>

- Bellini, S., Tommasi, T., Fino, D., 2022. Poly(3-hydroxybutyrate) biosynthesis by *Cupriavidus necator*: A review on waste substrates utilization for a circular economy approach. *Bioresource Technology Reports* 17, 100985. <https://doi.org/10.1016/j.biteb.2022.100985>
- Bernaerts, T.M.M., Gheysen, L., Foubert, I., Hendrickx, M.E., Van Loey, A.M., 2019. The potential of microalgae and their biopolymers as structuring ingredients in food: A review. *Biotechnology Advances* 37, 107419. <https://doi.org/10.1016/j.biotechadv.2019.107419>
- Budde, C.F., Riedel, S.L., Hübner, F., Risch, S., Popović, M.K., Rha, C., Sinskey, A.J., 2011. Growth and polyhydroxybutyrate production by *Ralstonia eutropha* in emulsified plant oil medium. *Applied Microbiology and Biotechnology* 89, 1611–1619. <https://doi.org/10.1007/s00253-011-3102-0>
- Bugnicourt, E., Cinelli, P., Lazzeri, A., Alvarez, V., 2014. Polyhydroxyalkanoate (PHA): Review of synthesis, characteristics, processing and potential applications in packaging. *Express Polymer Letters* 8, 791–808. <https://doi.org/10.3144/expresspolymlett.2014.82>
- Buitrón, G., Coronado-Apodaca, K.G., 2022. Influence of the solids retention time on the formation of the microalgal-bacterial aggregates produced with municipal wastewater. *Journal of Water Process Engineering* 46, 102617. <https://doi.org/10.1016/j.jwpe.2022.102617>
- Chai, W.S., Tan, W.G., Halimatul Munawaroh, H.S., Gupta, V.K., Ho, S.-H., Show, P.L., 2021. Multifaceted roles of microalgae in the application of wastewater biotreatment: A review. *Environmental Pollution* 269, 116236. <https://doi.org/10.1016/j.envpol.2020.116236>
- Chandel, P., Mahajan, D., Thakur, K., Kumar, R., Kumar, S., Brar, B., Sharma, D., Sharma, A.K., 2023. A review on plankton as a bioindicator: A promising tool for monitoring water quality. *World Water Policy* 1–20. <https://doi.org/10/gs4qkm>
- Chandra, R., Iqbal, H.M.N., Vishal, G., Lee, H.-S., Nagra, S., 2019. Algal biorefinery: A sustainable approach to valorize algal-based biomass towards multiple product recovery. *Bioresource Technology* 278, 346–359. <https://doi.org/10.1016/j.biortech.2019.01.104>
- Cheah, W.Y., Er, A.C., Aiyub, K., Mohd Yasin, N.H., Ngan, S.L., Chew, K.W., Khoo, K.S., Ling, T.C., Juan, J.C., Ma, Z., Show, P.L., 2023. Current status and perspectives of algae-based bioplastics: A reviewed potential for sustainability. *Algal Research* 71, 103078. <https://doi.org/10.1016/j.algal.2023.103078>
- Chen, G., van Loosdrecht, M.C.M. van, Ekama, G.A., Brdjanovic, D., 2020. *Biological Wastewater Treatment: Principles, Modelling and Design*, IWA Publishing, London.

- Chong, J.W., Tan, X., Khoo, K.S., Ng, H.S., Jonglertjunya, W., Yew, G.Y., Show, P.L., 2022. Microalgae-based bioplastics: Future solution towards mitigation of plastic wastes. *Environmental Research* 206, 112620. <https://doi.org/10.1016/j.envres.2021.112620>
- Chu, F.-F., Chu, P.-N., Cai, P.-J., Li, W.-W., Lam, P.K.S., Zeng, R.J., 2013. Phosphorus plays an important role in enhancing biodiesel productivity of *Chlorella vulgaris* under nitrogen deficiency. *Bioresource Technology* 134, 341–346. <https://doi.org/10.1016/j.biortech.2013.01.131>
- Cinar, S.O., Chong, Z.K., Kucuker, M.A., Wieczorek, N., Cengiz, U., Kuchta, K., 2020. Bioplastic production from microalgae: A review. *International Journal of Environmental Research and Public Health* 17, 1–21. <https://doi.org/10.3390/ijerph17113842>
- CONAGUA, 2021. Inventario Nacional de Plantas Municipales de Potabilización y de Tratamiento de Aguas Residuales en Operación. CONAGUA, Ciudad de México.
- Cordeiro, E.C.N., Mógor, Á.F., Amatussi, J.O., Mógor, G., Marques, H.M.C., de Lara, G.B., 2022. Microalga biofertilizer improves potato growth and yield, stimulating amino acid metabolism. *Journal of Applied Phycology* 34, 385–394. <https://doi.org/10.1007/s10811-021-02656-0>
- Costa, S.S., Miranda, A.L., de Moraes, M.G., Costa, J.A.V., Druzian, J.I., 2019. Microalgae as source of polyhydroxyalkanoates (PHAs) — A review. *International Journal of Biological Macromolecules* 131, 536–547. <https://doi.org/10.1016/j.ijbiomac.2019.03.099>
- Dalton, B., Bhagabati, P., De Micco, J., Padamati, R.B., O'Connor, K., 2022. A Review on Biological Synthesis of the Biodegradable Polymers Polyhydroxyalkanoates and the Development of Multiple Applications. *Catalysts*, 12, 319–331. <https://doi.org/10.3390/catal12030319>
- Das, S.K., Sathish, A., Stanley, J., 2018. Production Of Biofuel And Bioplastic From *Chlorella Pyrenoidosa*. *Materials Today: Proceedings* 5, 16774–16781. <https://doi.org/10.1016/j.matpr.2018.06.020>
- de Oliveira, C.Y.B., Viegas, T.L., da Silva, M.F.O., Fracalossi, D.M., Lopes, R.G., Derner, R.B., 2020. Effect of trace metals on growth performance and accumulation of lipids, proteins, and carbohydrates on the green microalga *Scenedesmus obliquus*. *Aquaculture International* 28, 1435–1444. <https://doi.org/10.1007/s10499-020-00533-0>

- De Philippis, R., Ena, A., Guastiini, M., Sili, C., Vincenzini, M., 1992. Factors affecting poly- β -hydroxybutyrate accumulation in cyanobacteria and in purple non-sulfur bacteria. *FEMS Microbiology Letters* 103, 187–194. [https://doi.org/10.1016/0378-1097\(92\)90309-C](https://doi.org/10.1016/0378-1097(92)90309-C)
- Degrenne, B., Pruvost, J., Legrand, J., 2011. Effect of prolonged hypoxia in autotrophic conditions in the hydrogen production by the green microalga *Chlamydomonas reinhardtii* in photobioreactor. *Bioresource Technology* 102, 1035–1043. <https://doi.org/10.1016/j.biortech.2010.08.009>
- Dineshkumar, R., Subramanian, J., Arumugam, A., Ahamed Rasheeq, A., Sampathkumar, P., 2020. Exploring the Microalgae Biofertilizer Effect on Onion Cultivation by Field Experiment. *Waste and Biomass Valorization* 11, 77–87. <https://doi.org/10.1007/s12649-018-0466-8>
- dos Santos, A.J., Oliveira Dalla Valentina, L.V., Hidalgo Schulz, A.A., Tomaz Duarte, M.A., 2017. From Obtaining to Degradation of PHB:Material Properties. Part I. *Ingeniería y Ciencia* 13, 269–298. <https://doi.org/10.17230/ingciencia.13.26.10>
- dos Santos Neto, A.G., Barragán-Trinidad, M., Florêncio, L., Buitrón, G., 2023. Strategy for the formation of microalgae-bacteria aggregates in high-rate algal ponds. *Environmental Technology* 44, 1863–1876. <https://doi.org/10.1080/09593330.2021.2014577>
- Fernández-Domínguez, D., Patureau, D., Houot, S., Sertillanges, N., Zennaro, B., Jimenez, J., 2021. Prediction of organic matter accessibility and complexity in anaerobic digestates. *Waste Management* 136, 132–142. <https://doi.org/10.1016/j.wasman.2021.10.004>
- Fernández-Domínguez, D., Yekta, S.S., Hedenström, M., Patureau, D., Jimenez, J., 2023. Deciphering the contribution of microbial biomass to the properties of dissolved and particulate organic matter in anaerobic digestates. *Science of The Total Environment* 877, 162882. <https://doi.org/10.1016/j.scitotenv.2023.162882>
- Ferrentino, R., Langone, M., Fiori, L., Andreottola, G., 2023. Full-Scale Sewage Sludge Reduction Technologies: A Review with a Focus on Energy Consumption. *Water* 15, 615. <https://doi.org/10.3390/w15040615>
- Fradinho, J.C., Oehmen, A., Reis, M.A.M., 2019. Improving polyhydroxyalkanoates production in phototrophic mixed cultures by optimizing accumulator reactor operating conditions. *International Journal of Biological Macromolecules* 126, 1085–1092. <https://doi.org/10.1016/J.IJBIOMAC.2018.12.270>

- Saratale, R.G., Ponnusamy, V.K., Jeyakumar, R.B., Sirohi, R., Piechota, G., Shobana, S., Dharmaraja, J., Lay, C., Dattatraya Saratale, G., Seung Shin, H., Ashokkumar, V., 2022. Microalgae cultivation strategies using cost-effective nutrient sources: Recent updates and progress towards biofuel production. *Bioresource Technology* 361, 127691. <https://doi.org/10.1016/j.biortech.2022.127691>
- Gao, S., Edmundson, S., Huesemann, M., 2022. Oxygen stress mitigation for microalgal biomass productivity improvement in outdoor raceway ponds. *Algal Research* 68, 102901. <https://doi.org/10.1016/j.algal.2022.102901>
- Garcia-Garcia, D., Quiles-Carrillo, L., Balart, R., Torres-Giner, S., Arrieta, M.P., 2022. Innovative solutions and challenges to increase the use of Poly(3-hydroxybutyrate) in food packaging and disposables. *European Polymer Journal* 178, 111505. <https://doi.org/10.1016/j.eurpolymj.2022.111505>
- Gifuni, I., Olivieri, G., Pollio, A., Marzocchella, A., 2018. Identification of an industrial microalgal strain for starch production in biorefinery context: The effect of nitrogen and carbon concentration on starch accumulation. *New Biotechnology* 41, 46–54. <https://doi.org/10.1016/j.nbt.2017.12.003>
- Gomaa, M.A., Refaat, M.H., Salim, T.M., El-Sayed, A.E.K.B., Bekhit, M.M., 2019. Identification of Green Alga *Chlorella vulgaris* Isolated from Freshwater and Improvement Biodiesel Productivity via UV Irradiation. *Microbiology and Biotechnology Letters* 47, 381–389. <https://doi.org/10.4014/MBL.1812.12017>
- González, I., Ekelhof, A., Herrero, N., Siles, J.Á., Podola, B., Chica, A.F., Ángeles Martín, M., Melkonian, M., Izquierdo, C.G., Gómez, J.M., 2020. Wastewater nutrient recovery using twin-layer microalgae technology for biofertilizer production. *Water Science and Technology* 82, 1044–1061. <https://doi.org/10.2166/wst.2020.372>
- González-Resendiz, L., Sánchez-García, L., Hernández-Martínez, I., Viguera-Ramírez, G., Jiménez-García, L.F., Lara-Martínez, R., Morales-Ibarría, M., 2021. Photoautotrophic poly(3-hydroxybutyrate) production by a wild-type *Synechococcus elongatus* isolated from an extreme environment. *Bioresource Technology* 337, 125508. <https://doi.org/10.1016/j.biortech.2021.125508>
- Guleria, S., Singh, H., Sharma, V., Bhardwaj, N., Arya, S.K., Puri, S., Khatri, M., 2022. Polyhydroxyalkanoates production from domestic waste feedstock: A sustainable approach

- towards bio-economy. *Journal of Cleaner Production* 340, 130661. <https://doi.org/10.1016/j.jclepro.2022.130661>
- Güven, H., Özgün, H., Ersahin, M.E., Dereli, R.K., Sinop, I., Öztürk, I., 2019. High-rate activated sludge processes for municipal wastewater treatment: the effect of food waste addition and hydraulic limits of the system. *Environmental Science and Pollution Research* 26, 1770–1780. <https://doi.org/10.1007/s11356-018-3665-8>
- Hauer, T., Komárek, J., 2022. *CyanoDB 2.0 - On-line database of cyanobacterial genera*. University of South Bohemia & Institute of Botany of the Czech Academy of Sciences. <http://www.cyanodb.cz/>.
- Hermann, D.-R., Lilek, D., Daffert, C., Fritz, I., Weinberger, S., Rumpler, V., Herbinger, B., Prohaska, K., 2020. In situ based surface-enhanced Raman spectroscopy (SERS) for the fast and reproducible identification of PHB producers in cyanobacterial cultures. *The Analyst* 145, 5242–5251. <https://doi.org/10.1039/D0AN00969E>
- Herrera, A., D’Imporzano, G., Zilio, M., Pigoli, A., Rizzi, B., Meers, E., Schouman, O., Schepis, M., Barone, F., Giordano, A., Adani, F., 2022. Environmental Performance in the Production and Use of Recovered Fertilizers from Organic Wastes Treated by Anaerobic Digestion vs Synthetic Mineral Fertilizers. *ACS Sustainable Chemistry & Engineering* 10, 986–997. <https://doi.org/10.1021/acssuschemeng.1c07028>
- Huang, S.T., Goh, J.L., Ahmadzadeh, H., Murry, M.A., 2019. A rapid sampling technique for isolating highly productive lipid-rich algae strains from environmental samples. *Biofuel Research Journal* 6, 920–926. <https://doi.org/10.18331/BRJ2019.6.1.3>
- Huang, Wenli, Huang, Weiwei, Li, H., Lei, Z., Zhang, Z., Tay, J.H., Lee, D.-J., 2015. Species and distribution of inorganic and organic phosphorus in enhanced phosphorus removal aerobic granular sludge. *Bioresource Technology* 193, 549–552. <https://doi.org/10.1016/j.biortech.2015.06.120>
- Jayakrishnan, U., Deka, D., Das, G., 2021. Waste as feedstock for polyhydroxyalkanoate production from activated sludge: Implications of aerobic dynamic feeding and acidogenic fermentation. *Journal of Environmental Chemical Engineering* 9, 105550. <https://doi.org/10.1016/j.jece.2021.105550>
- Jeong, S.W., Nam, S.W., HwangBo, K., Jeong, W.J., Jeong, B., Chang, Y.K., Park, Y.-I., 2017. Transcriptional Regulation of Cellulose Biosynthesis during the Early Phase of Nitrogen

- Deprivation in *Nannochloropsis salina*. *Scientific Reports* 7, 5264. <https://doi.org/10.1038/s41598-017-05684-4>
- Jimenez, J., Aemig, Q., Doussiet, N., Steyer, J.-P., Houot, S., Patureau, D., 2015a. A new organic matter fractionation methodology for organic wastes: Bioaccessibility and complexity characterization for treatment optimization. *Bioresource Technology* 194, 344–353. <https://doi.org/10.1016/j.biortech.2015.07.037>
- Jimenez, J., Grigatti, M., Boanini, E., Patureau, D., Bernet, N., 2020. The impact of biogas digestate typology on nutrient recovery for plant growth: Accessibility indicators for first fertilization prediction. *Waste Management* 117, 18–31. <https://doi.org/10.1016/j.wasman.2020.07.052>
- Jimenez, J., Latrille, E., Harmand, J., Robles, A., Ferrer, J., Gaida, D., Wolf, C., Mairet, F., Bernard, O., Alcaraz-Gonzalez, V., Mendez-Acosta, H., Zitomer, D., Totzke, D., Spanjers, H., Jacobi, F., Guwy, A., Dinsdale, R., Premier, G., Mazhegrane, S., Ruiz-Filippi, G., Seco, A., Ribeiro, T., Pauss, A., Steyer, J.-P., 2015b. Instrumentation and control of anaerobic digestion processes: a review and some research challenges. *Reviews in Environmental Science and Bio/Technology* 14, 615–648. <https://doi.org/10.1007/s11157-015-9382-6>
- Jimenez, J., Lei, H., Steyer, J.-P., Houot, S., Patureau, D., 2017. Methane production and fertilizing value of organic waste: Organic matter characterization for a better prediction of valorization pathways. *Bioresource Technology* 241, 1012–1021. <https://doi.org/10.1016/j.biortech.2017.05.176>
- Jokel, M., Nagy, V., Tóth, S.Z., Kosourov, S., Allahverdiyeva, Y., 2019. Elimination of the flavodiiron electron sink facilitates long-term H₂ photoproduction in green algae. *Biotechnology for Biofuels* 12, 280. <https://doi.org/10.1186/s13068-019-1618-1>
- Jothibas, K., Muniraj, I., Jayakumar, T., Ray, B., Dhar, D.W., Karthikeyan, S., Rakesh, S., 2022. Impact of microalgal cell wall biology on downstream processing and nutrient removal for fuels and value-added products. *Biochemical Engineering Journal* 187, 108642. <https://doi.org/10.1016/j.bej.2022.108642>
- Kamravamanesh, D., Pflügl, S., Nischkauer, W., Limbeck, A., Lackner, M., Herwig, C., 2017. Photosynthetic poly- β -hydroxybutyrate accumulation in unicellular cyanobacterium *Synechocystis* sp. PCC 6714. *AMB Express* 7, 143. <https://doi.org/10.1186/s13568-017-0443-9>

- Kamravamanesh, D., Slouka, C., Limbeck, A., Lackner, M., Herwig, C., 2019. Increased carbohydrate production from carbon dioxide in randomly mutated cells of cyanobacterial strain *Synechocystis* sp. PCC 6714: Bioprocess understanding and evaluation of productivities. *Bioresource Technology* 273, 277–287. <https://doi.org/10.1016/j.biortech.2018.11.025>
- Kannah, R.Y., Kumar, M.D., Kavitha, S., Banu, J.R., Tyagi, V.K., Rajaguru, P., Kumar, G., 2022. Production and recovery of polyhydroxyalkanoates (PHA) from waste streams – A review. *Bioresource Technology* 366, 128203. <https://doi.org/10.1016/j.biortech.2022.128203>
- Kassambara, A., 2023. rstatix: Pipe-Friendly Framework for Basic Statistical Tests. The Comprehensive R Archive Network. <https://cran.r-project.org/web/packages/rstatix/index.html>
- Kazbar, A., Cogne, G., Urbain, B., Marec, H., Le-Gouic, B., Tallec, J., Takache, H., Ismail, A., Pruvost, J., 2019. Effect of dissolved oxygen concentration on microalgal culture in photobioreactors. *Algal Research* 39, 101432. <https://doi.org/10.1016/j.algal.2019.101432>
- Keramidas, K., Fosse, F., Diaz Vazquez, A., Dowling, P., Garaffa, R., Després, J., Russ, H.P., Schade, B., Schmitz, A., Soria Ramirez, A., Vandyck, T., Weitzel, M., Tchong-Ming, S., Diaz Rincon, A., Rey Los Santos, L., Wojtowicz, K., 2021. Global Energy and Climate Outlook 2021: Advancing towards climate neutrality. Publications Office of the European Union, Luxembourg. <https://doi.org/10.2760/410610>
- Khalaf, Alaa.H., Ibrahim, W.A., Fayed, M., Eloffy, M.G., 2021. Comparison between the performance of activated sludge and sequence batch reactor systems for dairy wastewater treatment under different operating conditions. *Alexandria Engineering Journal* 60, 1433–1445. <https://doi.org/10.1016/j.aej.2020.10.062>
- Khoo, K.S., Chia, W.Y., Chew, K.W., Show, P.L., 2021. Microalgal-Bacterial Consortia as Future Prospect in Wastewater Bioremediation, Environmental Management and Bioenergy Production. *Indian Journal of Microbiology* 61, 262–269. <https://doi.org/10.1007/s12088-021-00924-8>
- Kim, B.H., Ramanan, R., Kang, Z., Cho, D.H., Oh, H.M., Kim, H.S., 2016. *Chlorella sorokiniana* HS1, a novel freshwater green algal strain, grows and hyperaccumulates lipid droplets in seawater salinity. *Biomass and Bioenergy* 85, 300–305. <https://doi.org/10.1016/j.biombioe.2015.12.026>

- Koch, M., Bruckmoser, J., Scholl, J., Hauf, W., Rieger, B., Forchhammer, K., 2020a. Maximizing PHB content in *Synechocystis* sp. PCC 6803: a new metabolic engineering strategy based on the regulator PirC. *Microbial Cell Factories* 19, 231. <https://doi.org/10.1186/s12934-020-01491-1>
- Koch, M., Doello, S., Gutekunst, K., Forchhammer, K., 2019. PHB is Produced from Glycogen Turn-over during Nitrogen Starvation in *Synechocystis* sp. PCC 6803. *International Journal of Molecular Sciences* 20, 1942. <https://doi.org/10.3390/ijms20081942>
- Koch, M., Forchhammer, K., 2021. Polyhydroxybutyrate: A Useful Product of Chlorotic Cyanobacteria. *Microbial Physiology* 31, 67–77. <https://doi.org/10.1159/000515617>
- Koch, M., Orthwein, T., Alford, J.T., Forchhammer, K., 2020b. The Slr0058 Protein From *Synechocystis* sp. PCC 6803 Is a Novel Regulatory Protein Involved in PHB Granule Formation. *Frontiers in Microbiology* 11. <https://doi.org/10.3389/fmicb.2020.00809>
- Kovalcik, A., Meixner, K., Mihalic, M., Zeilinger, W., Fritz, I., Fuchs, W., Kucharczyk, P., Stelzer, F., Drog, B., 2017. Characterization of polyhydroxyalkanoates produced by *Synechocystis salina* from digestate supernatant. *International Journal of Biological Macromolecules* 102, 497–504. <https://doi.org/10.1016/j.ijbiomac.2017.04.054>
- Kumar, A.N., Katakajwala, R., Amulya, K., Mohan, S.V., 2021. Polyhydroxybutyrate production from dark-fermentative effluent and composite grafting with bagasse derived α -cellulose in a biorefinery approach. *Chemosphere* 279, 130563. <https://doi.org/10.1016/j.chemosphere.2021.130563>
- Kumari, K., Samantaray, S., Sahoo, D., Tripathy, B.C., 2021. Nitrogen, phosphorus and high CO₂ modulate photosynthesis, biomass and lipid production in the green alga *Chlorella vulgaris*. *Photosynthesis Research* 148, 17–32. <https://doi.org/10.1007/s11120-021-00828-0>
- Kumari, P., Ravi Kiran, B., Venkata Mohan, S., 2022. Polyhydroxybutyrate production by *Chlorella sorokiniana* SVMIICT8 under Nutrient-deprived mixotrophy. *Bioresource Technology* 354, 127135. <https://doi.org/10.1016/j.biortech.2022.127135>
- Lakatos, G.E., Rangelová, K., Câmara Manoel, J., Grivalský, T., Masojídek, J., 2021. Photosynthetic monitoring techniques indicate maximum glycogen accumulation in nitrogen-limited *Synechocystis* sp. PCC 6803 culture. *Algal Research* 55, 102271. <https://doi.org/10.1016/j.algal.2021.102271>

- Lee, J.J.-S.S., Park, H.J., Moon, M., Lee, J.J.-S.S., Min, K., 2021. Recent progress and challenges in microbial polyhydroxybutyrate (PHB) production from CO₂ as a sustainable feedstock: A state-of-the-art review. *Bioresource Technology* 339, 125616. <https://doi.org/10.1016/j.biortech.2021.125616>
- Li, S.F., Fanesi, A., Martin, T., Lopes, F., 2021. Biomass production and physiology of *Chlorella vulgaris* during the early stages of immobilized state are affected by light intensity and inoculum cell density. *Algal Research* 59, 102453. <https://doi.org/10.1016/j.algal.2021.102453>
- Llewellyn, C.A., Kapoore, R.V., Lovitt, R.W., Greig, C., Fuentes-Grünewald, C., Kultschar, B., 2019. Deriving Economic Value from Metabolites in Cyanobacteria, In: Hallmann, A., Rampelotto, P.H., Grand Challenges in Biology and Biotechnology. Springer International Publishing, Cham, pp. 535–576. https://doi.org/10.1007/978-3-030-25233-5_15
- López Rocha, C.J., Álvarez-Castillo, E., Estrada Yáñez, M.R., Bengoechea, C., Guerrero, A., Orta Ledesma, M.T., 2020. Development of bioplastics from a microalgae consortium from wastewater. *Journal of Environmental Management* 263, 110353. <https://doi.org/10.1016/j.jenvman.2020.110353>
- Lopez-Arenas, T., González-Contreras, M., Anaya-Reza, O., Sales-Cruz, M., 2017. Analysis of the fermentation strategy and its impact on the economics of the production process of PHB (polyhydroxybutyrate). *Computers & Chemical Engineering*, 107, 140–150. <https://doi.org/10.1016/j.compchemeng.2017.03.009>
- Lu, J.-J., Dong, Z.-J., Li, P., Yan, W.-J., Yuan, J.-J., Dong, W.-Y., Sun, F.-Y., Shao, Y.-X., 2022. Reduction of greenhouse gas (GHG) emission in the vegetation-activated sludge process (V-ASP) involving decontaminated plants for decentralized wastewater treatment. *Journal of Cleaner Production* 362, 132341. <https://doi.org/10.1016/j.jclepro.2022.132341>
- Lu, Q., Xiao, Y., 2022. From manure to high-value fertilizer: The employment of microalgae as a nutrient carrier for sustainable agriculture. *Algal Research* 67, 102855. <https://doi.org/10.1016/j.algal.2022.102855>
- Ma, M., Wei, C., Wang, H., Sha, C., Chen, M., Gong, Y., Hu, Q., 2019. Isolation and evaluation of a novel strain of *Chlorella sorokiniana* that resists grazing by the predator *Poteroioochromonas malhamensis*. *Algal Research* 38, 101429. <https://doi.org/10.1016/j.algal.2019.101429>

- Madadi, R., Maljaee, H., Serafim, L.S., Ventura, S.P.M., 2021. Microalgae as contributors to produce biopolymers. *Marine Drugs* 19, 1–27. <https://doi.org/10.3390/MD19080466>
- Maltsev, Y., Maltseva, K., Kulikovskiy, M., Maltseva, S., 2021. Influence of Light Conditions on Microalgae Growth and Content of Lipids, Carotenoids, and Fatty Acid Composition. *Biology* 10, 1060. <https://doi.org/10.3390/biology10101060>
- Mariotto, M., Egloff, S., Fritz, I., Refardt, D., 2023. Cultivation of the PHB-producing cyanobacterium *Synechococcus leopoliensis* in a pilot-scale open system using nitrogen from waste streams. *Algal Research* 70, 103013. <https://doi.org/10.1016/j.algal.2023.103013>
- Markov, S.A., Eivazova, E.R., Greenwood, J., 2006. Photostimulation of H₂ production in the green alga *Chlamydomonas reinhardtii* upon photoinhibition of its O₂-evolving system. *International Journal of Hydrogen Energy* 31, 1314–1317. <https://doi.org/10.1016/j.ijhydene.2005.11.017>
- Marquez, F.J., Sasaki, K., Nishio, N., Nagai, S., 1995. Inhibitory effect of oxygen accumulation on the growth of *Spirulina platensis*. *Biotechnology Letters* 17, 225–228. <https://doi.org/10.1007/BF00127993>
- Mastropetros, S.G., Pispas, K., Zagklis, D., Ali, S.S., Kornaros, M., 2022. Biopolymers production from microalgae and cyanobacteria cultivated in wastewater: Recent advances. *Biotechnology Advances* 60, 107999. <https://doi.org/10.1016/J.BIOTECHADV.2022.107999>
- Mathiot, C., Ponge, P., Gallard, B., Sassi, J.F., Delrue, F., Le Moigne, N., 2019. Microalgae starch-based bioplastics: Screening of ten strains and plasticization of unfractionated microalgae by extrusion. *Carbohydrate Polymers* 208, 142–151. <https://doi.org/10.1016/j.carbpol.2018.12.057>
- Meixner, K., Daffert, C., Bauer, L., Drosig, B., Fritz, I., 2022. PHB Producing Cyanobacteria Found in the Neighborhood— Their Isolation, Purification and Performance Testing. *Bioengineering* 9. <https://doi.org/10.3390/bioengineering9040178>
- Meixner, K., Fritz, I., Daffert, C., Markl, K., Fuchs, W., Drosig, B., 2016. Processing recommendations for using low-solids digestate as nutrient solution for poly-β-hydroxybutyrate production with *Synechocystis salina*. *Journal of Biotechnology* 240, 61–67. <https://doi.org/10.1016/j.jbiotec.2016.10.023>

- Mendiburu, F. de, 2023. agricolae: Statistical Procedures for Agricultural Research. The Comprehensive R Archive Network. <https://cran.r-project.org/web/packages/agricolae/index.html>
- Milferstedt, K., Hamelin, J., Park, C., Jung, J., Hwang, Y., Cho, S.-K., Jung, K.-W., Kim, D.-H., 2017a. Biogranules applied in environmental engineering. *International Journal of Hydrogen Energy* 42, 27801–27811. <https://doi.org/10.1016/j.ijhydene.2017.07.176>
- Milferstedt, K., Kuo-Dahab, W.C., Butler, C.S., Hamelin, J., Abouhend, A.S., Stauch-White, K., McNair, A., Watt, C., Carbajal-González, B.I., Dolan, S., Park, C., 2017b. The importance of filamentous cyanobacteria in the development of oxygenic photogranules. *Scientific Reports* 7, 17944. <https://doi.org/10.1038/s41598-017-16614-9>
- Montaño San Agustín, D., Orta Ledesma, M.T., Monje Ramírez, I., Yáñez Noguez, I., Luna Pabello, V.M., Velasquez-Orta, S.B., 2022. A non-sterile heterotrophic microalgal process for dual biomass production and carbon removal from swine wastewater. *Renewable Energy* 181, 592–603. <https://doi.org/10.1016/j.renene.2021.09.028>
- Montiel-Corona, V., Buitrón, G., 2022. Polyhydroxybutyrate production in one-stage by purple phototrophic bacteria: Influence of alkaline pH, ethanol, and C/N ratios. *Biochemical Engineering Journal* 189, 108715. <https://doi.org/10.1016/j.bej.2022.108715>
- Morales-Plasencia, M.E., Ibarra-Castro, L., Martínez-Brown, J.M., Nieves-Soto, M., Bermúdez-Lizárraga, J.F., Rojo-Cebreros, A.H., 2023. The effect of nitrogen limitation on carbohydrates and β -glucan accumulation in *Nannochloropsis oculata*. *Algal Research* 72, 103125. <https://doi.org/10.1016/j.algal.2023.103125>
- More, T.T., Yadav, J.S.S., Yan, S., Tyagi, R.D., Surampalli, R.Y., 2014. Extracellular polymeric substances of bacteria and their potential environmental applications. *Journal of Environmental Management* 144, 1–25. <https://doi.org/10.1016/j.jenvman.2014.05.010>
- Morillas-España, A., Lafarga, T., Sánchez-Zurano, A., Acién-Fernández, F.G., González-López, C., 2022. Microalgae based wastewater treatment coupled to the production of high value agricultural products: Current needs and challenges. *Chemosphere* 291, 132968. <https://doi.org/10.1016/j.chemosphere.2021.132968>
- Mourão, M.M., Gradíssimo, D.G., Santos, A.V., Schneider, M.P.C., Faustino, S.M.M., Vasconcelos, V., Xavier, L.P., 2020. Optimization of Polyhydroxybutyrate Production by

- Amazonian Microalga *Stigeoclonium* sp. B23. *Biomolecules* 10, 1628.
<https://doi.org/10.3390/biom10121628>
- Mückschel, F., Ollo, E., Glaeser, S.P., Düring, R., Yan, F., Velten, H., Theilen, U., Frei, M., 2023. Nitrogen use efficiency of microalgae application in wheat compared to mineral fertilizer. *Journal of Plant Nutrition and Soil Science* 186, 522-531.
<https://doi.org/10.1002/jpln.202300125>
- Muller, M., Jimenez, J., Antonini, M., Dudal, Y., Latrille, E., Vedrenne, F., Steyer, J.-P., Patureau, D., 2014. Combining chemical sequential extractions with 3D fluorescence spectroscopy to characterize sludge organic matter. *Waste Management* 34, 2572–2580.
<https://doi.org/10.1016/j.wasman.2014.07.028>
- Nadarajan, S., Sukumaran, S., 2021. Chemistry and toxicology behind chemical fertilizers, In: Lewu, F.B., Volova, T., Thomas, S., Rakhimol, K.R. (Eds.), *Controlled Release Fertilizers for Sustainable Agriculture*. Elsevier, Amsterdam, pp. 195–229.
<https://doi.org/10.1016/B978-0-12-819555-0.00012-1>
- Nanda, N., Bharadvaja, N., 2022. Algal bioplastics: current market trends and technical aspects. *Clean Technologies and Environmental Policy* 24, 2659–2679.
<https://doi.org/10.1007/s10098-022-02353-7>
- Narayanan, M., Kandasamy, S., Kumarasamy, S., Gnanavel, K., Ranganathan, M., Kandasamy, G., 2020. Screening of polyhydroxybutyrate producing indigenous bacteria from polluted lake soil. *Heliyon* 6. <https://doi.org/10.1016/j.heliyon.2020.e05381>
- Neumann, N., Doello, S., Forchhammer, K., 2021. Recovery of Unicellular Cyanobacteria from Nitrogen Chlorosis: A Model for Resuscitation of Dormant Bacteria. *Microbial Physiology* 31, 78–87. <https://doi.org/10.1159/000515742>
- Noyola, A., Paredes, M.G., Morgan-Sagastume, J.M., Güereca, L.P., 2016. Reduction of Greenhouse Gas Emissions From Municipal Wastewater Treatment in Mexico Based on Technology Selection. *CLEAN Soil Air Water* 44, 1091–1098.
<https://doi.org/10.1002/clen.201500084>
- OECD, 2022. Global Plastics Outlook: Policy Scenarios to 2060. OECD Publishing, Paris, <https://doi.org/10.1787/aa1edf33-en>.
- Paliwal, C., Pancha, I., Ghosh, T., Maurya, R., Chokshi, K., Vamsi Bharadwaj, S.V., Ram, S., Mishra, S., 2015. Selective carotenoid accumulation by varying nutrient media and salinity

- in *Synechocystis* sp. CCNM 2501. *Bioresource Technology* 197, 363–368. <https://doi.org/10.1016/j.biortech.2015.08.122>
- Panda, B., Mallick, N., 2007. Enhanced poly- β -hydroxybutyrate accumulation in a unicellular cyanobacterium, *Synechocystis* sp. PCC 6803. *Letters in Applied Microbiology* 44, 194–198. <https://doi.org/10.1111/j.1472-765X.2006.02048.x>
- Park, Y.-K., Lee, J., 2023. Achievements in the production of bioplastics from microalgae. *Phytochemistry Reviews* 22, 1147–1165. <https://doi.org/10.1007/s11101-021-09788-8>
- Phalanisong, P., Plangklang, P., Reungsang, A., González-Fernandez, C., Gouveia, L., 2021. Photoautotrophic and Mixotrophic Cultivation of Polyhydroxyalkanoate-Accumulating Microalgae Consortia Selected under Nitrogen and Phosphate Limitation. *Molecules*, Vol. 26, 7613–7626. <https://doi.org/10.3390/molecules26247613>
- Posadas, E., García-Encina, P.-A., Soltau, A., Domínguez, A., Díaz, I., Muñoz, R., 2013. Carbon and nutrient removal from centrates and domestic wastewater using algal–bacterial biofilm bioreactors. *Bioresource Technology* 139, 50–58. <https://doi.org/10.1016/j.biortech.2013.04.008>
- Price, S., Kuzhiumparambil, U., Pernice, M., Ralph, P.J., 2020. Cyanobacterial polyhydroxybutyrate for sustainable bioplastic production: Critical review and perspectives. *Journal of Environmental Chemical Engineering* 8, 104007. <https://doi.org/10.1016/j.jece.2020.104007>
- Quijano, G., Arcila, J.S., Buitrón, G., 2017. Microalgal-bacterial aggregates: Applications and perspectives for wastewater treatment. *Biotechnology Advances* 35, 772–781. <https://doi.org/10.1016/j.biotechadv.2017.07.003>
- Rajpoot, A.S., Choudhary, T., Chelladurai, H., Nath Verma, T., Shende, V., 2022. A comprehensive review on bioplastic production from microalgae. *Materials Today: Proceedings* 56, 171–178. <https://doi.org/10.1016/j.matpr.2022.01.060>
- Raso, S., van Genugten, B., Vermuë, M., Wijffels, R.H., 2012. Effect of oxygen concentration on the growth of *Nannochloropsis* sp. at low light intensity. *Journal of Applied Phycology* 24, 863–871. <https://doi.org/10.1007/s10811-011-9706-z>
- Ray, A., Nayak, M., Ghosh, A., 2022. A review on co-culturing of microalgae: A greener strategy towards sustainable biofuels production. *Science of The Total Environment* 802, 149765. <https://doi.org/10.1016/j.scitotenv.2021.149765>

- Razzak, S.A., Lucky, R.A., Hossain, M.M., deLasa, H., 2022. Valorization of Microalgae Biomass to Biofuel Production: A review. *Energy Nexus* 7, 100139. <https://doi.org/10.1016/j.nexus.2022.100139>
- Riffat, R., Husnain, T., 2022. Fundamentals of Wastewater Treatment and Engineering, CRC Press, London. <https://doi.org/10.1201/9781003134374>
- Rohit, M.V., Venkata Mohan, S., 2018. Quantum Yield and Fatty Acid Profile Variations With Nutritional Mode During Microalgae Cultivation. *Frontiers in Bioengineering and Biotechnology* 6, 111. <https://doi.org/10.3389/fbioe.2018.00111>
- Romero-Frasca, E., Velasquez-Orta, S.B., Escobar-Sánchez, V., Tinoco-Valencia, R., Orta Ledesma, M.T., 2021. Bioprospecting of wild type ethanologenic yeast for ethanol fuel production from wastewater-grown microalgae. *Biotechnology for Biofuels* 14, 93. <https://doi.org/10.1186/s13068-021-01925-x>
- Ruangsomboon, S., Ganmanee, M., Choochote, S., 2013. Effects of different nitrogen, phosphorus, and iron concentrations and salinity on lipid production in newly isolated strain of the tropical green microalga, *Scenedesmus dimorphus* KMITL. *Journal of Applied Phycology* 25, 867–874. <https://doi.org/10.1007/s10811-012-9956-4>
- Rueda, E., Álvarez-González, A., Vila, J., Díez-Montero, R., Grifoll, M., García, J., 2022a. Inorganic carbon stimulates the metabolic routes related to the polyhydroxybutyrate production in a *Synechocystis* sp. strain (cyanobacteria) isolated from wastewater. *Science of The Total Environment* 829, 154691. <https://doi.org/10.1016/j.scitotenv.2022.154691>
- Rueda, E., García-Galán, M.J., Díez-Montero, R., Vila, J., Grifoll, M., García, J., 2020a. Polyhydroxybutyrate and glycogen production in photobioreactors inoculated with wastewater borne cyanobacteria monocultures. *Bioresource Technology* 295, 122233. <https://doi.org/10.1016/j.biortech.2019.122233>
- Rueda, E., García-Galán, M.J., Ortiz, A., Uggetti, E., Carretero, J., García, J., Díez-Montero, R., 2020b. Bioremediation of agricultural runoff and biopolymers production from cyanobacteria cultured in demonstrative full-scale photobioreactors. *Process Safety and Environmental Protection* 139, 241–250. <https://doi.org/10.1016/j.psep.2020.03.035>
- Rueda, E., Gonzalez-Flo, E., Roca, L., Carretero, J., García, J., 2022b. Accumulation of polyhydroxybutyrate in *Synechocystis* sp. isolated from wastewaters: Effect of salinity,

- light, and P content in the biomass. *Journal of Environmental Chemical Engineering* 10, 107952. <https://doi.org/10.1016/j.jece.2022.107952>
- Rumin, J., Bonnefond, H., Saint-Jean, B., Rouxel, C., Sciandra, A., Bernard, O., Cadoret, J.P., Bougaran, G., 2015. The use of fluorescent Nile red and BODIPY for lipid measurement in microalgae. *Biotechnology for Biofuels* 8, 1–16. <https://doi.org/10.1186/s13068-015-0220-4>
- Safi, C., Cabas Rodriguez, L., Mulder, W.J., Engelen-Smit, N., Spekking, W., van den Broek, L.A.M., Olivieri, G., Sijtsma, L., 2017. Energy consumption and water-soluble protein release by cell wall disruption of *Nannochloropsis gaditana*. *Bioresource Technology* 239, 204–210. <https://doi.org/10.1016/j.biortech.2017.05.012>
- Safi, C., Ursu, A.V., Laroche, C., Zebib, B., Merah, O., Pontalier, P.-Y., Vaca-Garcia, C., 2014. Aqueous extraction of proteins from microalgae: Effect of different cell disruption methods. *Algal Research* 3, 61–65. <https://doi.org/10.1016/j.algal.2013.12.004>
- Saidu, H., Mohammed Ndejiko, J., Abdullahi, N., Bello Mahmoud, A., Eva Mohamad, S., 2022. Microalgae: a cheap tool for wastewater abatement and biomass recovery. *Environmental Technology Reviews* 11, 202–225. <https://doi.org/10.1080/21622515.2022.2147453>
- Sayara, T., Khayat, S., Saleh, J., Abu-Khalaf, N., van der Steen, P., 2021. Algal–bacterial symbiosis for nutrients removal from wastewater: The application of multivariate data analysis for process monitoring and control. *Environmental Technology & Innovation* 23, 101548. <https://doi.org/10.1016/j.eti.2021.101548>
- Selvaraj, K., Vishvanathan, N., Dhandapani, R., 2021. Screening, optimization and characterization of poly hydroxy butyrate from fresh water microalgal isolates. *International Journal of Biobased Plastics* 3, 139–162. <https://doi.org/10.1080/24759651.2021.1926621>
- Senatore, V., Rueda, E., Bellver, M., Díez-Montero, R., Ferrer, I., Zarra, T., Naddeo, V., García, J., 2023. Production of phycobiliproteins, bioplastics and lipids by the cyanobacteria *Synechocystis* sp. treating secondary effluent in a biorefinery approach. *Science of The Total Environment* 857, 159343. <https://doi.org/10.1016/j.scitotenv.2022.159343>
- Shahid, A., Khan, F., Ahmad, N., Farooq, M., Mehmood, M.A., 2020. Microalgal Carbohydrates and Proteins: Synthesis, Extraction, Applications, and Challenges, In: Alam, Md.A., Xu, J.-L., Wang, Z. (Eds.), *Microalgae Biotechnology for Food, Health and High Value Products*.

- Springer International Publishing, Singapore, pp. 433–468. https://doi.org/10.1007/978-981-15-0169-2_14
- Sharma, A.K., Sahoo, P.K., Singhal, S., Patel, A., 2016. Impact of various media and organic carbon sources on biofuel production potential from *Chlorella* spp. *3 Biotech* 6, 116. <https://doi.org/10.1007/S13205-016-0434-6>
- Shishatskaya, E., Nemtsev, I., Lukyanenko, A., Vasiliev, A., Kiselev, E., Sukovatyi, A., Volova, T., 2020. Polymer Films of Poly-3-hydroxybutyrate Synthesized by *Cupriavidus necator* from Different Carbon Sources. *Journal of Polymers and the Environment*. <https://doi.org/10.1007/s10924-020-01924-3>
- Shriwastav, A., Mohamed, J., Bose, P., Shekhar, M., 2015. Deconvoluting algal and bacterial biomass concentrations in algal-bacterial suspensions. *Journal of Applied Phycology* 27, 211–222. <https://doi.org/10.1007/s10811-014-0302-x>
- Shukla, R., Ahammad, S.Z., 2022. Performance evaluation and microbial community structure of a modified trickling filter and conventional activated sludge process in treating urban sewage. *Science of The Total Environment* 853, 158331. <https://doi.org/10.1016/j.scitotenv.2022.158331>
- Siddiki, S.Y.A., Mofijur, M., Kumar, P.S., Ahmed, S.F., Inayat, A., Kusumo, F., Badruddin, I.A., Khan, T.M.Y., Nghiem, L.D., Ong, H.C., Mahlia, T.M.I., 2022. Microalgae biomass as a sustainable source for biofuel, biochemical and biobased value-added products: An integrated biorefinery concept. *Fuel* 307, 121782. <https://doi.org/10.1016/j.fuel.2021.121782>
- Silva, D.F.S., Speranza, L.G., Quartaroli, L., Moruzzi, R.B., Silva, G.H.R., 2021. Separation of microalgae cultivated in anaerobically digested black water using *Moringa Oleifera* Lam seeds as coagulant. *Journal of Water Process Engineering* 39, 101738. <https://doi.org/10.1016/j.jwpe.2020.101738>
- Singh, A.K., Mallick, N., 2017. Advances in cyanobacterial polyhydroxyalkanoates production. *FEMS Microbiology Letters* 364, 1–13. <https://doi.org/10.1093/femsle/fnx189>
- Singh, A.K., Sharma, L., Mallick, N., Mala, J., 2017. Progress and challenges in producing polyhydroxyalkanoate biopolymers from cyanobacteria. *Journal of Applied Phycology* 29, 1213–1232. <https://doi.org/10.1007/s10811-016-1006-1>

- Singhon, P., Phoraksa, O., Incharoensakdi, A., Monshupanee, T., 2021. Increased bioproduction of glycogen, lipids, and poly(3-hydroxybutyrate) under partial supply of nitrogen and phosphorus by photoautotrophic cyanobacterium *Synechocystis* sp. PCC 6803. *Journal of Applied Phycology* 33, 1–11. <https://doi.org/10.1007/s10811-021-02494-0>
- Sirohi, R., Lee, J.S., Yu, B.S., Roh, H., Sim, S.J., 2021. Sustainable production of polyhydroxybutyrate from autotrophs using CO₂ as feedstock: Challenges and opportunities. *Bioresource Technology* 341, 125751. <https://doi.org/10.1016/j.biortech.2021.125751>
- Slompo, N.D.M., Quartaroli, L., Fernandes, T.V., Silva, G.H.R. da, Daniel, L.A., 2020. Nutrient and pathogen removal from anaerobically treated black water by microalgae. *Journal of Environmental Management* 268, 110693. <https://doi.org/10.1016/j.jenvman.2020.110693>
- Soares, F., Trovão, J., Portugal, A., 2022. Phototrophic and fungal communities inhabiting the Roman cryptoporticus of the national museum Machado de Castro (UNESCO site, Coimbra, Portugal). *World Journal of Microbiology and Biotechnology* 38, 1–16. <https://doi.org/10.1007/s11274-022-03345-x>
- Sukkasam, N., Incharoensakdi, A., Monshupanee, T., 2022. Chemicals Affecting Cyanobacterial Poly(3-hydroxybutyrate) Accumulation: 2-Phenylethanol Treatment Combined with Nitrogen Deprivation Synergistically Enhanced Poly(3-hydroxybutyrate) Storage in *Synechocystis* sp. PCC6803 and *Anabaena* sp. TISTR8076. *Plant and Cell Physiology* 63, 1253–1272. <https://doi.org/10.1093/pcp/pcac100>
- Tamis, J., Lužkov, K., Jiang, Y., Loosdrecht, M.C.M. van, Kleerebezem, R., 2014. Enrichment of *Plasticicumulans acidivorans* at pilot-scale for PHA production on industrial wastewater. *Journal of Biotechnology* 192, 161–169. <https://doi.org/10.1016/j.jbiotec.2014.10.022>
- Tang, Y., Dai, X., Dong, B., Guo, Y., Dai, L., 2020. Humification in extracellular polymeric substances (EPS) dominates methane release and EPS reconstruction during the sludge stabilization of high-solid anaerobic digestion. *Water Research* 175, 115686. <https://doi.org/10.1016/j.watres.2020.115686>
- Tchobanoglous, G., Stensel, H.D., Tsuchihashi, R., Burton, F.L., Abu-Orf, M.M., Bowden, G., Pfrang, W., 2014. Wastewater engineering: treatment and resource recovery. McGraw-Hill Education, New York.

- Tharasirivat, V., Jantaro, S., 2023. Increased Biomass and Polyhydroxybutyrate Production by *Synechocystis* sp. PCC 6803 Overexpressing RuBisCO Genes. *International Journal of Molecular Sciences* 24, 6415. <https://doi.org/10.3390/IJMS24076415/S1>
- Tian, D., Li, Z., O'Connor, D., Shen, Z., 2020. The need to prioritize sustainable phosphate-based fertilizers. *Soil Use and Management* 36, 351–354. <https://doi.org/10.1111/sum.12578>
- Toro-Huertas, E.I., Franco-Morgado, M., de los Cobos Vasconcelos, D., González-Sánchez, A., 2019. Photorespiration in an outdoor alkaline open-photobioreactor used for biogas upgrading. *Science of The Total Environment* 667, 613–621. <https://doi.org/10.1016/j.scitotenv.2019.02.374>
- Trakunjae, C., Boondaeng, A., Apiwatanapiwat, W., Kosugi, A., Arai, T., Sudesh, K., Vaithanomsat, P., 2021. Enhanced polyhydroxybutyrate (PHB) production by newly isolated rare actinomycetes *Rhodococcus* sp. strain BSRT1-1 using response surface methodology. *Scientific Reports* 11, 1896. <https://doi.org/10.1038/s41598-021-81386-2>
- Trebuch, L.M., Sohier, J., Altenburg, S., Oyserman, B.O., Pronk, M., Janssen, M., Vet, L.E.M., Wijffels, R.H., Fernandes, T.V., 2023. Enhancing phosphorus removal of photogranules by incorporating polyphosphate accumulating organisms. *Water Research* 235, 119748. <https://doi.org/10.1016/j.watres.2023.119748>
- van Alphen, P., Abedini Najafabadi, H., Branco dos Santos, F., Hellingwerf, K.J., 2018. Increasing the Photoautotrophic Growth Rate of *Synechocystis* sp. PCC 6803 by Identifying the Limitations of Its Cultivation. *Biotechnology Journal* 13, 1700764. <https://doi.org/10.1002/biot.201700764>
- Vital-Jácome, M., Díaz-Zamorano, A.L., Cuautle-Marín, M., Moreno, G., Buitrón, G., Muñoz, R., Quijano, G., 2020. Microalgal–bacterial aggregates with flue gas supply as a platform for the treatment of anaerobic digestion centrate. *Journal of Chemical Technology & Biotechnology* 95, 289–296. <https://doi.org/10.1002/jctb.6235>
- Vu, C.H.T., Lee, H.G., Chang, Y.K., Oh, H.M., 2018. Axenic cultures for microalgal biotechnology: Establishment, assessment, maintenance, and applications. *Biotechnology Advances* 36, 380–396. <https://doi.org/10.1016/J.BIOTECHADV.2017.12.018>
- Vuppaladadiyam, A.K., Prinsen, P., Raheem, A., Luque, R., Zhao, M., 2018. Microalgae cultivation and metabolites production: a comprehensive review. *Biofuels, Bioproducts and Biorefining* 12, 304–324. <https://doi.org/10.1002/bbb.1864>

- Wang, Q., Jin, W., Zhou, X., Guo, S., Gao, S.-H., Chen, C., Tu, R., Han, S.-F., Jiang, J., Feng, X., 2019. Growth enhancement of biodiesel-promising microalga *Chlorella pyrenoidosa* in municipal wastewater by polyphosphate-accumulating organisms. *Journal of Cleaner Production* 240, 118148. <https://doi.org/10.1016/j.jclepro.2019.118148>
- Wanner, J., 2021. The development in biological wastewater treatment over the last 50 years. *Water Science and Technology* 84, 274–283. <https://doi.org/10.2166/wst.2021.095>
- Wehr, J.D., Sheath, R.G., Kocielek, J.P., 2015. *Freshwater Algae of North America: Ecology and Classification*. Elsevier, Amsterdam. <https://doi.org/10.1016/C2010-0-66664-8>
- Wu, Q., Guo, L., Li, X., Wang, Y., 2021. Effect of phosphorus concentration and light/dark condition on phosphorus uptake and distribution with microalgae. *Bioresource Technology* 340, 125745. <https://doi.org/10.1016/j.biortech.2021.125745>
- Xie, B., Gong, W., Tian, Y., Qu, F., Luo, Y., Du, X., Tang, X., Xu, D., Lin, D., Li, G., Liang, H., 2018. Biodiesel production with the simultaneous removal of nitrogen, phosphorus and COD in microalgal-bacterial communities for the treatment of anaerobic digestion effluent in photobioreactors. *Chemical Engineering Journal* 350, 1092–1102. <https://doi.org/10.1016/j.cej.2018.06.032>
- Xin, L., Hong-ying, H., Ke, G., Ying-xue, S., 2010. Effects of different nitrogen and phosphorus concentrations on the growth, nutrient uptake, and lipid accumulation of a freshwater microalga *Scenedesmus* sp. *Bioresource Technology* 101, 5494–5500. <https://doi.org/10.1016/j.biortech.2010.02.016>
- Yan, H., Lu, R., Liu, Y., Cui, X., Wang, Y., Yu, Z., Ruan, R., Zhang, Q., 2022. Development of microalgae-bacteria symbiosis system for enhanced treatment of biogas slurry. *Bioresource Technology* 354, 127187. <https://doi.org/10.1016/j.biortech.2022.127187>
- Yashavanth, P.R., Das, M., Maiti, S.K., P R., Y., Das, M., Maiti, S.K., 2021. Recent progress and challenges in cyanobacterial autotrophic production of polyhydroxybutyrate (PHB), a bioplastic. *Journal of Environmental Chemical Engineering* 9, 105379. <https://doi.org/10.1016/j.jece.2021.105379>
- Yu, T.-H., Lin, A.Y.-C., Lateef, S.K., Lin, C.-F., Yang, P.-Y., 2009. Removal of antibiotics and non-steroidal anti-inflammatory drugs by extended sludge age biological process. *Chemosphere*, 175–181. <https://doi.org/10.1016/j.chemosphere.2009.07.049>

- Zanchetta, E., Damergi, E., Patel, B., Borgmeyer, T., Pick, H., Pulgarin, A., Ludwig, C., 2021. Algal cellulose, production and potential use in plastics: Challenges and opportunities. *Algal Research* 56, 102288. <https://doi.org/10.1016/j.algal.2021.102288>
- Zhang, B., Li, W., Guo, Y., Zhang, Z., Shi, W., Cui, F., Lens, P.N.L.L., Tay, H., Tay, J.H., 2020. Microalgal-bacterial consortia: From interspecies interactions to biotechnological applications. *Renewable and Sustainable Energy Reviews* 118, 109563. <https://doi.org/10.1016/j.rser.2019.109563>
- Zhang, C., Show, P.L., Ho, S.H., 2019a. Progress and perspective on algal plastics – A critical review. *Bioresource Technology* 289, 121700. <https://doi.org/10.1016/j.biortech.2019.121700>
- Zhang, Y., Wu, H., Yuan, C., Li, T., Li, A., 2019b. Growth, biochemical composition, and photosynthetic performance of *Scenedesmus acuminatus* during nitrogen starvation and resupply. *Journal of Applied Phycology* 31, 2797–2809. <https://doi.org/10.1007/s10811-019-01783-z>
- Zhao, X., Zhou, Y., Huang, S., Qiu, D., Schideman, L., Chai, X., Zhao, Y., 2014. Characterization of microalgae-bacteria consortium cultured in landfill leachate for carbon fixation and lipid production. *Bioresource Technology* 156, 322–328. <https://doi.org/10.1016/j.biortech.2013.12.112>
- Zhou, Y., Nguyen, B.T., Zhou, C., Straka, L., Lai, Y.S., Xia, S., Rittmann, B.E., 2017. The distribution of phosphorus and its transformations during batch growth of *Synechocystis*. *Water Research* 122, 355–362. <https://doi.org/10.1016/j.watres.2017.06.017>

Thesis products

Research papers:

- Romero-Frasca, E., Buitrón, G., 2023. Assessment of polyhydroxyalkanoates and polysaccharides production in native phototrophic consortia under nitrogen and phosphorous-starved conditions. *International Journal of Environmental Science and Technology*. <https://doi.org/10.1007/s13762-023-05332-7>
- Romero-Frasca, E., Buitrón, G., González-Sánchez, A., Etchebehere, C. 2024. Effect of dissolved oxygen concentration on polyhydroxybutyrate production by *Synechocystis* sp. grown in mineral medium and wastewater. *Submitted for publication*.
- Romero-Frasca, E., Galea-Outón, S., Coronado-Apodaca, K.G., Milferstedt, K., Jimenez, J., Hamelin, J., Buitrón, G., 2024. Bioaccessibility characterization of organic matter, nitrogen, and phosphorus from microalgae-bacteria aggregates. *Waste and Biomass Valorization*. <https://doi.org/10.1007/s12649-024-02495-3>

Book chapters:

- Romero-Frasca, E., Buitrón, G. (2022). Determinación de carbohidratos totales por fenol-sulfúrico (DuBois-Gilles-Hamilton). In: Gouveia, L., Navarro, J.M. (Eds.), *Protocolos de Microalgas de la Red RENUWAL I*, pp. 62-68. Programa Iberoamericano de Ciencia y Tecnología para el Desarrollo, Madrid.
- Romero-Frasca, E., Buitrón, G. (2024). Long-term storage of photoautotrophic microorganisms on solid culture medium. In: Álvarez-Montenegro, X., Mercado-Reyes, I. (Eds.), *Microalgae Protocols II*, pp. 80-84. Programa Iberoamericano de Ciencia y Tecnología para el Desarrollo, Madrid.

Conference participations:

- Romero-Frasca, E, Buitrón, G. Obtención de polihidroxiálcanoatos a partir de consorcios de cianobacterias procedentes de aguas residuales. XIX Congreso Nacional de Biotecnología y Bioingeniería de la Sociedad Mexicana de Biotecnología y Bioingeniería (SMBB). September 2021.

- Romero-Frasca E, Galea-Outón S, Buitrón G, Jimenez J, Hamelin J, Milferstedt K. Accessibility and complexity of nutrients present in residual microalgal-bacterial biomass for soil conditioning. 4th International Conference for Bioresource Technology for Bioenergy, Bioproducts & Environmental Sustainability. Lake Garda, Italy. May 2023.
- Romero-Frasca, E., Buitrón, G. Assessment of polyhydroxyalkanoates production in photosynthetic communities from activated sludge and *Chlorella sorokiniana* consortium. 7th International Symposium on Environmental Biotechnology and Engineering. Marseille, France. May 2023.
- Romero-Frasca, E., Buitrón, G. Effect of dissolved oxygen levels on photoautotrophic polyhydroxybutyrate production in mixed cyanobacteria consortium. International Conference on Algal Biomass, Biofuels and Bioproducts (AlgalBBB 2023). Hawaii, USA. June 2023.
- Romero-Frasca, E, Buitrón, G. Effect of dissolved oxygen on photoautotrophic polyhydroxybutyrate production by *Synechocystis* sp. XX Congreso Nacional de Biotecnología y Bioingeniería de la Sociedad Mexicana de Biotecnología y Bioingeniería (SMBB). September 2023.

Workshops and seminars:

- Romero-Frasca, E. Obtención de polihidroxiálcanoatos a partir de consorcios de cianobacterias procedentes de aguas residuales. Universidad Autónoma de Querétaro. 12 November 2021.
- Romero-Frasca, E., Buitrón, G. Recuperación de recursos durante el tratamiento de aguas bajo el concepto de economía circular. 6th Conference IWA-YWP Mexico. 24 May 2022.

Supplementary material

Figures

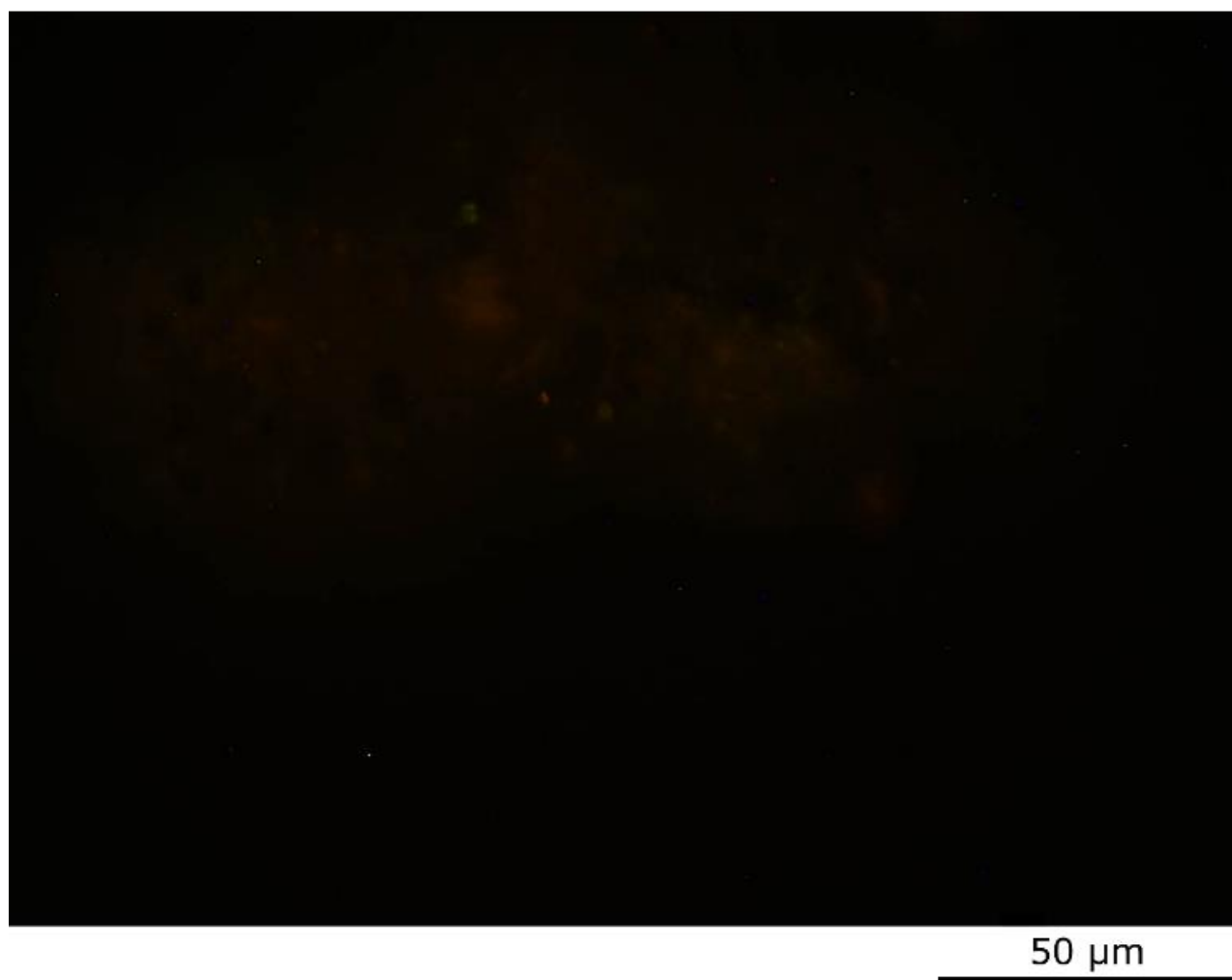


Figure S0.1. Microscopic imaging of non-stressed polymer accumulating photoautotrophic strains observed under fluorescence microscope at 40X after straining with Nile red dye. Any observed fluorescence, only a dark field.

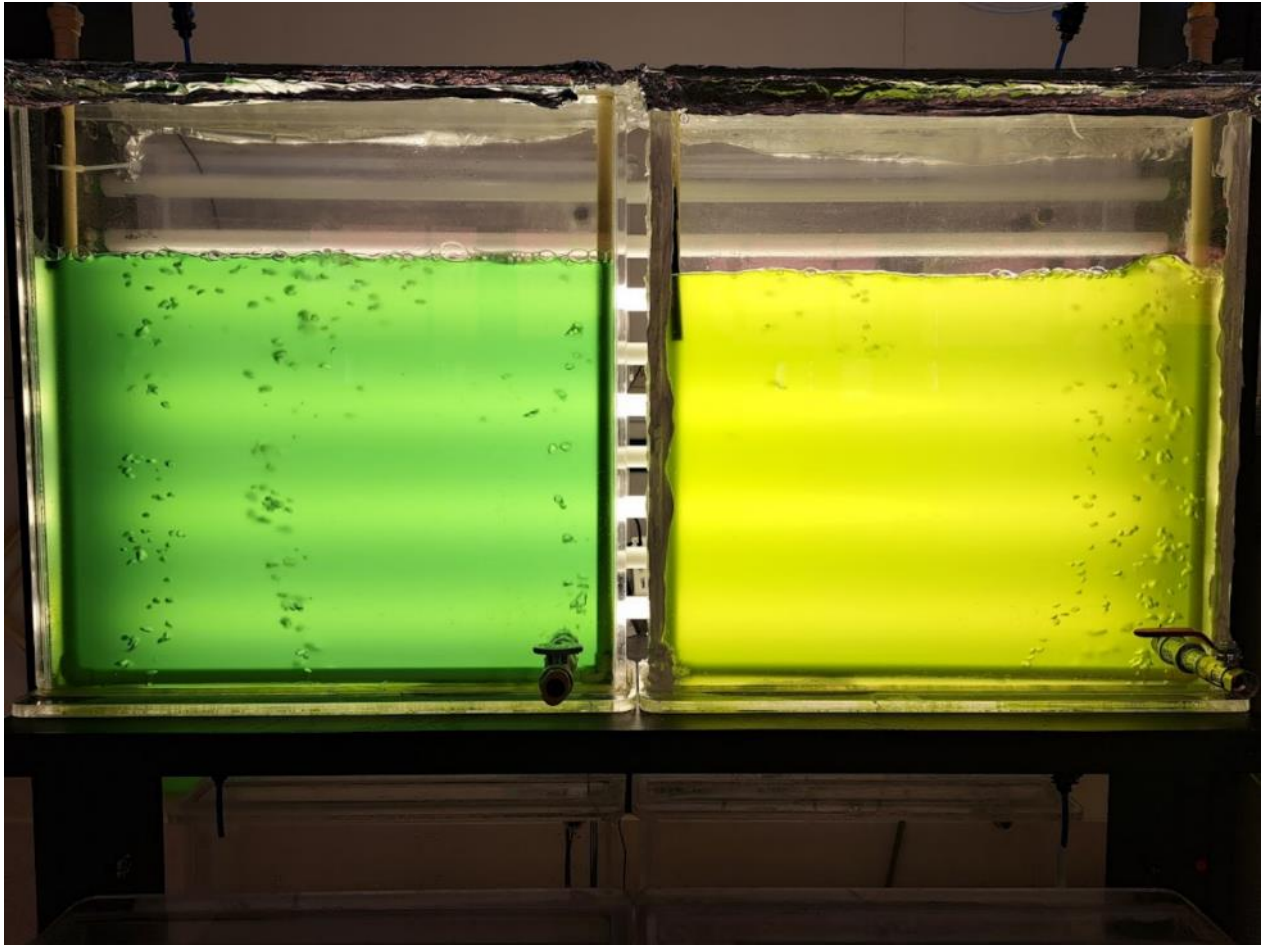


Figure S0.2. Indoor cultivation of *C. sorokiniana* dominated consortium in FP-PBR under nutrient-rich (left) and nutrient-unbalanced (right) conditions. Note yellowish color.

Tables

Table S5.1. Organic matter content in each fraction extracted from microalgae-bacteria aggregates. Lowercase letters indicate whether there are significant differences ($p \leq 0.05$) between fractions extracted for each sample. Percentage in terms of Total Organic Matter content.

Sample type	Organic matter (mgCOD·g dry matter ⁻¹)					Total organic matter (mgCOD·g dry matter ⁻¹)
	Soluble extractable	Readily extractable	Slowly extractable	Poorly extractable	Non-extractable	
Loose flocs	108 ± 1 ^a (10%)	101 ± 1 ^c (10%)	116 ± 3 ^c (12%)	177 ± 10 ^b (18%)	502 ± 11 ^a (50%)	1004 ± 2 ^c
Consolidated flocs	186 ± 7 ^a (17%)	359 ± 1 ^a (33%)	304 ± 1 ^a (28%)	182 ± 13 ^b (16%)	66 ± 38 ^c (6%)	1097 ± 17 ^b
Smooth granules	181 ± 53 ^a (15%)	207 ± 17 ^b (17%)	157 ± 17 ^b (13%)	168 ± 9 ^b (14%)	495 ± 25 ^a (41%)	1208 ± 71 ^a
Filamentous granules	111 ± 5 ^a (9%)	121 ± 7 ^c (10%)	157 ± 8 ^b (13%)	478 ± 15 ^a (39%)	356 ± 25 ^b (29%)	1223 ± 1 ^a

Table S5.2. Nitrogen content in each fraction extracted from microalgae-bacteria aggregates. Lowercase letters indicate whether there are significant differences ($p \leq 0.05$) between fractions extracted for each sample. Percentage in terms of Total Nitrogen content.

Sample type	Nitrogen (mgTN·g dry matter ⁻¹)					Total nitrogen (mgTN·g dry matter ⁻¹)
	Soluble extractable	Readily extractable	Slowly extractable	Poorly extractable	Non- extractable	
Loose flocs	22 ± 1 ^a (23%)	9 ± 1 ^c (10%)	11 ± 1 ^a (12%)	11 ± 1 ^b (12%)	40 ± 1 ^a (43%)	93 ± 3 ^a
Consolidated flocs	21 ± 9 ^a (24%)	36 ± 2 ^a (41%)	16 ± 2 ^a (18%)	8 ± 1 ^c (9%)	7 ± 5 ^b (8%)	88 ± 4 ^a
Smooth granules	12 ± 1 ^a (20%)	21 ± 1 ^b (36%)	15 ± 4 ^a (25%)	7 ± 1 ^c (12%)	4 ± 4 ^b (7%)	59 ± 3 ^c
Filamentous granules	6 ± 1 ^a (8%)	11 ± 1 ^b (15%)	15 ± 1 ^a (21%)	33 ± 1 ^a (45%)	8 ± 1 ^b (11%)	73 ± 2 ^b

Table S5.3. Total bioavailable phosphorous content in each fraction extracted from microalgae-bacteria aggregates. Lowercase letters indicate whether there are significant differences ($p \leq 0.05$) between fractions extracted for each sample. Percentage in terms of Total Bioavailable Phosphorous content.

Sample type	Bioavailable phosphorous (mg TBP·g dry matter ⁻¹)		Total bioavailable phosphorous (mg TBP·g dry matter ⁻¹)
	Inorganic phosphorous	Organic phosphorous	
Loose flocs	11 ± 1 ^b (81%)	3 ± 1 ^a (19%)	14 ± 1 ^b
Consolidated flocs	16 ± 1 ^a (93%)	1 ± 1 ^a (7%)	17 ± 1 ^a
Smooth granules	15 ± 1 ^a (92%)	2 ± 1 ^a (8%)	17 ± 1 ^a
Filamentous granules	8 ± 1 ^b (70%)	5 ± 1 ^a (30%)	13 ± 1 ^b

Table S5.4. Initial concentration of the BG-11 growth medium used for the cultivation of loose flocs under nutrient reduced conditions for bioaccessibility of organic matter, nitrogen, and phosphorous and molecular complexity assessment.

Component	Concentration (mg·L ⁻¹)	Difference with BG-11 growth medium described in section 4.2.1 (%)
Na ₂ MgEDTA	1.4	
(NH ₄) ₅ [Fe(C ₆ H ₄ O ₇) ₂]	6.0	
C ₆ H ₈ O ₇ ·H ₂ O	6.0	
CaCl ₂ ·2H ₂ O	6.0	
MgSO ₄ ·7H ₂ O	75	
K ₂ HPO ₄	192	
Na ₂ CO ₃	20	none
H ₃ BO ₃	2.9	
MnCl ₂ ·4H ₂ O	1.8	
ZnSO ₄ ·7H ₂ O	0.22	
Na ₂ MoO ₄ ·2H ₂ O	0.39	
CuSO ₄ ·5H ₂ O	0.079	
Co(NO ₃) ₂ ·6H ₂ O	0.0494	
NaNO ₃	0	-100%

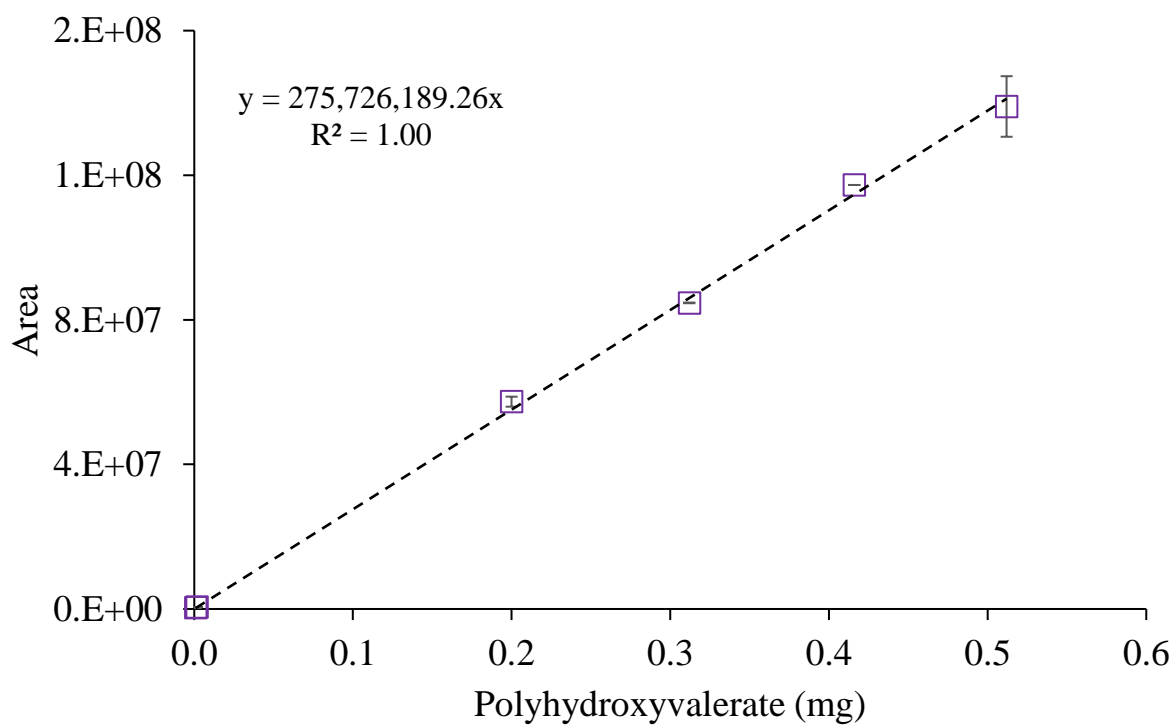
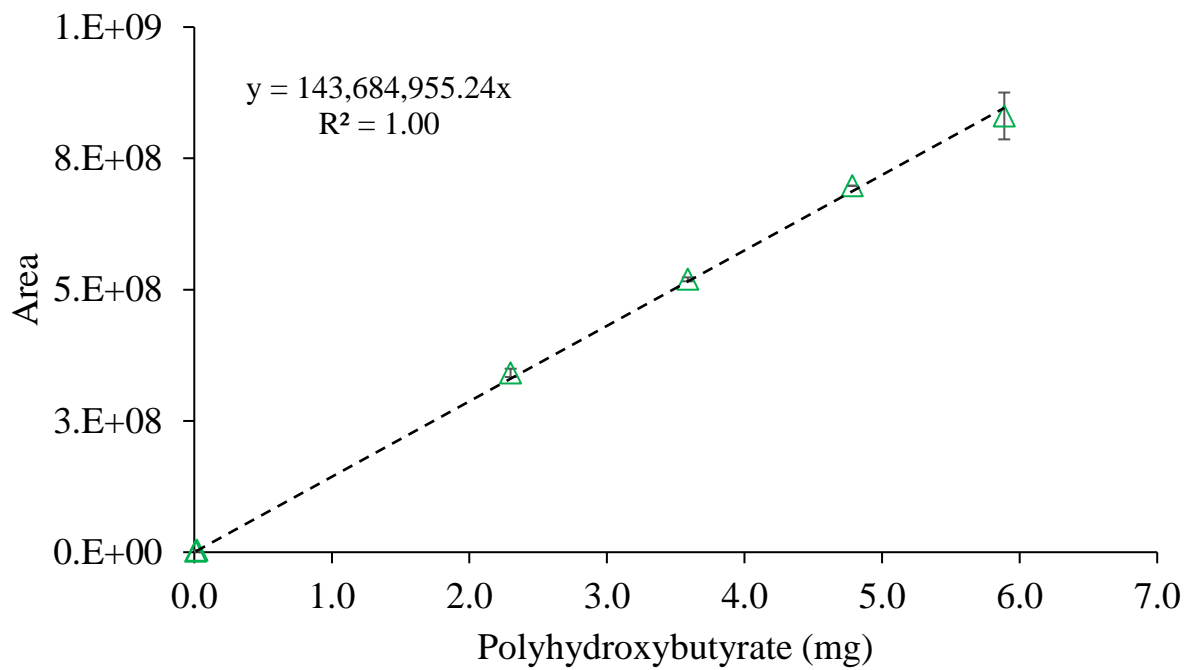
Table S5.5. Initial concentration of the nitrate mineral salt growth medium used for the cultivation of filamentous granules under nutrient reduced conditions for bioaccessibility of organic matter, nitrogen, and phosphorous and molecular complexity assessment.

Component	Concentration (mg·L ⁻¹)	Difference with nitrate mineral salt growth medium described in section 4.2.1 (%)
CH ₃ COONa	62	
KH ₂ PO ₄	1.4	
Na ₂ HPO ₄ ·12H ₂ O	2.8	
(NH ₄) ₂ SO ₄	25	
Na ₂ EDTA·2H ₂ O	0.625	
Na ₂ MoO ₄ ·2H ₂ O	0.00025	
FeSO ₄ ·7H ₂ O	0.0025	
H ₃ BO ₃	0.005	-75%
ZnSO ₄ ·7H ₂ O	0.001	
MnCl ₂	0.00025	
CoCl ₂ ·6H ₂ O	0.0025	
CuSO ₄ ·5H ₂ O	0.0035	
FeCl ₃	0.05	
NiCl ₂ ·6H ₂ O	0.00025	

Methods

Polyhydroxyalkanoates content using gas chromatography

1. Take 25 mL of the desired culture and place it in a 50 mL Falcon tube. Harvest the cells by centrifuging at 3000 *g* for 20 min. Thoroughly discard the supernatant.
2. Spread the cell pellets in plastic trays and freeze for at least 4 h at -2 °C. Afterwards, freeze-dried the sample at -85°C and 0.05 hPa for 24 h.
3. Retrieve dried biomass using a spatula, place it in a 50 mL Falcon tube, and ground using 4.8-mm stainless steel beads in a bead mill for 6 min.
4. Weight 10-20 mg of freeze-dried biomass in a 10 mL glass test tube with a Teflon liner screw cap and add 2.0 mL volume of acidified (2 % v/v H₂SO₄) methanol and 2.0 mL of chloroform. Vortex for 1 min.
5. Place the tubes in a dry bath at 120 °C for 2 h. Then, let the sample cool at room temperature for 15 min. Add 1.0 mL of distilled water to the sample and vortex again for 1 min to facilitate the solvent separation by density.
6. Retrieve the bottom layer using a glass Pasteur pipette and filter through a 0.45µm pore-size nylon membrane filter.
7. Take a small aliquot from the glass test tube (1.0 µL) and inject into the gas chromatograph. Polyhydroxyalkanoates were determined as polyhydroxybutyrates and polyhydroxyvalerate. A calibration curve was also performed following the steps before using Poly[(R)-3-hydroxybutyric acid-co-(R)-3-hydroxyvaleric acid] of natural origin.



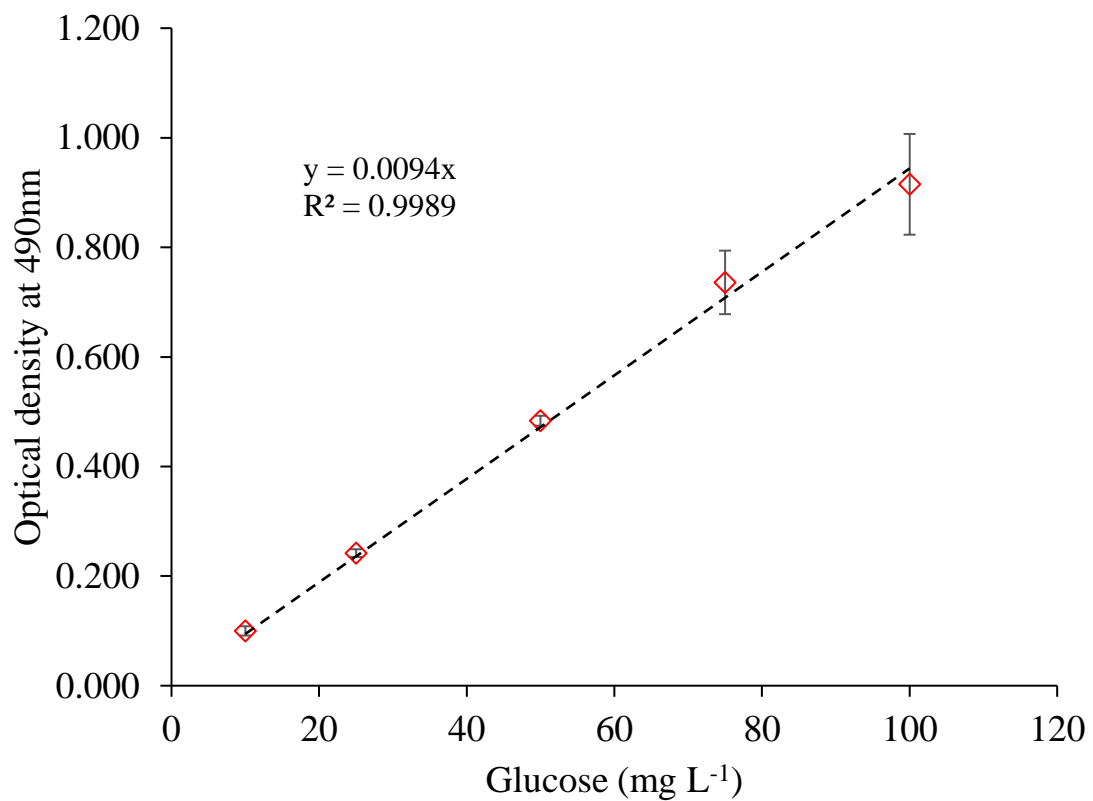
Polyhydroxyalkanoates using Nile red fluorescent staining

1. Take 10 mL of the desired culture and place it in a 15 mL Falcon tube. Harvest the cells by centrifuging at 3000 g for 20 min.
2. Discard the supernatant and resuspended cell pellets in 1.0 mL of Nile red dye (100 $\mu\text{g mL}^{-1}$ dissolved in Dimethyl Sulfoxide (DMSO)). Incubate for 10 min at room temperature.
3. Retrieve 20 μL of the stained cell pellets with a micropipette and place it in a glass-slide. Heat-fixed the sample using a Bunsen burner. Remove excess dye with distilled water.
4. Place the slide in a fluorescence microscope equipped with an excitation filter (450–490 nm), emission filter (515 nm), and a dichroic beam splitter (500 nm). Polyhydroxyalkanoates, more specifically polyhydroxybutyrates, granules would take a bright red color.

Polysaccharides content using phenol-sulfuric method.

1. Take 10 mL of the desired culture and place it in a 15 mL Falcon tube. Harvest the cells by centrifuging at 3000 g for 20 min. Thoroughly discard the supernatant.
2. Spread the cell pellets in plastic trays and freeze for at least 4 h at $-2\text{ }^{\circ}\text{C}$. Afterwards, freeze-dried the sample at -85°C and 0.05 hPa for 24 h. Retrieve dried biomass using a spatula, place it in a 50 mL Falcon tube, and ground using 4.8-mm stainless steel beads in a bead mill for 6 min.
3. Weight 1-2 mg of freeze-dried biomass in a 10 mL glass test tube with a Teflon liner screw cap and add 1.0 mL of HCl with a concentration of 1.0 M. Vortex for 1 min. Place the tubes in a dry bath at $100\text{ }^{\circ}\text{C}$ for 2 h. Then, let the sample cool at room temperature for 15 min.
4. Take 1.0 mL of the sample and place it in in a 10 mL glass test tube with a Teflon liner screw cap. Add 1.0 mL of 5.0% m/V phenol solution and 5.0 mL of concentrated (36 N) H_2SO_4 . Vortex for 10 s.

5. Incubate for 10 min at room temperature. Then, place the glass test tube in a lukewarm water bath (25 to 30 °C) for another 15 min.
6. Take a small aliquot from the glass test tube and measure the absorbance in a spectrophotometer at 490 nm. A calibration curve was also performed following the steps before using glucose solutions in concentrations from 2 to 100 mg L⁻¹.



Storage of photoautotrophic microorganisms

1. Prepare the recommended solid culture medium for the isolated cyanobacteria or microalgae strain. Recommended growth media for cyanobacteria is BG-11, for freshwater microalgae is Basal Bold Medium or BBM, for *Spirulina* is Zarrouk, for diatoms and coastal seaweeds is f/2 and for marine algae is Artificial Seawater or ASN-III. Sterilize at 15 psi for 30 minutes at 121°C.
2. Disinfect a designated workspace using 5% v/v NaOCl. Then, place the strain to be inoculated and sterilized glassware (Petri dishes, sterilized medium, inoculation loop, etc.) within a 15-25 cm radius from the Bunsen burner flame.
3. After 10 minutes, pour enough culture medium into a Petri dish to reach one-third of the total container height. Allow it to solidify at room temperature within the sterilized area and on a flat surface.
4. If the strain is on a solid medium, allow the inoculation loop to heat up until red-hot in the Bunsen burner flame and let it cool behind the flame. Take a sample using the loop's tip and perform a basic streak on the culture medium surface. Seal the Petri dish with parafilm and masking tape when finished.
5. If the strain is in a liquid medium, retrieve a known volume of the strain using a previously cleaned pipette behind the Bunsen burner. Empty the sample into the Petri dish, close the lid, and gently spread the liquid in circular movements by gently tilting the Petri dish around the worktable. Seal with plastic wrap and masking tape.
6. Finally, incubate the Petri dishes at room temperature in a well-lit room or area. Repeat the process up to every three months for maintaining inoculums at an exponential phase.